

**DEVELOPMENT OF EFFECTIVE STRUCTURES AND
METHODS FOR CALCULATING PARAMETERS OF
HARNESS-LEVER COUPLINGS OF CARDAN
MECHANISMS WITH ELASTIC ELEMENTS**

**B.N. DAVIDBAEV, A. JURAEV,
S.M. ZULPIEV ,N.B. DAVIDBAEVA**

ISBN:- 978-1-957653-20-4

PUBLISHED DATE:- 30 NOVEMBER 2023

DOI:- <https://doi.org/10.37547/gbps-15>

**MINISTRY OF HIGHER EDUCATION, SCIENCE AND
INNOVATION OF THE REPUBLIC OF UZBEKISTAN**

Fergana Polytechnic Institute

**B.N. DAVIDBAEV, A. JURAEV,
S.M. ZULPIEV, N.B. DAVIDBAEVA**

**DEVELOPMENT OF EFFECTIVE STRUCTURES AND
METHODS FOR CALCULATING PARAMETERS OF
HARNESS-LEVER COUPLINGS OF CARDAN MECHANISMS
WITH ELASTIC ELEMENTS**

Fergana - 2023

UDK: 621.01

B.N. Davidbaev, A. Juraev, S.M. Zulpiev, N.B. Davidbaeva

Development of effective structures and methods for calculating parameters of harness-lever couplings of cardan mechanisms with elastic elements. Fergana 2023, 149 p.

The monograph considers the analysis of the design features of lever-hinge couplings with elastic elements. The methods and results of structural, kinematic and dynamic analysis of lever - articulated couplings with elastic joints of cardan mechanisms. The results of experimental studies on the determination of the loading of the shafts of the coupling halves at various values of the angles of divergence of the shafts and technological loads are given. The monograph is intended for researchers, graduate students and students.

Reviewers:

Doctor of Technical Sciences, Prof.
Doctor of Technical Sciences, Prof.

M.T.Mansurov
T.S. Nabiev

ISBN: - 978-1-957653-20-4

DOI: - <https://doi.org/10.37547/gbps-15>

INTRODUCTION

In the main directions of development of the national economies of the states of Central Asia, the leading place is occupied by the development of mechanical engineering and related industries. Solving the problems of the development of the machine-building sector is a defining link in the entire strategy of the transition of these states to the market. In this case, transport means and communications play an important role. Moments, powers over long distances are transmitted by cardan shafts. At the same time, during the operation of these shafts, misalignment and misalignment of the axes of these shafts occur. This leads to premature failure of the transmission. In addition, the transmission efficiency is significantly reduced. Usually, in these transmissions of vehicle drives, lever couplings, in particular "crosses", are used. The kinematic capabilities of existing lever couplings are limited. At the present stage of development of vehicles, technological machines, the main trend is based on an increase in power, speed, at minimal cost, with high efficiency.

Therefore, the creation of more efficient designs of lever couplings for cardan mechanisms of vehicles, providing an increase in the kinematic and operational characteristics of the drive, is an important problem.

The main goal of the work is the development of a new design and the creation of methods for the structural, kinematic and dynamic analysis of a lever-hinge coupling with elastic elements of the cardan mechanism. Research tasks include:

- to develop a new design of a lever-articulated coupling with elastic elements of the cardan mechanism. Develop a classification of lever-articulated couplings;
- to develop a method of structural and metric analysis of a lever-hinge coupling;

- to carry out a kinematic analysis of the lever-articulated coupling of the cardan mechanism;

- to develop dynamic and mathematical models of a machine unit with a lever-articulated clutch. Based on the numerical solution of problems, determine the patterns of movement of the drive and driven shafts of the coupling, justify the inertial and elastic-dissipative parameters of the system;

- develop a methodology for experimental studies and substantiate the parameters of shafts and elastic elements that provide the necessary uneven rotation of the coupling shafts.

The results obtained expand the general theory of machines and mechanisms to improve the designs of lever-articulated couplings of cardan mechanisms, the development of methods for their structural, kinematic and dynamic analysis.

1. ANALYSIS OF THE WORK OF THE STRUCTURE OF HINGE , GARDEN MECHANISMS AND METHODS OF THEIR IMPROVEMENT

1.1. Overview of the work of articulated-cardan mechanisms

When analyzing the structure of cardan mechanisms, analysis methods are used that are described in the works [4,5,6]. Currently, to assess the rationality of the design of the mechanism, the method of L.N. Reshetov and his followers is used [7-10]. In this case, a technique is used that has proven itself when studying the possibility of assembling the mechanism contour without interference. Since to prove the synchronism of the mechanism it is sufficient to check the equality of the angles of rotation of the shafts in one complete revolution, the application of the analytical geometry formula quite easily and convincingly solved the problem [11]. As for the metric analysis and synthesis of the mechanism, they were carried out by the method of closed vector contours, developed by V.A. Zinoviev and other researchers [12-21]. Methods for studying the kinematics of widely known cardan mechanisms have also been adopted, the results of which are presented in [22-25, 26-32]. Determining the position of links of lever-hinge mechanisms, including articulated-cardan mechanisms, was solved by the method of coordinate transformation - the method of Yu.F. Moroshkin [6,33-36], as well as the method of conditional opening of the circuit [37,38,39]. In the kinematic analysis and synthesis of these mechanisms, the method of coordinate transformation in matrix form is successfully used [40-51]. The kinematic Euler equations, known from theoretical mechanics [52], are also used. The study of the action of force factors on the links of the lever-hinge mechanism, there are methods of vector calculus with consideration of the balance of the links [53-63], which most clearly illustrate the actions of forces. In a number of cases, attention is paid to the development of the theory of calculation of some details of the mechanism based on the methods of strength of materials [64, 65]. For the theoretical and

experimental determination of the efficiency of the new mechanism, the methods described in the work of A.I. Soloviev [66] and others [67, 68] are used.

History developed universal joints. The first mention of the hinge dates back to the 4th century BC. This is how Philo von Bizantz describes an inkpot located inside several concentric, movably connected rings, allowing the liquid to always be in a strictly horizontal position. This design later became the prototype for the creation of a ship's compass in 1550. Its creator is the Italian physician, philosopher and mathematician Geranimo Cardano. In 1664, the Englishman Robert Hooke received a patent for a cross hinge, which later became a classic. And only in 1898, Louis Renault, in his first, personally designed car, installed a shaft with cross joints, called the Cardan or "Hook shaft". Later, the shaft was divided into two parts, inserting a third knee. In 1903, Clarence Spicer completed and patented the design of a splined bushing, which made it possible to compensate for linear elongation and achieve hitherto unseen characteristics [69].

Inventors Carl Weiss (1923), Jean Albert Gregoire (1925) and Alfred Rzeppa "(1927) patented synchronous joints, which later received the names Trakta, Bendix-Weiss, Rzeppa. Moreover, J. A. Gregoire and M .D Orange developed the theoretical foundations of such joints in 1932. Thus , the designers of all-wheel drive vehicles received a whole arsenal of synchronous joints in addition to the already known double cardan joints and their varieties with a dividing ball, first proposed in 1931 by Hans Jung [70].

A further development of the ideas of A. Rzeppa are hinges manufactured by Liebro, Unicardan, Tripod, GKN, DANA-Spicer. Here it was possible to somewhat simplify the design of known synchronous hinges.

Today we can say with confidence that the right to life in the transmission of front-wheel drive models of cars with independent suspension has been won by Rzeppa joints and their derivatives, and on powerful heavy all-wheel drive

cars by cam-disc joints or dual universal joints [71]. It should be noted that during the operation of transport systems, depending on the conditions of their operation, it is possible to improve and modernize some elements, including cardan joints.

1.2 Analysis of design features and schemes of synchronous cardan mechanisms

According to the sources of information that we have, in creating a new design of synchronous cardan mechanisms operating, for example, at an angle of up to 60° or more, it has not been possible to find original solutions so far. Our attempt to fill this gap to a certain extent (by proposing a new design of such a mechanism) was the result of a comprehensive analysis of all existing designs and schemes that have found application in mechanical engineering and remained ideas not embodied in metal. The general design principles of synchronous cardan mechanisms were predicted in the prewar years by Academician E.A. Chudakov, based on the theory developed by him. According to this theory, all known synchronous mechanisms [1,2,3], despite the many varieties, as already noted, are based on the same principle. At the same time, an exception to the described principle are double single asynchronous cardan mechanisms (Hooke's joints) and cardans equipped with devices that allow dividing the angle of inclination of the shafts by a bisector plane [32]. Thus, a non-variable condition for the design of all synchronous cardan mechanisms is to ensure that the angle of inclination of the shaft is divided in half by the mentioned plane. All existing mechanisms are based on this principle, the bisector plane of which passes through the point of intersection of the axes of the shafts. With respect to it, any half, for example, the driven one, should be a mirror image of the other leading half. The design features of cardan mechanisms are important.

Ball joint by Karl Weiss. The widespread use of shaft connections in which forces are transmitted through balls is an example of the Karl Weiss ball joint. In such mechanisms, it is easy to achieve a constant gear ratio. However, the known designs of these mechanisms are characterized by a large number of redundant links. In the Weiss mechanism (see Fig . 1.1), the forces from the leading fork to the driven one are transmitted not through the cross, but through two balls that roll along the circular grooves made on the forks. The other two balls serve to transmit torque in the opposite direction. Currently, they are not used in transport systems.

The middle ball serves to center the forks. Due to the symmetry of the mechanism with respect to the driving and driven forks, their angular velocities are the same, so the gear ratio is constant and equal to one. The number of moving links (two forks and three balls) $n = 5$. When determining mobility, it should be remembered that each ball, due to possible slippage, has local (passive) mobility - rotation around three coordinate axes.

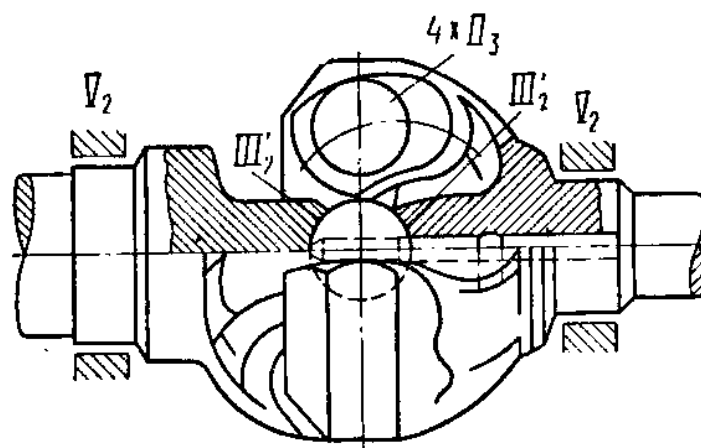


Figure 1.1. Weiss hinge

The mechanism can be improved if the double forks are replaced with triple ones and the torque is transmitted through three balls. Then the load of the ball will decrease by one and a half times: the middle ball is not needed, since three balls center the forks themselves.

These cardans are not designed to transmit high torques, since two balls are always involved in the work. The value of the angle at which rotation is transmitted to the driven shaft from the driving one does not exceed 40^0 [72,73].

High contact stresses in the ball-groove area (only two balls transmit torque at any given moment) significantly reduce the service life of these joints. In addition, it is difficult to manufacture and requires high-precision equipment, which makes the operation of this unit unprofitable economically.

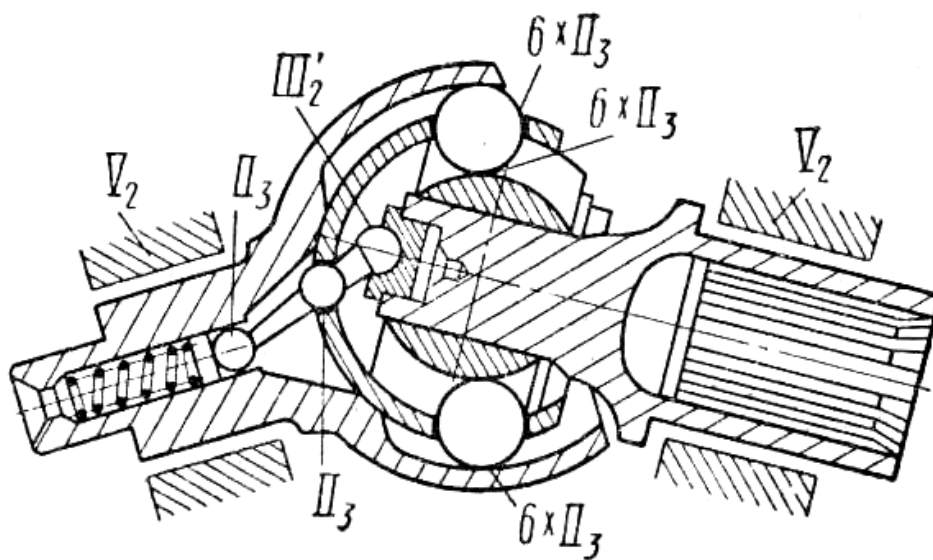


Figure. 1.2. Rzepp Hinge

Alfred Rzepp's ball joint. It is not surprising that this particular design has become the most common on modern front-wheel drive vehicles. The Rzepp joint differs from the considered Weiss joint in that it is equipped with six balls arranged with semicircular grooves, a dividing lever and a separator for balls.

The Rzepp hinge (Figure 1.2.) consists of spherical links with grooves for balls in the axial plane (meridional). One of the links has an outer spherical surface, and the other has an inner one. Balls (usually six pieces) are laid in the gutters, which, with the help of a separator and a dividing mechanism, are held in a plane dividing the angle between the axes in half. The mobility of the

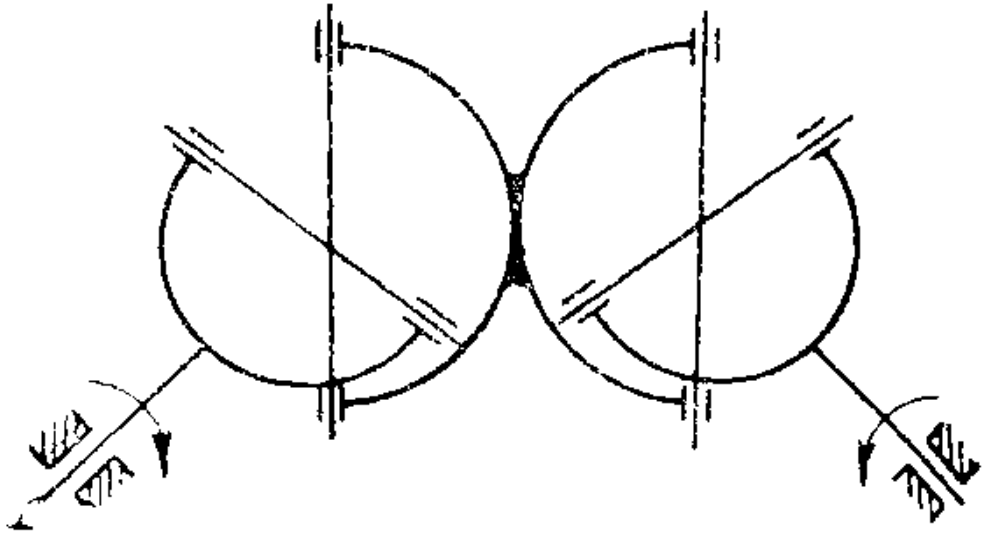
mechanism consists of the main mobility, the local mobility of six balls and the lever of the dividing mechanism.

Each ball is connected to separators and heads of the driving and driven shafts in three pairs Π_3 - annular. Two such pairs are available between the dividing lever and the head and the lever and separator. With such a huge number of redundant connections, the mechanism can only work if it is carried out very precisely. The separator is necessary so that the balls always lie on planes dividing the angle between the axes of the shafts into equal parts, and thereby guarantee the synchronism of the rotation of the shafts. Rceppa cardans are characterized by such disadvantages as the complexity of manufacturing and the need for high-precision equipment. Various firms (Birfield, Saginow, GKN, Lbro) have acquired licenses for the production of Rzepp's hinges. A further development of the ideas of A. Rcepp are hinges with three spherical rollers ("Lbro", "Tripod", "Unicardan"). Here it was possible to simplify the design and abandon the dividing lever. The grooves (with a modified section) are now placed not parallel to the hinge axis, but at an angle to it.

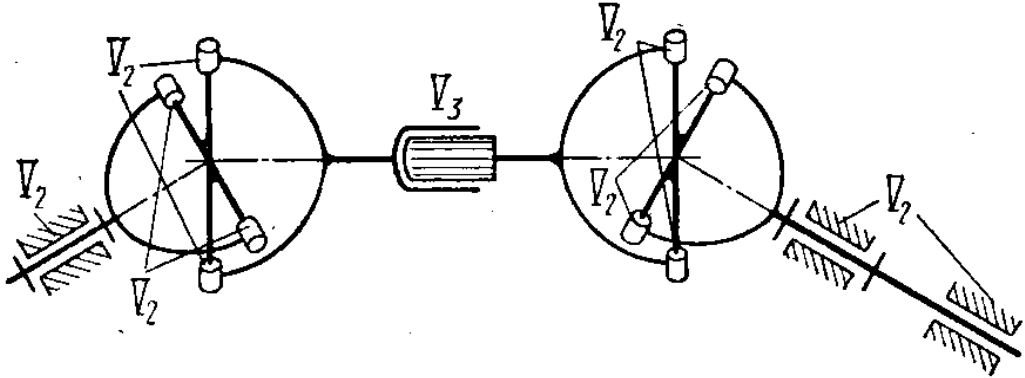
Double universal joint. Universal joint mechanisms are formed as a result of pairing of two single asynchronous cardans. Dual cardans practically carry out the transmission of rotation at an angle up to 30° and have large dimensions in the axial direction (Figure 1.3 a) [74,76]. They are sometimes made with centering devices to obtain synchronous rotation of the drive and driven shafts, as well as to reduce overall dimensions. To ensure synchronism, the forks of the intermediate link (shaft with forks at the ends) must lie in the same plane and the angles between the named link and the axes of the shafts must be equal.

Synchronous cardan mechanisms do not provide transmission of rotation at large angles, for example, 60° or more. Therefore, for the perfect need of mechanical engineering in more advanced mechanisms that meet modern requirements of technical progress, it leads to the search for new original designs, cardan mechanisms of a new generation. In practice, double cardans are

exclusively used. In "single cardan" automotive transmissions, there is usually a second cardan - flexible or toothed, eliminating redundant connections. Therefore, it is very important to properly design the double cardan mechanism. Double cardan ensures synchronous rotation of the driving and driven shafts. When the mechanism is made up of two cardan joints (Figure 1.4. *b*), then it is necessary to put a free spline connection on one of the shafts (driven, driven or intermediate) (translational pair V_3 class) [73].



a - Double universal joint



b - Double cardan.

Figure. 1.3.

In this case, the intermediate shaft must not have bearings. Then there are no redundant connections, i.e. and the mechanism will work reliably.

Connection remains, which in such mechanisms leads to breakage of parts. In the automotive industry for cars ZIL-130V, VAZ-2105,2107, AZLK-2140, GAZ-3101, etc., samples of new promising designs of cardan shafts with pipes made of composite material and forks made of light alloys based on a double cardan mechanism [77,78].

In these mechanisms, in order to avoid spline connection, it is possible if one or both universal joints are taken universal , i.e., allowing axial mobility. At (Figure 1.3.b); here one of the universal joints is toothed. In this case, the mechanism also works reliably [73]. The design of the double cardan mechanism with one universal gear cardan is shown in figure 1.4 *a*.

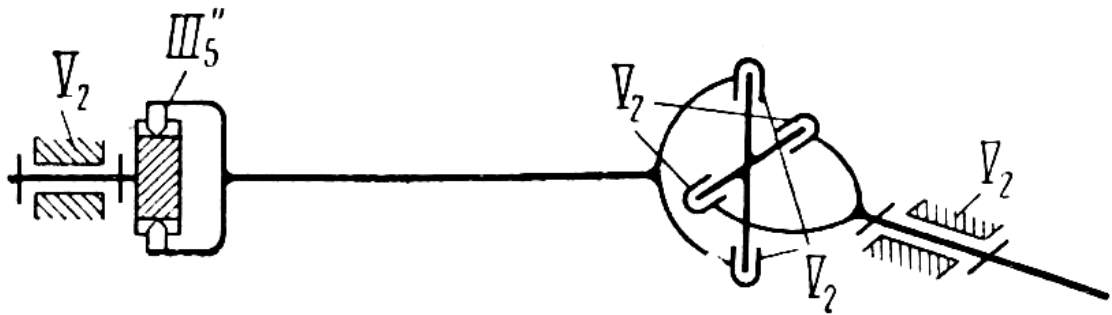
In these mechanisms, one should be careful not to use supports on the intermediate shaft of the double cardan mechanism, since they greatly increase the number of redundant links.

In rolling machines, double cardans are usually used. It should be remembered that the intermediate shaft has longitudinal mobility within the gaps. Therefore, the degree of mobility of the mechanism will be $\omega = 2$. The mechanism is especially beneficial for railway transport when making hinges on greasy blocks (on rubber).

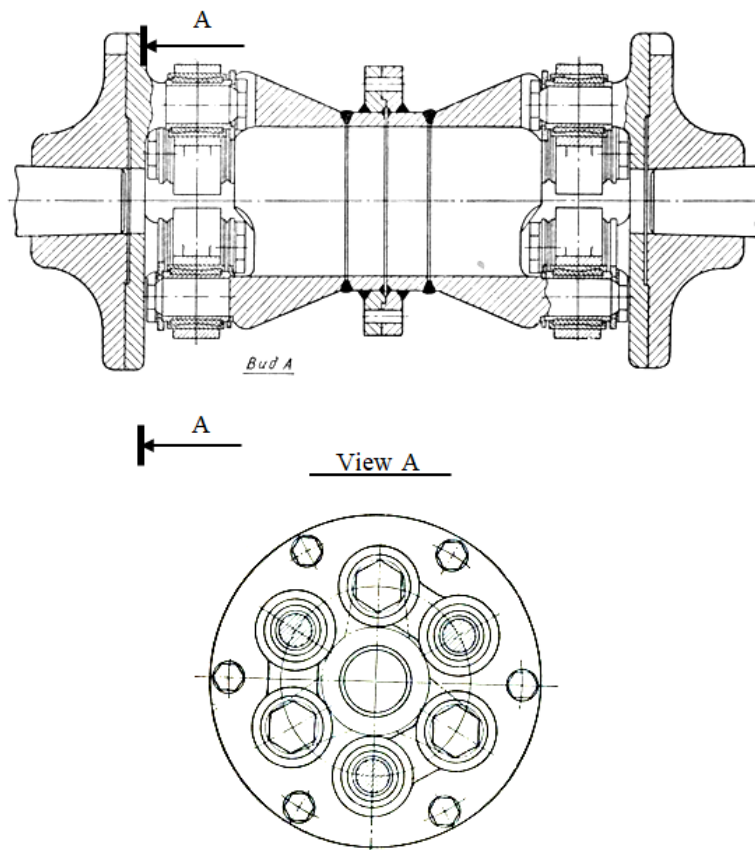
With small angles between the axes, they can also be performed on spherical rolling bearings. In Figure 1.4. *b* shows a double cardan joint with spherical pairs [73]. The bearings of the leading to the driven shafts - pairs V_2 are not shown. Connecting rods have local mobility - rotation around its axis, which gives six mobility.

In addition, there is axial mobility of the intermediate shaft within the gaps and the main mobility is the rotation of the mechanism .

The problem of eliminating redundant connections in the tract mechanism is interestingly resolved (Figure 1.5. *a*. Cardan of the tract).



a - double with one universal gear cardan



***b* - double cardan joint with spherical pairs.**

Figure 1.4

According to its kinematics, it represents a double cardan joint, but instead of six moving links, it has four [69,72,73].

These cardans are arranged as follows. The forks of the driving and driven shafts are connected by intermediate elements - cams with perpendicular

grooves and a ledge. Due to their compactness and ease of manufacture, these cardans are used to transmit rotation at an angle of up to 50° . However, they cannot be performed with rolling bearings and, therefore, their friction losses are higher than those of other universal joints, and as a result, increased heating of parts and the inadmissibility of working with a significant number of shaft revolutions.

The plane pair is made in the form of a deep groove on one link, into which the plate of the end of the other link enters. It provides the links with the same relative movement as in a conventional double gimbal.

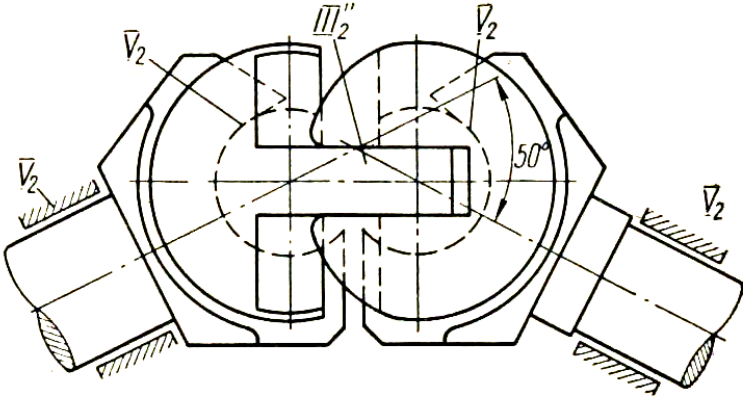
To assemble rotational pairs V_2 , the surface of the trunnions is sawn off. Insert them into the forks in a position rotated 90° . The Tract mechanism is very interesting in its idea. It is difficult to perform it alone on rolling bearings. To process its links, special devices are needed, without which it is difficult to fix them on the wall, so it is not suitable for individual production. In addition, it is difficult to obtain a large angle between the axes. Cardan "Trakta" works well at angles up to 50° and transmits significant torque, compact and simple, but leads to increased heat and noise, laborious operation, as well as complexity in the layout of the drive.

Such cardans of the 1920s and 30s were widely distributed and used on front-wheel drive models of cars of foreign Citroen companies. "Shtever" DKV, "Adler".

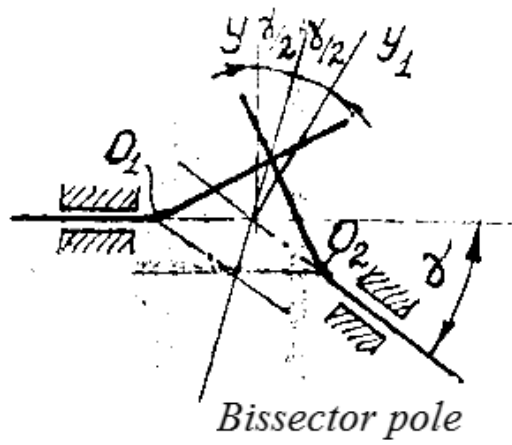
The prototype of known designs and schemes of synchronous cardan mechanisms is a spatial drive mechanism, the design of which is shown in Figure 1.5. *in* the spatial drive cardan mechanism [72] the axes of the driving and driven shafts intersect at one point R . Moreover, the plane passing through the point P and the point *And* the contact of the leashes, rigidly connected with the shafts, is bisector. For synchronous rotation of the shafts, it is necessary that the distances from the point of intersection of the axes of the shafts and to the points of connection of the drivers with the shafts O_1 and O_2 must be equal. In

addition, the point of contact of the drivers A must lie in a plane that bisects the angle formed by the axes of the shafts. It follows from the foregoing that the planes of rotation of the leashes make an angle with the bisector plane equal to half the angle between the axes of the shafts. Therefore, the bisector plane is also the plane of symmetry. Thus, a regularity is revealed that all synchronous cardan mechanisms should be structurally performed to ensure the symmetry of the elements of the intermediate links with respect to the bisector plane.

Recently, flexible shaft connections have begun to be widely used [72, 73]. They do not require lubrication, are not afraid of contamination, are not subject to wear, and when properly designed, they work without fail. On figure 1.6. *and* shows a double flexible cardan Brown - Boveri, used in railway transport [73]. The cardan shaft runs inside the hollow shaft of the electric motor. This explains the unusual arrangement of the supports. Typically, electric locomotives use a double cardan. For simplicity, a single one is considered, considering the shaft bearings in pairs V_2 and III_2' , as they do with any universal cardan. It consists of a flexible steel sheet to which the forks of the drive and driven shafts are attached. The sheet imposes three link conditions, i.e. is the pair III_4'' that is required for a universal gimbal. Flexible cardans are placed openly and are not closed with any casings.

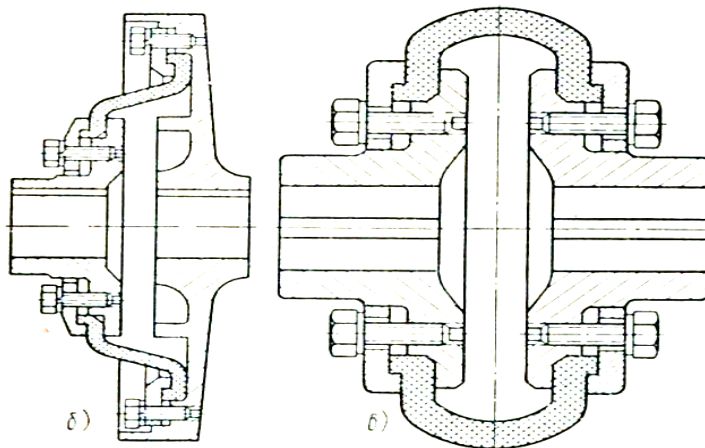
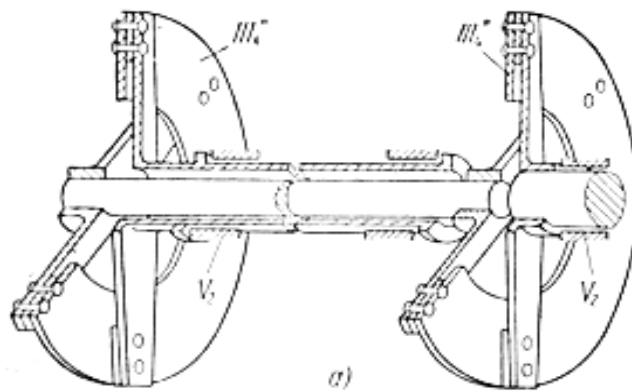


a - Cardan Trakta



b - Spatial drive cardan mechanism

Figure 1.5



a) double Brown Boveri; b) single rubber; c) double type car tire.

Figure 1.6. flexible gimbal

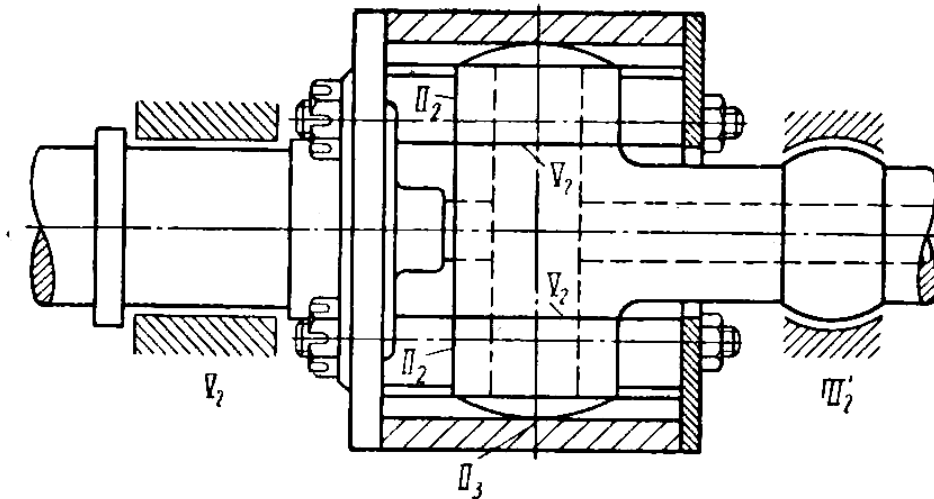
The angle between the axles is small, which contributes to the durability of the mechanism, despite its speed and large transmitted moments.

Rubber flexible shaft connections are also used: in the form of a sheet (see Figure. 1.6.b) or in the form of a car tire (see Figure 1.6.c). The latter corresponds to a double compound of the first type. Such gimbal connections are used in cars VAZ, Mercedes, BMW with rear wheel drive. The universal bell cardan (see figure. 1.7. a) is universal, i.e. allows both angular and axial movement of the shafts [7,8,9]. Therefore, it does not require axial mobility in the bearings. The latter is performed: one as a rotational pair V_2 , the other as a spherical pair III_2' . Each roller works on two surfaces - a plane and a cylinder, and itself consists of a cylindrical and spherical working surfaces. Therefore, these sections must be considered as separate pairs of II_2 and II_3 . Only one roller can be pressed in the radial direction, and both can be pressed in the circumferential direction, therefore $p_{II} = 3$. The disadvantage of these mechanisms is that very precise manufacturing of parts is required, as well as careful assembly of the mechanism.

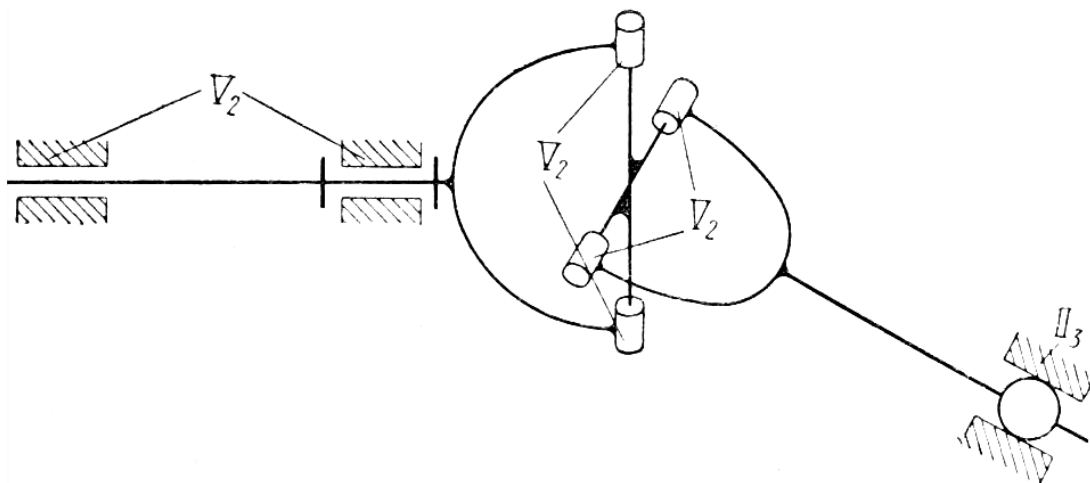
1.3. Some design features of asynchronous cardan mechanisms

In asynchronous cardan articulated mechanisms, unlike synchronous ones, there are some discrepancies between the angular velocities of the drive and driven shafts of the mechanism. There are a number of designs of asynchronous cardan mechanisms that are used in mechanical engineering, especially in vehicles.

One of these mechanisms is the Cardan (Hooke) hinge, shown in Figure 1.8. In this mechanism, all kinematic pairs, except for one, perform rotational V_2 cylindrical with rims [7,8,11]. The connection between the fork and the cross should be considered as one kinematic pair, despite the fact that this connection consists of two parts. The fact is that these parts can be made in one piece. Therefore, the coincidence of their axes is performed with great accuracy.



a - Universal bell cardan.



b - Single universal joint

Figure 1.7

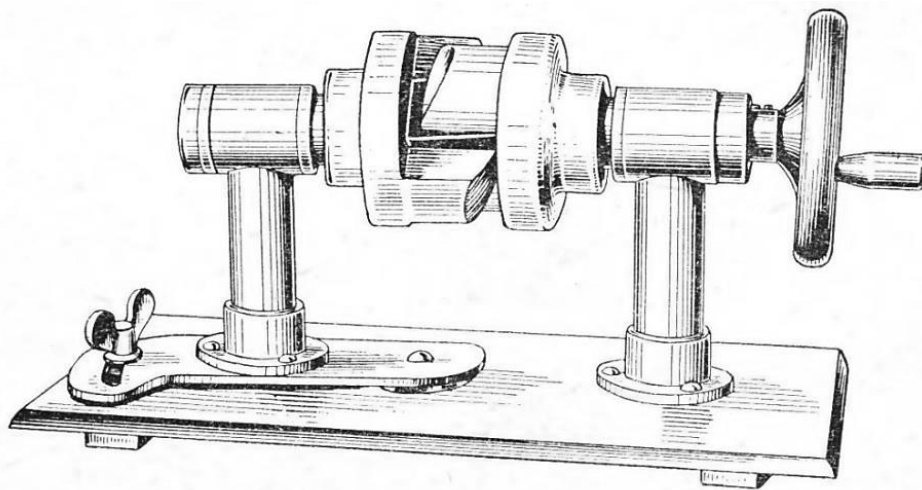
In a cardan joint for small loads on plain bearings, the kinematic pair can be made as a cylindrical pair without flanges with gaps, provided that it is sufficiently removed from the center of the hinge (5-10 fork radii) and the liner is short (no more than the shaft diameter).

The gaps in the kinematic pairs increase the angular movements and affect the linear movements. Therefore, the gaps made in the cylindrical pair IV_2 turn it into a pair II_4 . In practice, there may be cases when rotational pairs of class V_5 are required on both the driving and driven shafts, i.e., a pair of II_3 cannot be installed on any of them (shaft oscillations are unacceptable). In this case, you can use a double

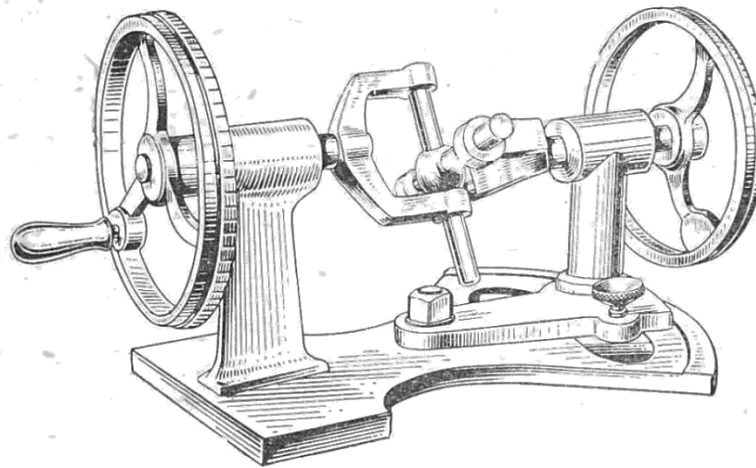
cardan or a cardan with a cube (Figure 1.8. *a*). This mechanism, in the presence of a gap in the axial direction between the cube and the fork, allows a certain angle between the axes of the shafts. In addition, this can be achieved by beveling the corners of the cube. The allowable angle depends on the clearance or bevel of the corners of the cube [73]. It should be noted that this mechanism as a cardan joint is still pores were not used and it was considered possible to use it only with parallel axes, i.e., as an Oldghem coupling. Even in the classic version, the Oldghem coupling, in the presence of a gap in the axial direction, can serve as a cardan joint.

In this mechanism, a planar pair III_2 ", applied between the cross and the fork, allows relative rotation, that is, it can replace the rotational pair. This results in a non-constant gear ratio with a coefficient of unevenness, approximately equal to the square of the angle (in radians) between the axes. However, it cannot serve as a cardan joint, since in the presence of a shift of the axes and the angle between them, the shaft with the IV_2 pair oscillates along the axis with twice the frequency. The amplitude can be adjusted by shifting the axes or changing the angle between them.

Therefore, the mechanism can be used to convert rotational motion into translational motion when amplitude adjustment is required (see Fig. 1.8. *b*).



***a* - Cardan with a cube**



***b* - Gimbal with IV_s**

Figure 1.8

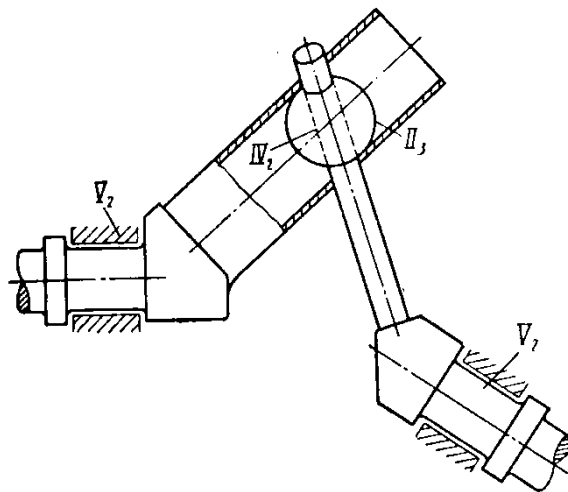
The design of the cardan mechanism of asynchronous rotation between the shafts, proposed by M.I. Lysov has no redundant connections. The scheme given by M.I. Lysov [80] the roller is made spherical and the corresponding gutter is cylindrical (see .r Figure 1.9. *a*). The mechanism transmits only force (one connection condition), therefore the supports of both shafts are made on rotational pairs V_2 . Mobility $\omega = 2$ (basic and slip roller). Excess connections $Q = 0$. The bearings of this mechanism are loaded with circumferential force. This mechanism is sometimes called a universal joint with a ball.

IV_4 can also serve as a cardan joint , which gives the necessary four connection conditions (Figure 1.9. *b* - Cardan mechanism with a chain pair) [74]. Due to poor contact and large gaps, such a hinge is not suitable for a mechanical drive and can only be used with a manual drive (for opening doors, shutters, blinds). For the same purposes, a pair IV_3 - ball with a pin can serve. The disadvantages of such a cardan mechanism can be said to be a large gap between the kinematic pairs. This is limited at high angular speeds of the shafts. It does not work well with reverse rotation of the shafts.

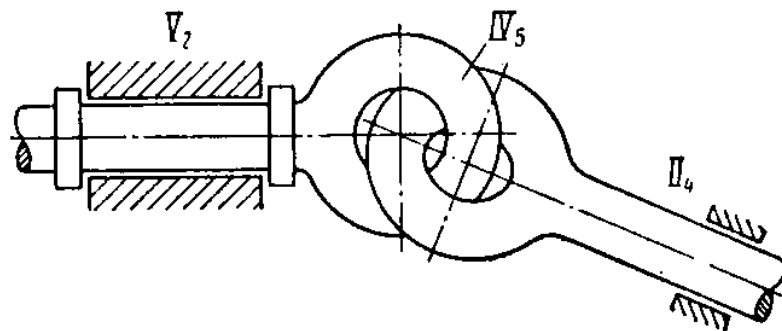
1.4. Development of new schemes of articulated-lever couplings

From the analysis of cardan mechanisms, the following shortcomings can be noted: limited kinematic capabilities, limited speed modes; increased wear of kinematic pairs and low durability; limited angle between the shafts, a large discrepancy between the kinematic characteristics of the driving and driven shafts; limited use in industry, especially in transport and agricultural machinery.

To eliminate these shortcomings, we have developed a number of new designs of cardan mechanisms in the form of articulated-lever couplings.



a - Cardan mechanism of M.I. Lysov.



b - Cardan mechanism with a chain pair

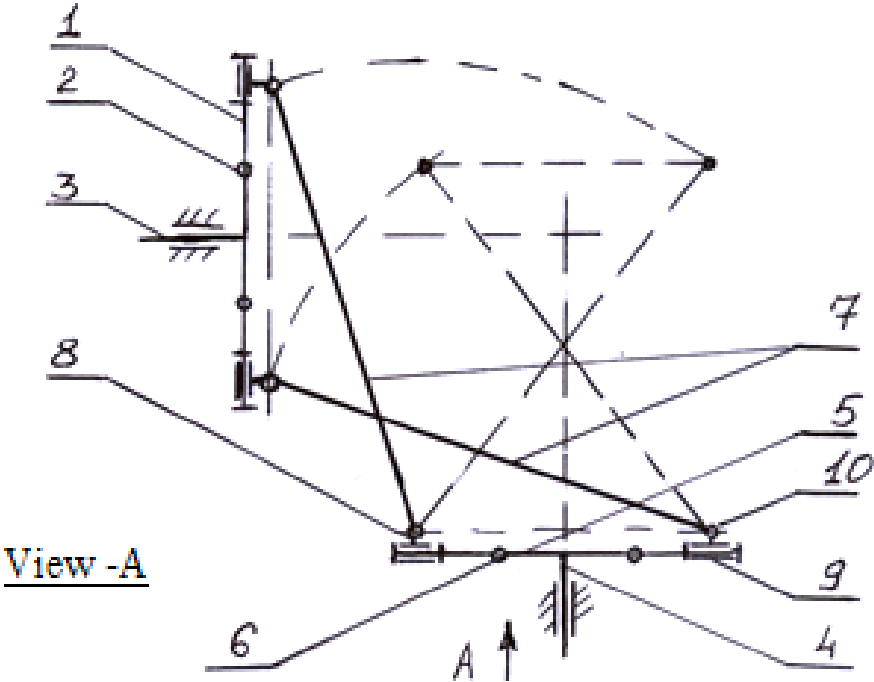
Figure 1.9.

Figure 1.10.a shows a diagram of an articulated-lever coupling, which contains two composite cranks 1, 5 and two crossed bracket-shaped connecting rods 7 located between them. In the composite crank 1, a spring 2, a drive shaft 3, a driven shaft 4 are installed. A composite crank 5 is installed in the driven shaft, and in the driven part of the mechanism the composite crank has a spring 6 and is connected to the lever 8. The lever 8 is connected by one end of the bracket-shaped connecting rod 7 through a spherical hinge 10, and the other end with a composite crank 5 through a cylindrical hinge 9. The lever clutch transmits rotational movements at an angle of the shaft axes 0 to 90° . This ensures smooth rotation of the driven shaft. This reduces vibrations and oscillations and also reduces the peak load of the cardan shaft. The toggle coupling can be used in agricultural machines [81].

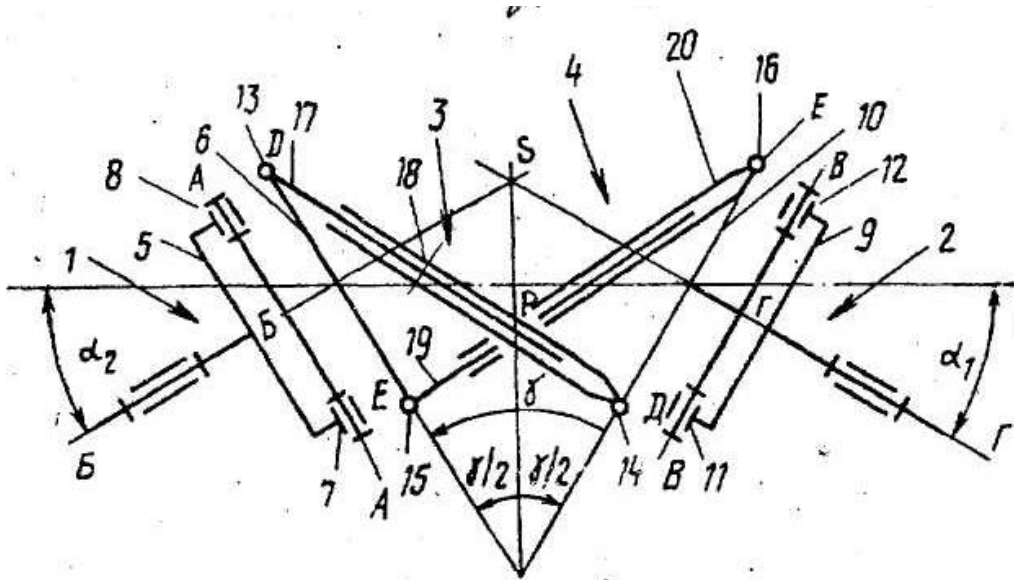
Figure 1.10.b shows a hinged coupling with extended kinematic characteristics [82]. The articulated coupling contains two coupling halves 1 and 2 and two crossed bracket-shaped connecting rods 3 and 4 located between them. The half-coupling 1 contains a fork 5, and an earring 6 connected to one another by means of cylindrical hinges 7 and 8, the axis A-A, which is located at right angles to the axis B-B of the fork 5. The half-coupling 2 contains a fork 9 and an earring 10, connected one on the other hand, by means of cylindrical hinges 11 and 12, the axis B-B of which is located at right angles to the axis G-D of the fork 9. The connecting rod 3 is connected at one end to the earring 6 by means of a cylindrical hinge 13, and at the other end to the earring 10 by means of a cylindrical hinge 14. The connecting rod 4 is connected at one end to the earring 10 through a cylindrical hinge 15, and at the other end to the earring 6 through a cylindrical hinge 16. Two parts 17 and 18 connected to one another with the possibility of mutual movement in the direction of the axis D-D, perpendicular to the axes of the hinges 13 and 14, and the connecting rod 4 is made of two parts 19 and 20 connected to one another with the possibility of mutual movement in the direction of the axis E-E, perpendicular to the axes of

the hinges 15 and 16. Axes A -A, B-B, C-C and G-D in one of the positions shown in the drawing are located in the same plane (in the plane of the drawing). In this case , the hinge axes 13.14,15 and 16 are located in a plane perpendicular to the drawing.

When transmitting torque from half-coupling 1 to half-coupling 2, the point 5 of the intersection of the axes B-B and G-D, as well as the point P of the intersection of the axes D-D and E-E, are located in the bisector plane dividing the angle in half.



a - articulated- lever clutch with composite cranks.



b - articulated-lever coupling with composite connecting rods.

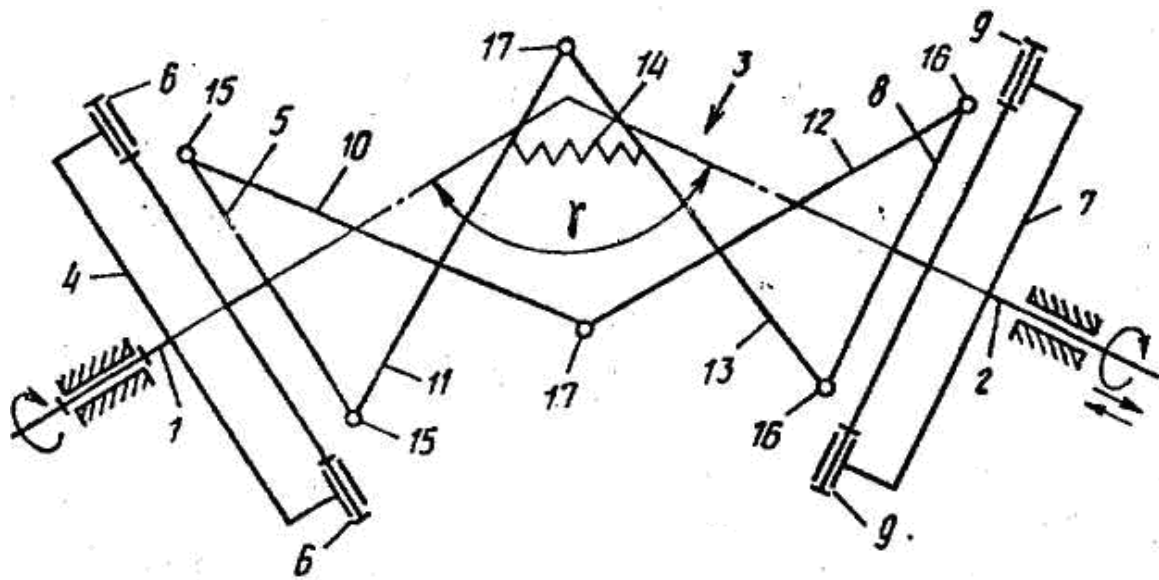
Figure 1.10. Hinge - lever coupling

The execution of the connecting rods 3 and 4 of the components 17, 18 and 19, 20 provides the ability to compensate not only for the angular displacement of the forks but also axial, in the direction of the axes B-B and G-G, as well as radial in the direction of the axes A-A and C - In this way, the expansion of the functionality of the clutch is achieved.

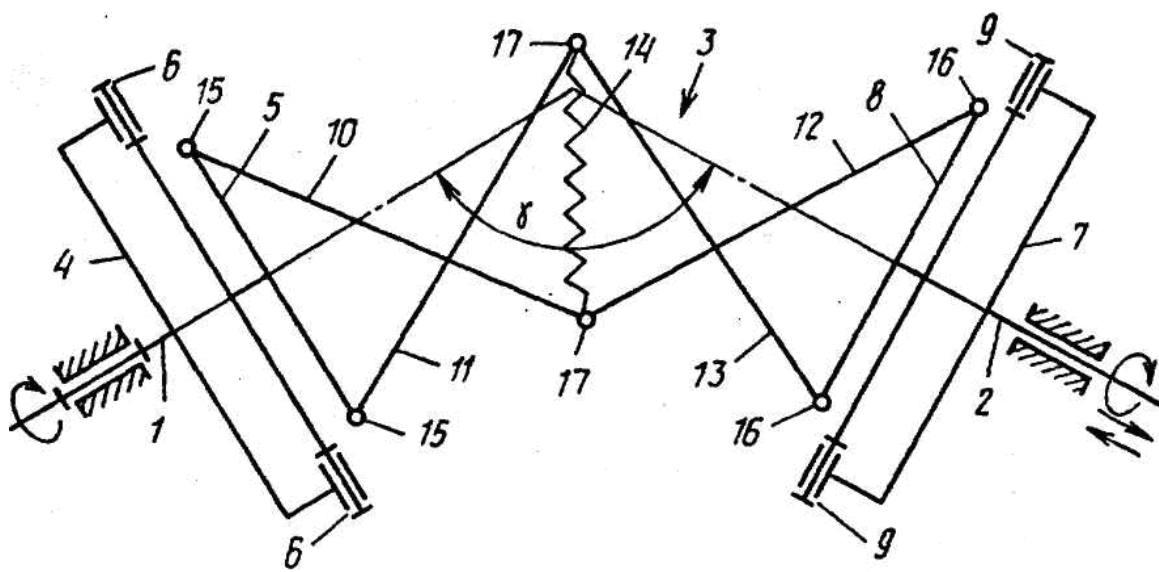
In the next developed design of the articulated coupling [83], the kinematic possibility is expanded due to the use of an elastic connection of the spring.

Figure.1.11. *a* shows a kinematic diagram of a clutch with an elastic element located between two levers connected to each other; figure1.11. *b* - the same, with an elastic element located between the levers of one pair; figure1.11. *c* - the same, with an elastic element located between one of the levers and the earring.

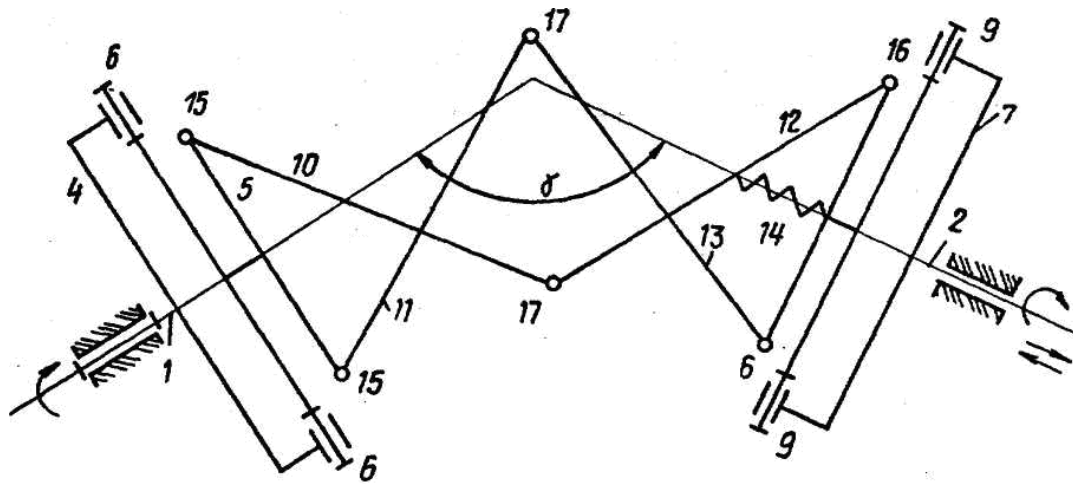
The articulated coupling contains a driving half-coupling 1, a driven half-coupling 2 and an intermediate device 3 located between them . driven coupling half 2 also



a - with an elastic connection between the levers.



b - with an elastic connection between the levers of one pair.



c - with an elastic connection between the levers and the earring.

Figure 1.11. Swivel Coupling with Elastic Links

contains links in the form of a fork 7 and an earring 8 connected to each other by means of hinges 9, the axis of which is perpendicular to the axis of rotation and parallel to the axis of the hinges 6. The intermediate device 3 contains two pairs of crossing levers 10, 11 and 12, 13 and an elastic element 14. The levers 10 and 11 are connected to the earring 5 by means of hinges 15. The levers 12 and 13 are connected to the earring 8 by means of hinges 16. The levers 10, 12 and 11, 13 are connected to each other by means of hinges 17. The axes of hinges 15 and 16 are arranged parallel to one another and perpendicular hinge axes 6 and 9. Forks 4 and 7, earrings 5 and 8, levers 10-13, hinges 6,9 and 15-17 can be made, respectively, the same. The elastic element 14 can be located between the levers of one pair, as well as between one of the levers and the earring. The articulated coupling can be made with several elastic elements 14 located between the links, the connection points of which with the elastic element can change the distance between them during operation. The articulated coupling works as follows.

When transmitting torque between coupling halves located at an angle γ one to the other, the levers 10-13 change the mutual angular position relative to each other, as well as relative to the earrings 5 and 8. i.e. the distance between any points of the mentioned links is continuously changing. Installation between

the said points of the elastic element 14 provides a reduction in the change in this distance, which leads to axial multidirectional movements of the driven half-coupling 2. The execution of the well-known articulated coupling with the elastic element 14 located between the points of the links, the distance between which changes, provides additional axial reciprocating movements of the driven coupling half during its rotation, which allows the coupling to be used as a drive of the working body that performs axial movements.

In order to increase the reliability of operation and increase the kinematic capability, a new design scheme of the articulated coupling is recommended, which is shown in Fig. 1.12 [84,85]. In this design, the damping of the reaction forces is carried out through the use of composite hinges between the earrings and forks, including elastic (rubber) bushings between the outer cylinder of the fork and the inner axis of the earring. In addition, the driving and driven shafts are mounted on bearings, which are connected to the housing by means of oval elastic bushings, and the major axis of the oval is set perpendicular to the plane of the housing base. This ensures smoothing of the moment transmitted by the clutch.

The drawing shows a kinematic diagram of the proposed articulated coupling, where Figure 1.12. *a* - a general scheme of the articulated coupling, in Figure 1.12. *b* - section A-A and in Figure 1.12. *c* - *section B- B* , 1.12.d - section B - B.

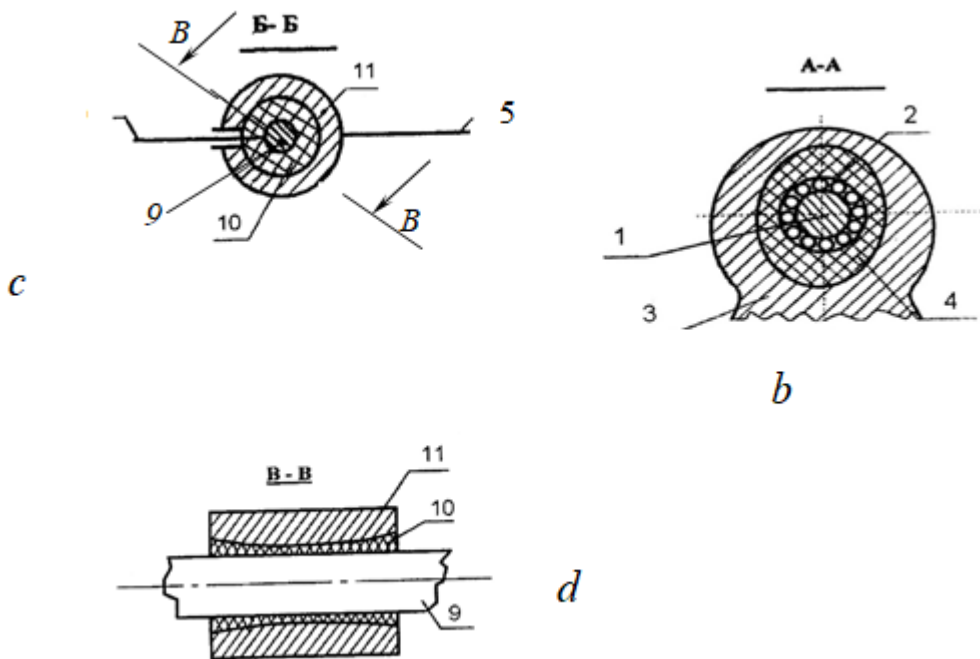
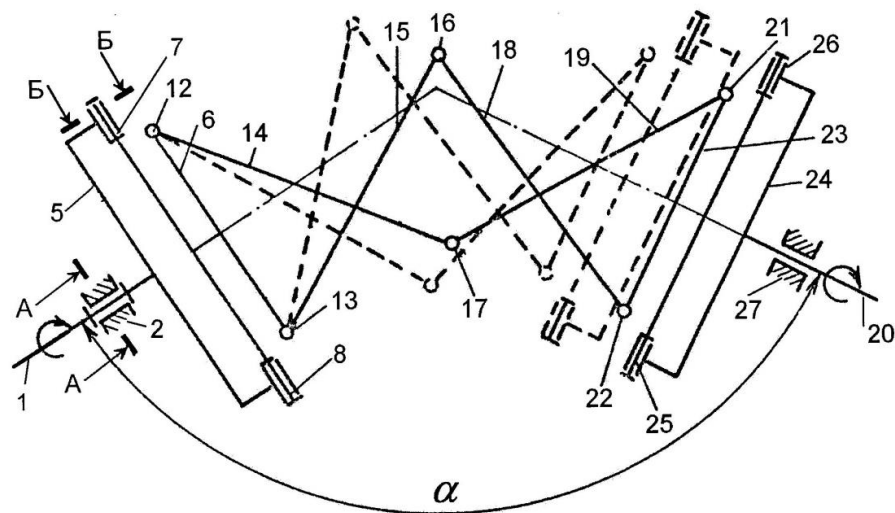
The clutch contains a drive half-coupling, consisting of a drive shaft 1 mounted on a bearing 2, which is connected to the housing 3 through an oval rubber bushing 4, and the major axis of the oval 4 is installed perpendicular to the plane of the base of the housing 3. The shaft 1 is rigidly connected to the fork 5, which in its queue is connected to the earring 6 by means of a hinge 7 and 8 . Hinges 7 and 8 are made composite , including axle 9 rigidly connected to fork 5, rubber bushing 10 put on it and cylinder 11 clasping it from the outside, rigidly connected to earring 6. At the same time, the outer surface of

rubber bushing 10 is made concave. With the earring 6 by means of cylindrical hinges 12,13 on both sides are connected bracket-shaped connecting rods 14,15. The other ends of the connecting rods 14 and 15 are connected by hinges 16 and 17 with another pair of connecting rods 18,19 of the driven half-coupling of the shaft 20. The connecting rods 18 and 19 are connected by other ends by hinges 21,22 to the earring 23, which is connected to the fork 24 by means of hinges 25,26. Hinges 25 and 26 are also made composite and have the same design with hinges 7 and 8. Fork 24 is rigidly connected to driven shafts 20, which is mounted on a support 27 identical to the support 2 of the shaft 1. The hinge axes 12,13,16,17,21,22 are parallel to each other. Shafts 1 and 20 are set at a certain angle α .

During the operation of the articulated coupling, the torque from the input shaft 1 is transmitted to the driven shaft 20 through the forks 5 and 24 and then through the earrings 6 and 23, connecting rods 14,15, 18,19.

During operation, the angular and axial compensation of the location of the forks 5 and 24 is achieved due to the swivel joints 7,8, 12, 13, 16, 17, 21, 22, 25, 26. In addition, the peak values of fluctuations in the reaction forces in the hinges and in bearing supports are amortized, smoothed out by elastic elements in composite hinges 7, 8 and 25, 26, as well as in composite bearing supports 2,27 of shafts 1 and 20.

The expansion of the kinematic capabilities of the articulated coupling is achieved by increasing speed modes by reducing the peak components of the transmitted moment for due to the use of composite elastic supports and composite elastic joints of the coupling. That is, the speed mode is increased by increasing the reliability of the articulated coupling.



a - general scheme, b - section of the support 2, c - section of the hinge 7 and d - axial section of the hinge 7.

Figure 1.12. Swivel coupling with elastic elements

1.5. Classification of articulated couplings in cardan mechanisms

Based on the analysis of existing designs of articulated couplings in cardan mechanisms, as well as taking into account the developed schemes of articulated-lever couplings with elastic elements, a classification of articulated

couplings has been developed, which is shown in Figure 1.13. At the same time, the articulated couplings are divided into two groups according to the relationship between the speed modes of the drive and driven shafts of the cardan mechanism: synchronous and asynchronous. Each of these groups is divided into the use of kinematic pairs of higher and lower classes. In addition, the designs of hinged couplings are divided into two groups according to their parameters: with constant geometric and kinematic parameters; with variable settings.

The recommended designs of swivel couplings mainly belong to the group with variable parameters. The studies carried out mainly concern the design of the articulated-lever coupling with composite kinematic pairs and elastic shock absorbers recommended by us. Based on the above, the following conclusions can be drawn :

- based on the analysis of works on the designs of articulated couplings in cardan gears, their main shortcomings in terms of kinematic and experimental characteristics were identified: limited kinematic capabilities, limited speed modes; increased wear of kinematic pairs and low durability; limited angle between the shafts, a large discrepancy between the kinematic characteristics of the driving and driven shafts; limited use in industry, especially in transport and agricultural machinery;

- new design schemes of articulated-lever couplings with improved kinematic and operational characteristics have been developed. The design of an articulated lever clutch with shock-absorbing properties of reactions in the kinematic pairs of the mechanism is proposed;

- A new classification of articulated couplings in cardan mechanisms has been developed, taking into account the design, geometric and kinematic features.

2. STRUCTURAL AND METRIC ANALYSIS OF A HINGE COUPLING

2.1. Structural Analysis of Swivel Couplings

In the general theory of machines and mechanisms, in terms of structural analysis, the number of moving links, kinematic pairs, the degree of mobility of the mechanism and excess connections are mainly revealed.

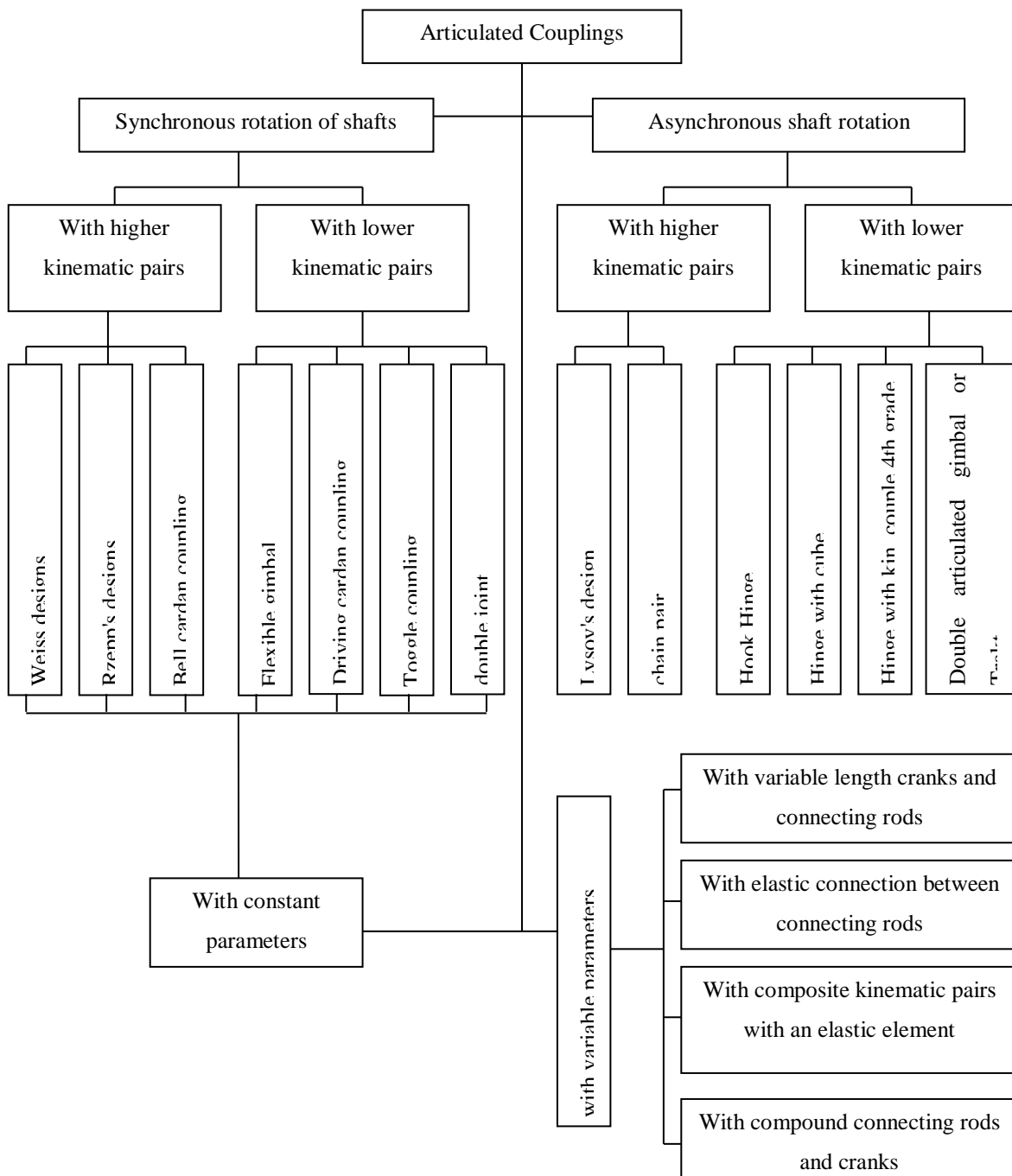


Figure. 1.13. Joint Classification

Determination of the degree of mobility of lever mechanisms is carried out by the methods proposed by Chebyshev, Ozol, Somov - Malyshev and Reshetov [4,5]. At the same time, redundant links in the lever mechanisms are also determined. In addition, consideration of the zero degree of mobility of mechanisms is reduced to a special system, which is called Assur groups [4,5,6].

The mechanisms we are considering, articulated couplings, belong to a spatial articulated-lever mechanism. In Figure 2.1. the kinematic diagram of the articulated coupling is presented, which consists of a driving 1 and a driven 2 shafts, rigidly connected to the forks 3 and 4, two earrings 5 and 6 and connecting rods 7 and 8, that is, the mechanism consists of 6 movable links interconnected 8-and rotational kinematic pairs of the fifth class. Using the Somov-Malyshev formula [4,5], it is possible to determine the degree of mobility of the considered articulated coupling:

$$W = 6n - 5P_5 \quad (2.1)$$

where n - is the number of moving links, P_5 is the number of kinematic pairs of the fifth class.

Analysis of the kinematic scheme shows that the degree of mobility of the considered mechanism is equal to one, has one generalized coordinate. In addition, it is known [10] that the mechanism acquires an extra degree of mobility in the case of the intersection of the axes of two pairs of the fifth class or the location of these axes in parallel. Therefore, when determining the degree of mobility of lever mechanisms under the above conditions it is considered expedient to take into account excess connections in the mechanism, then according to [4,86] we have:

$$W = 6n - 5P_5 + q \quad (2.2)$$

where, q - is the number of redundant links.

Taking into account the fact that $W = 1$, $n = 6$, $P_5 = 8$, we can determine

$$q = W - 6n + 5P_5 = 5 \quad (2.3)$$

The resulting number of redundant bonds can also be determined using the Ozol formula [4]

$$q = W + 6k - f = 1 + 6 \cdot 2 - 8 = 5 \quad (2.4)$$

where, k - is the number of independent circuits in the mechanism, f - is the total number of mobility, or the number of kinematic pairs of the fifth class.

In a rectangular spatial coordinate system $OXYZ$, the X axis is directed parallel to the axis passing through the centers of the forks of shafts 1 and 2, the Y axis is perpendicular to the drawing plane, and the Z axis is perpendicular to the plane of the intermediate links. In this case, the designations of linear and angular mobility of the kinematic pairs of the lever coupling (see Figure 2.1) are accepted: f_x, f_y, f_z - linear displacements along the axes X, Y, Z ; f_x^1, f_y^1, f_z^1 - angular displacement along the axes X, Y, Z . Shafts 1 and 2 do not have linear mobility along the X axis, since they have rotational kinematic pairs of the fifth class with a rack.

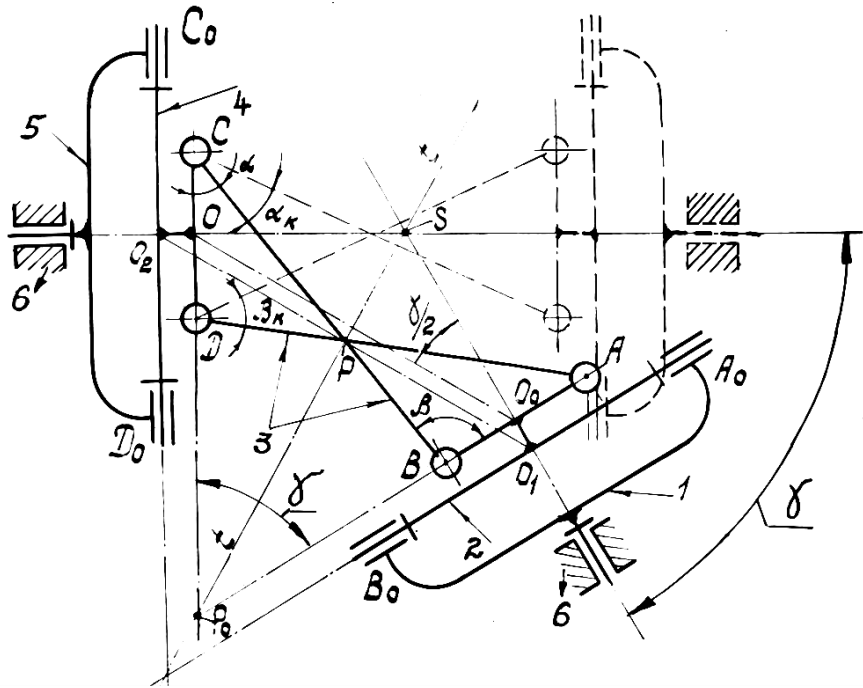


Fig.2.1. Kinematic diagram of the articulated coupling

Thus, two more kinematic pairs of the fifth class do not have linear movements along the Y axis and four kinematic pairs of the fifth class do not

have non-linear movements along the Z axis . Thus, it should be noted that in the mechanism there are no kinematic pairs having linear mobility f_x, f_y, f_z equal to zero. The driving and driven shafts 1 and 2 have angular mobility to the X axis . The replacement of the missing linear mobility along the X axis with angular mobility is carried out due to the reciprocating movement of the points O and O_o , the axes passing through the hinges A and B, C and D earrings 2 and 4 are mixed relative to the axis of the forks A_o, B_o and C_o, D_o , while $OO_o < OO_1$ and $O_1O_o = O_2O$ [87]. Such an arrangement of the axes s allows a change in the distance between O_1 and O_2 , the above conditions are met. So, one mobility f_x is used to close the circuit, and the second is the mobility of the mechanism. Angular mobility relative to the axis $f_z=2$. In this case, the Z axis is directed parallel to the axes of the forks of the shafts. Angular movements around the Y axis , $f_y \u003d y$, since the axes of the hinged joints of the connecting rods with the earrings are parallel to the Y axis . In this case, the missing linear movements along the X, Y and Z axes are replaced by angular movements about the Y and Z axes . Then four angular mobilities are used, one to replace f_x , one to replace f_z , and two to close the circuit. Also mobilities $f_z=2$, one is used to replace f_y and one for closing the circuit of the articulated coupling mechanism. It has been established from the analysis that the articulated coupling mechanism under consideration no longer has redundant connections, $q = 0$.

Table 2.1 presents the characteristics of the structure of the mechanisms of articulated couplings, various versions. According to the first scheme of the articulated-lever clutch, the excess connection according to formula (2.3) is equal to five, and taking into account the replacement of mobility and analysis of the scheme of the mechanism, in fact, the excess connection $q = 0$.

In the second scheme of the articulated-lever coupling (see Table 2.1, 2nd line), two pairs of levers (rods) are used . For this mechanism, redundant connections:

$$q = W + 6n - f = 1 + 12 - 10 = 3$$

It should be noted that with four connecting rods (2-circuit) of the mechanism, excess connections $q = 3$. The source of excess connections is the connecting rod levers of the articulated coupling contours, forming in the same plane between themselves and with the earrings with parallel rotational pairs. At the same time, the connections imposed by paired connecting rods are repeated, and some of them are redundant. At reducing the contours (one pair of connecting rods) eliminates excess connections, $q = 0$ (see table . 2.1, 3rd line).

In the following kinematic diagram of the lever-articulated clutch mechanism, three links and three rotary kinematic pairs of the fifth class, which leads to the elimination of redundant connections (see table 2.1, 4th line).

To reduce excess links in the lever-hinge coupling, elastic links are included between adjacent links, in the form of one spring between the connecting rods (5-line, tab 2.1), in the form of three springs between the connecting rods, between opposite rotational kinematic pairs and between the right connecting rod with an earring, (6-line, table 2.1). In addition, rotational pairs of the fifth class can be made composite, including elastic bushings (7-line, Table 2.1). According to the existing calculation method, the excess connections in these articulated couplings will be $q = 3$

2.2 . Structural Analysis of Swivel Couplings with Elastic Elements

In the general theory of mechanisms and machines, each elastic link available in a mechanism increases the degree of mobility by one. The influence of elastic bonds in mechanisms at the determination of the degrees of mobility of mechanisms was not taken into account. Thus, when using rotary kinematic pairs as composite ones, they are also not taken into account when determining the degree of mobility of the lever-articulated coupling of the cardan mechanism. It should be noted that the inclusion of elastic elements in the system reduces the excessive connections of the mechanism. Therefore, a new

formula is proposed for determining the degree of mobility of articulated-lever mechanisms, taking into account elastic elements:

$$W = 6n - 5P_5 + n_y + q \quad (2.5)$$

where, n_y is the number of elastic links between links and kinematic pairs, as well as elastic elements in composite kinematic pairs.

For a lever-articulated coupling shown in Figure 2.2, we determine the degree of mobility according to (2.5):

$$W = 6 \cdot 8 - 5 \cdot 10 + 1 + q = 1 \quad (2.6)$$

As seen from Figure 2.2 that the mechanism has one degree of freedom. Therefore, from (2.6) one can determine the number of redundant connections.

$$q = W - 6n + 5P_5 - n_y = 1 - 48 + 50 - 1 = 2$$

This means that one elastic bond reduces the number of redundant bonds by one. Therefore, in order to eliminate redundant connections in lever-articulated couplings, the following condition is necessary:

$$q = n_y;$$

Then, taking into account the inclusion in the mechanism of the required number of elastic elements, it is possible to eliminate redundant connections, $q = 0$.

Wherein:

$$W - 6n + 5P_5 - n_y = 0 \text{ or } n_y = W - 6n + 5P_5 \quad (2.8)$$

For the mechanism under consideration (see .p and 2.2) $n_y = 3$.

Taking into account the proposed formulas (2.5) and (2.8), we can transform the Ozol formula [4] to the following form:

$$q = W + 6k - f - n_y \quad (2.9)$$

where, K - is the number of independent circuits in the articulated coupling, for the case under consideration, $k = 2$; $f = 10$; $n_y = 3$; $q = 0$.

Figure 2.3 shows a diagram of a lever-articulated coupling with composite rotational kinematic pairs. For this mechanism, without taking into account elastic elements in kinematic pairs;

$$q = W - 6n - 5P_5 = 1 - 6 \cdot 8 - 5 \cdot 10 = -3$$

into account the elastic elements in the three rotational kinematic pairs of the coupling, taking (2.5) and (2.9) we have:

$$n_y = W - 6n + 5P_5 = 1 - 6 \cdot 8 + 5 \cdot 10 = 3$$

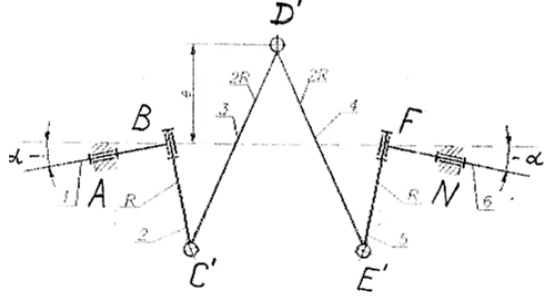
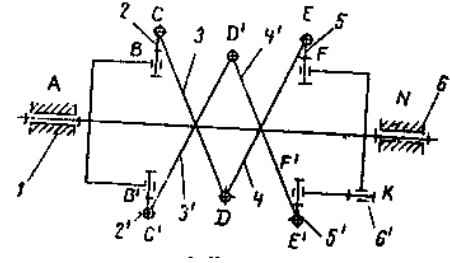
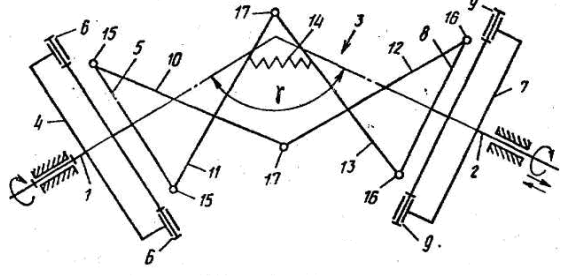
$$\text{or } q = W - 6n + 5P_5 - n_y - q = 1 - 6 \cdot 8 + 5 \cdot 10 - 3 - 0 = 0$$

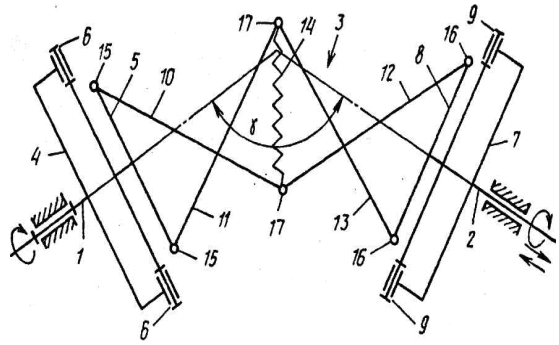
$$q = W + 6k - f - n_y = 1 + 6 \cdot 2 - 10 - 3 = 0$$

Table 2.1. Structural characteristics of hinged couplings

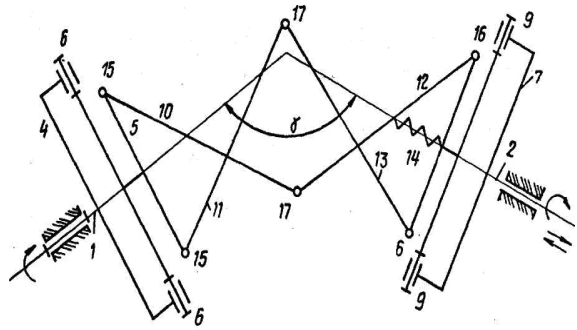
No	Scheme of articulated couplings	n	P5	k	W	q	Linear movements			Angular movements		
							f_{x-}	f_y	f_{z-}	f'_x	f'_y	f'_z
1		6	8	2	1	5/0	$\frac{0}{f'_x \rightarrow 1}$ $f'_y \rightarrow 1$	$\frac{0}{f'_z \rightarrow 1}$	$\frac{0}{f'_y \rightarrow 1}$	$\frac{2}{1}$	$\frac{4}{2}$	$\frac{2}{1}$
2		8	10	2	1	3/0	$\frac{0}{f'_y \rightarrow 2}$	0	$\frac{0}{f'_y \rightarrow 2}$	$\frac{2}{2}$	$\frac{6}{2}$	$\frac{2}{2}$

Continuation of table 2.1

							$\frac{0}{0}$	$\frac{0}{f'_y \rightarrow 1}$	$\frac{0}{f'_z \rightarrow 1}$	$\frac{0}{f'_y \rightarrow 1}$	$\frac{2}{2}$	$\frac{3}{1}$	$\frac{2}{1}$
		le v e n	3				$\frac{0}{0}$	$\frac{0}{f'_y \rightarrow 2}$	$\frac{0}{f'_z \rightarrow 2}$	$\frac{0}{f'_y \rightarrow 2}$	$\frac{3}{3}$	$\frac{6}{2}$	$\frac{4}{2}$
		0					$\frac{3}{3}$	$\frac{0}{f'_y \rightarrow 2}$	$\frac{0}{f'_z \rightarrow 1}$	$\frac{0}{f'_y \rightarrow 2}$	$\frac{2}{1}$	$\frac{6}{2}$	$\frac{2}{2}$



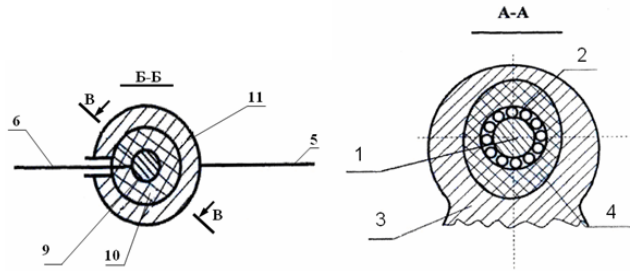
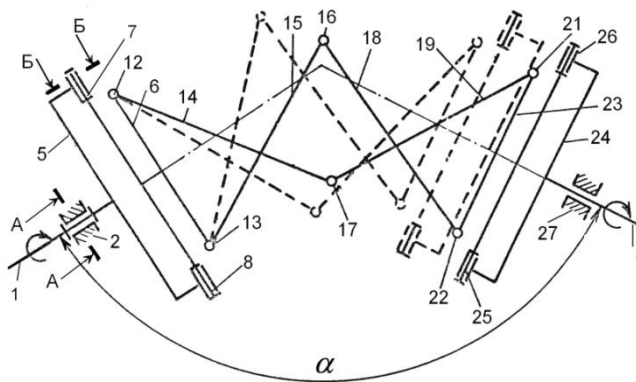
b



V

0

$\frac{3}{3}$	$\frac{0}{f_y' \rightarrow 2}$	$\frac{0}{f_z' \rightarrow 1}$	$\frac{0}{f_y' \rightarrow 2}$	$\frac{2}{1}$	$\frac{6}{2}$	$\frac{2}{1}$
---------------	--------------------------------	--------------------------------	--------------------------------	---------------	---------------	---------------



0

$\frac{3}{3}$	$\frac{0}{f_y' \rightarrow 1}$	$\frac{0}{f_z' \rightarrow 1}$	$\frac{0}{f_y' \rightarrow 2}$	$\frac{2}{1}$	$\frac{6}{2}$	$\frac{2}{1}$
---------------	--------------------------------	--------------------------------	--------------------------------	---------------	---------------	---------------

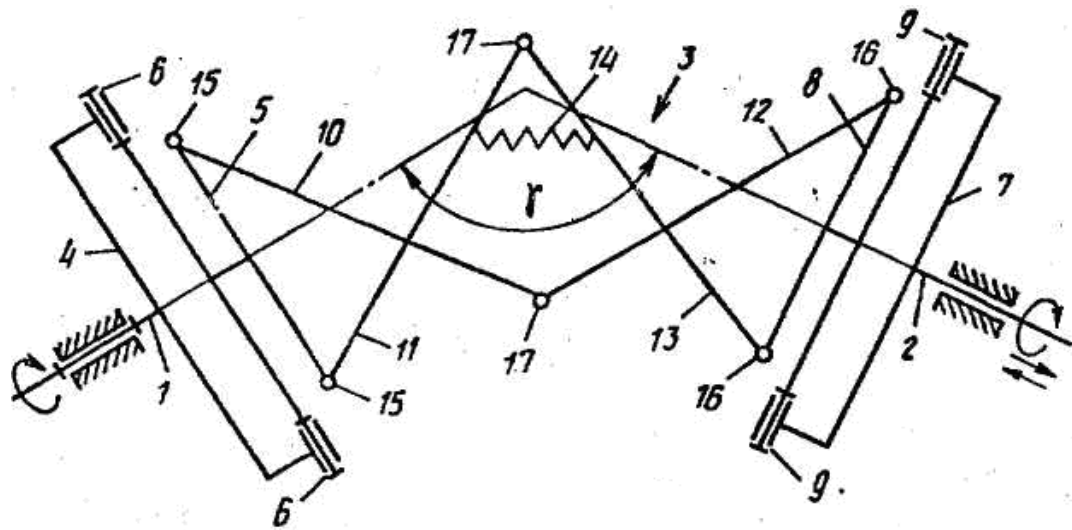


Figure 2.2 Lever-articulated couplings with elastic links between the levers

Thus, the proposed method of including the required number of elastic elements in the lever-hinge couplings made it possible to eliminate excessive connections.

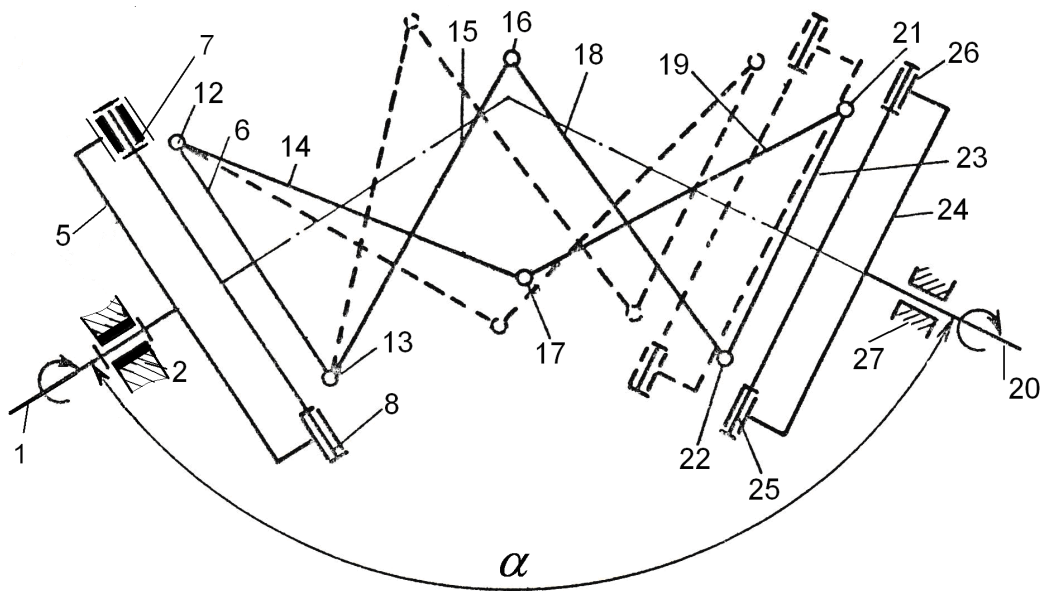


Figure 2.3. Lever-hinge coupling with compound rotational kinematic pairs and elastic elements

2.3. Metric mechanism analysis

A distinctive feature of the mechanism under consideration is the composite hinges with elastic elements. During the operation of the articulated coupling, these elastic elements are deformed, thereby leading to a change in positions, as well as to an increase or decrease in the length of the links of the mechanism.

The main task of the metric analysis of the proposed articulated coupling is to determine the distance between the centers of the articulated joints of the drive and driven shafts with earrings, as well as the choice of the length of the earrings and levers (rods) of the lever-articulated coupling, taking into account the maximum values of deformations of the elastic elements of the composite hinges.

To solve the problem, the axes of the shafts of the mechanism are located in the same plane (see Figure 2.4.) with a deviation from the axis 0-0, respectively, at angles α_1 and α_2 , with the possibility of their symmetrical change from 0° to 90° in such a way that the hinges D_1 and E earrings rested in extreme straight positions between themselves.

We take the length of the earrings as the initial size $l_{DD_1} = l_{EE_1} = 2R$. To determine the distance between the centers of the hinged joints of the driving and driven coupling halves with earrings, perpendiculars to the 0-0 axis are drawn from points D_1 and E_1 , which intersect it at points K_1 and K_2 . It should be noted that composite hinges with elastic elements can be installed both in the driving and driven shafts, as well as in the rotational hinges of the earrings. For example, consider composite hinges at points A and D_1 of a lever-articulated coupling.

In this case, due to deformations of the elastic sleeve in the hinge A, its position at the point C_1 changes; we will denote them through the points C_1' and

C_2' . In this case, the distances are the minimum values of displacements at the maximum deformation of the bushings at point A. In a similar way, points $C_1C_1' = C_1C_2''$ and \mathcal{D}_1'' can be designated \mathcal{D}_1' , which are obtained due to the deformation of the elastic sleeve at point A. In this case, due to the deformation of the elastic element of the composite hinge at point D_1 , the radius of the earring DD changes l_1 . Then, taking into account the maximum deformations of the elastic elements of the hinges at points A and D_1 , we can write:

$$X_1 = C_1K_1 = C_1\mathcal{D}_1 \sin \alpha_1 = R_1 \sin \alpha_1;$$

$$X_1' = C_1'K_1' = C_1'\mathcal{D}_1' \sin \alpha_1 = (C_1'C_1 + C_1\mathcal{D}_1') \sin \alpha_1 = (R_1 + \Delta\mathcal{D}_1) \sin \alpha_1;$$

$$X_1'' = (R_1 - \Delta\mathcal{D}_1) \sin \alpha_1, \quad X_2 = R_2 \sin \alpha_2 \quad (2.10)$$

Then the distance between the centers of the hinged connections of the driving and driven shafts with sergs C_1 and F in the absence of deformation of the elastic elements of the composite hinges A and D_1 will be:

$$X = R_1 \sin \alpha_1 + R_2 \sin \alpha_2 + K_1K_2 \quad (2.11)$$

Now let's determine this distance at the minimum and maximum values of the radius of the earring C_1D_1 due to deformations of the elastic elements of the composite hinges at the points A and D_1 :

$$X_{max} = C_1'F = \sqrt{\Delta C_1^2 \cos^2 \alpha_1 + (R_1 \sin \alpha_1 + R_2 \sin \alpha_2 + K_1E_1 + \Delta C_1 \sin \alpha_1)^2};$$

$$X_{min} = C_1''F = \sqrt{\Delta C_1^2 \cos^2 \alpha_1 + (R_1 \sin \alpha_1 + R_2 \sin \alpha_2 + K_1E_1 - \Delta C_1 \sin \alpha_1)^2}$$

(2.12)

where, $\Delta C_1 = C_1'C_1 = C_1''C_1$ - is the value of the deformation of the elastic element at points A. The length of the earring DD_1 is determined by:

$$\text{at } \Delta C_1 = 0, \quad l_1 = l_{\mathcal{D}_1} = 2R_1;$$

$$\text{at } \Delta C_1 = C_1C_1'; \quad l_{1max} = \mathcal{D}'C_1' + C_1'\mathcal{D}_1' + \mathcal{D}_1'\mathcal{D}_0' = R + R_1 + \Delta\mathcal{D}_1 = 2R_1 + \Delta\mathcal{D}_1; \quad (2.13)$$

$$\text{at } l_{1min} = \mathcal{D}''C_1'' + C_1''\mathcal{D}_1'' - \mathcal{D}_1''\mathcal{D}_0'' = 2R_1 - \Delta\mathcal{D}_1;$$

where, ΔD_1 is the linear deformation of the elastic element of the composite hinge at the point D_1 . This means that the distance between the centers of the hinges of the shafts with shackles can be taken on average equal to the length of the shackles, but in this case it is necessary to sum up the value of the deformation of the elastic elements of the composite hinges in the zero dead

position, $\alpha_1 = \alpha_2 = \frac{\pi}{2}$ i.e. at $\frac{\pi}{2}$. The lengths of connecting rods DO_1 , EO , and D_1M , E_1M are determined using the design scheme of the articulated coupling shown in figure 2.5.

The length of the connecting rod EE_1 is determined from $\Delta EO_1E'$

$$l_{EO_1} = \sqrt{(EE')^2 + (O_1E')^2} \quad (2.14)$$

From $\Delta EFE'$ we have:

$$EE' = EF \cos \alpha_2 = R_2 \cos \alpha_2; \quad FE' = EF \sin \alpha_2 = R_2 \sin \alpha_2 \quad (2.15)$$

Then the distance O_1E' will be:

$$O_1E' = O_1F + FE' = \frac{1}{2}(R_1 \sin \alpha_1 + R_2 \sin \alpha_2 + K_1K_2) + R_2 \sin \alpha_2 \quad (2.16)$$

At the same time, substituting (2.15) and (2.16) into (2.14) we obtain:

$$l_{EO_1} = \sqrt{\frac{1}{4}(R_1 \sin \alpha_1 + R_2 \sin \alpha_2 + K_1K_2 + R_2 \sin \alpha_2)^2 + R_2^2 \cos^2 \alpha_2} \quad (2.17)$$

Consider $\Delta D_3D'O_1$ to determine the length of the lever TO_1 consider

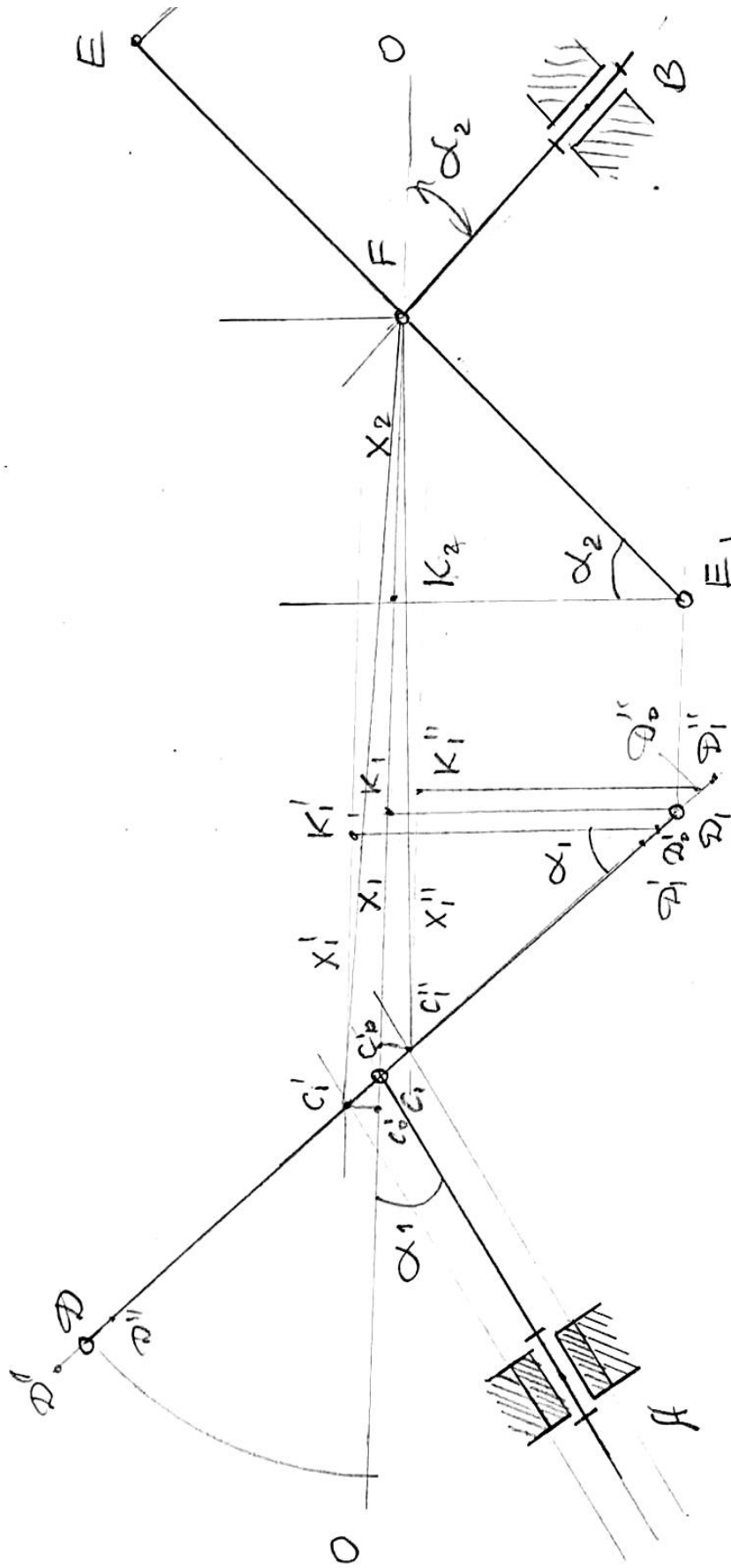


Figure. 2.4 Calculation scheme for metric analysis of a hinged coupling, taking into account the

$$\Delta D_3 D' O_1, \Delta D_3 D'' O_1$$

$$D_3 O_1 = O_1 F = \frac{1}{2} (R_1 \sin \alpha_1 + R_2 \sin \alpha_2 + K_1 K_2);$$

$$D'_3 O_1 = D'_3 O_1 + C_3 O_1 = (R_1 - \Delta D) \sin \alpha_1 + \frac{1}{2} (R_1 \sin \alpha_1 + R_2 \sin \alpha_2 + K_1 K_2);$$

$$D''_3 O_1 = D''_3 O_1 + C_1 O_1 = (R_1 - \Delta D) \sin \alpha_1 + \frac{1}{2} (R_1 \sin \alpha_1 + R_2 \sin \alpha_2 + K_1 K_2);$$

$$D' D'_3 (R_1 + \Delta D) \cos \alpha_1; D'' D''_3 (R_1 - \Delta D) \cos \alpha$$

$$\Delta D = \Delta D' = \Delta D''; \Delta D = \Delta C \quad (2.18)$$

Then the length of the lever DO_1 will be:

$$l_{DO_1} = l_{EO_1} = \sqrt{\frac{1}{4} (R_1 \sin \alpha_1 + R_2 \sin \alpha_2 + K_1 K_2 + R_1 \sin \alpha_1)^2 + R_1^2 \cos^2 \alpha_1}$$

(2.19)

In this case, the maximum $l_{D'O_1}$ and minimum values $l_{D''O_1}$ of the lever length TO_1 will be:

$$l_{D'O_1} = \sqrt{(R_1 + \Delta D)^2 \cos^2 \alpha_1 + \left[(R_1 + \Delta D) \sin \alpha_1 + \frac{1}{2} (R_1 \sin \alpha_1 + R_2 \sin \alpha_2 + K_1 K_2) \right]^2};$$

$$l_{D''O_1} = \sqrt{(R_1 - \Delta D)^2 \cos^2 \alpha_1 + \left[(R_1 - \Delta D) \sin \alpha_1 + \frac{1}{2} (R_1 \sin \alpha_1 + R_2 \sin \alpha_2 + K_1 K_2) \right]^2}$$

(2.20)

The analysis of the obtained expressions for determining the distance between the centres of the hinged joints of the driving and driven half-couplings shows that when $\alpha = 90^\circ$ ($\alpha_1 = \alpha_2$) the earrings DD_1 and EE_1 are located on the O-O axis and the maximum value of the distance between the axes will be equal to $(2R + \Delta D_1)$. This value in the calculations we get $2.04R$, and the minimum value is $1.95R$ at $K_1 K_2 \approx 0.02R$, $\Delta D_1 \approx 0.01R$. Table 2.2 shows the values l_{DO_1} , $l_{D'O_1}$, and $l_{D''O_1}$, and in Fig. 2.6. a are graphical dependences of the

change in the center-to-center distance as a function of the angle α . It can be seen from Table 2.2 that if the angle α is increased from 0° to 90° , then the value of the centre-to-centre distance changes from $1.95R$ to $2.055 R$. Choosing the optimal length of the distance between the centres of the hinged joints of the driving and driven coupling halves with earrings, taking into account the deformations of the elastic elements in the support A and in the hinge D_1 we produce from the following conditions:

Distance $C_1 F$ excluding deformations in the hinges A and D with $l_{C_1 F} < 2R + K_1 K_2$ and with an increase in α from 0° to 90° , the value $l_{C_1 F}$ changes from 0 to $2R$. For each value of α there corresponds a certain value of $l_{C_1 F}$. For the obtained values, $l_{C_1 F} = R \dots 1.9R$ the angle α is used within $30^\circ \dots 75^\circ$. At angle $\beta=0$, the mechanism goes into a dead position. When taking into account the deformation of compound hinges A and D, at $K_1 K_2 = 0$, $\Delta C_1 = 0.02R$, the smallest value of the centre distance length $l_{C_1 F}$ at $\alpha = 30^\circ \dots 75^\circ$ is $0.985 R \dots 1.88R$. Here, too, at the angle $\beta=0$, the mechanism goes into a dead position. In addition, at an angle $\alpha=90^\circ$ and $K_1 K_2 = 0$, the hinges E_1 and D_1 can rest against each other without reaching the O-O axis. An increase in the values of ΔC_1 and $K_1 K_2$ eliminates this situation. Then the dimensions of the hinges E_1 and D_1 must be less than the dimensions of the sum $\Delta C_1 + K_1 K_2$. Patterns of changes in the center distance of the earrings as a function of the angle α are shown in Figure 2.6. a, b.

Consider when the deformations in the composite hinge D_1 and A leads to an increase in the distance between the centers of the hinged connections of the driving and driven coupling halves with earrings. With a change in the angle α from 0° to 90° , the value $l_{C_1 F}$ is given in tables 2.2 and 2.3, as well as in fig. 2.6. a, b. In the range of angle α from 15° to 90° , the value $l_{C_1 F}$

is within $0.517R \dots 2.02R$. With an increase in the values of $K_1 K_2 \setminus u003d 0.02R$, the distance between the axes is within $(0.033 \div 2.072)R$

Then, at $\alpha = 90^\circ$, the earrings EE_1 and DD_1 are located on the axis $C'_1 F_1$ and the hinges E_1 and D'_1 in straight positions do not rest against each other. The range of the angle α depends on the angle β . When $\alpha = 90^\circ$ or $\beta = 0$, the mechanism passes the dead position. Therefore, it is advisable to choose the angle range within $\alpha = 30^\circ \dots 75^\circ$. Taking into account the linear deformations of the composite hinges D_1 and A the center distance between the earrings and the distance between the hinges D_1 and E_1 are recommended to be selected, $l_{C,F} = (2,08 \div 2.1)R$, $K_1 K_2 = 0,02R$.

It should be noted that with the correct choice of distance, $l_{C,F}$ the range of angle α from 0° to 90° also depends on the length of the levers (rods) of the articulated coupling. It is necessary to determine such values of the length of the clutch levers, at which the range of the angle α would be the largest. In this case, it is necessary to preserve the conditions for crossing levers in space, regardless of the range of angle α . To do this, we will draw up a diagram (see Fig. 2.5) by placing the hinge O_1 on the axis $O-O$ symmetrically to the hinges D_1 and E_1 without taking into account deformations in the composite hinges A and D_1 . Hinge O_1 , is the instantaneous center of rotation of hinges D_1 and E_1 with varying radii l_{DO_1} and l_{EO_1} . In this case, two symmetrically located triangles $DD_2 O_1$, and $EE' O_1$ are formed with side sizes that change with increasing angle α from 0 to 90° . Taking into account deformations in compound hinges A and D_1 , the actual length l_{DD_1} and l_{DO_1} varies depending on the angle α and the distance $K_1 K_2$.

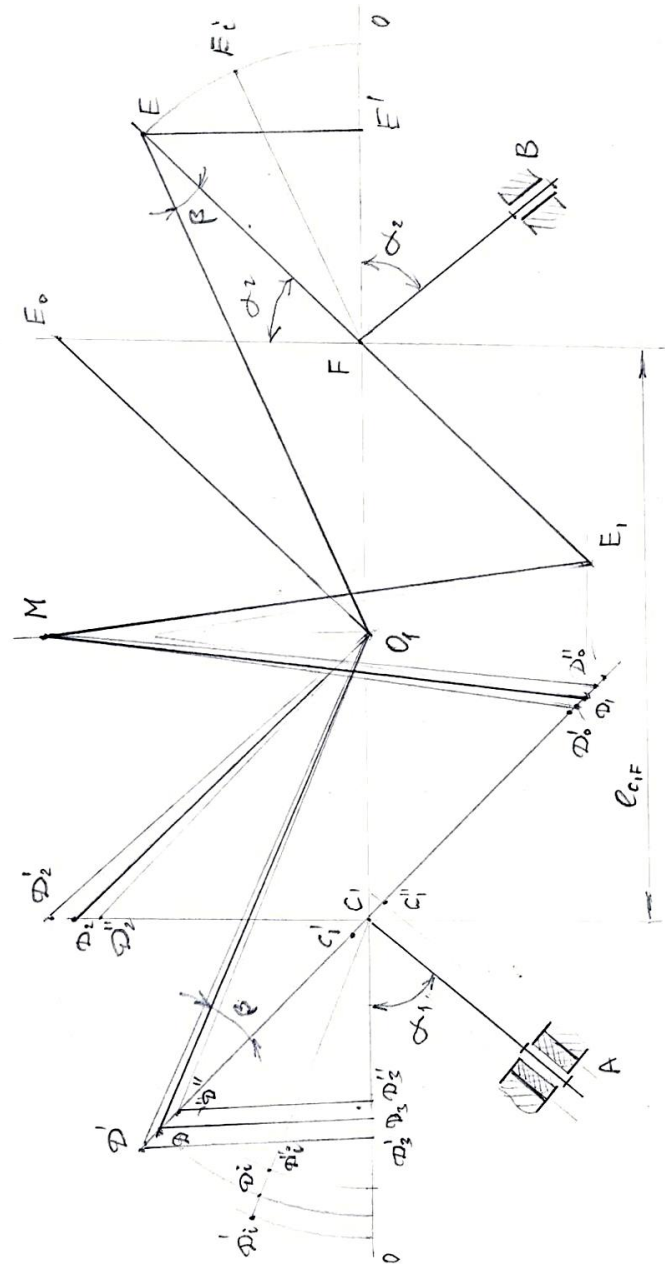


Figure. 2.5 Calculation diagram for determining the length of the levers of a lever-joint coupling with composite joints

Table 2.2. Estimated values of the length of the levers of the lever-hinge coupling

No.	α_1	α_2	$2l_{C_1D_1} = 2l_{E_1F}$	$l_{C_1O_1}$	l_{FO_1}	$l_{C_1'F}$	$l_{C_1''F}$	l_{C_1F}	ΔC_1	K_1K_2
1.	0	0	2R	0	0	0	0	0	0.02R	0
2.	15°	15°	2 R	0.25R	0.25R	0.517R	0.483R	0.5R	0.02R	0
3.	30°	30°	2 R	0.5R	0.5R	1.015R	0.985R	R	0.02R	0
4.	45°	45°	2 R	0.7R	0.7R	1.418R	1.382R	$\sqrt{2}$ R	0.02R	0
5.	60°	60°	2R	0.85R	0.85R	1.729R	1.671R	$\sqrt{3}$ R	0.02R	0

6.	75^0	75^0	2 R	0.95R	0.95R	1.92R	1.88R –	$\sqrt{1,9}$ R	0.02 R	0
7.	90^0	90^0	2R –	R	R	2.02R	1.98R –	2R –	0.02R –	0

Table 2.3. Estimated values of the length of the levers of the lever-hinge coupling

No.	α_1	α_2	$2l_{C_1D_1} = 2l_{E_1F}$	$l_{C_1O_1}$	l_{FO_1}	$l_{C_1'F}$	$l_{C_1''F}$	l_{C_1F}	ΔC_1	K_1K_2
1.	0	0	2 R	0.01 R –	0.01 R –	0.034R –	0.018R –	0.02 R –	0.04 R –	0.02 R –
2.	15_0	15_0	2 R	0.26R – –	0.26R – –	0.565R –	0.475R – –	0.52 R	0.04R – –	0.02R – –
3.	30_0	30_0	2 R	0.51R – –	0.51R – –	1.048R –	0.992 R –	1.02R –	0.04R – –	0.02R – –
4.	45_0	45_0	2 R	0.715R – –	0.715R – –	1.465R –	1.395R –	1.43 R	0.04R – –	0.02 R –
5.	60_0	60_0	2 R	0.865R – –	0.865R – –	1.77R –	1.69R –	1.73R –	0.04R – –	0.02 R –
6.	75_0	75_0	2R –	0.96R –	0.96R –	1.96R –	1.89R –	1.92R –	0.04R – –	0.02 R –
7.	90_0	90_0	2R –	1.01R –	1.01R –	2.072R –	1.99R –	2.02 R	0.04 R –	0.02R – –

According to the obtained analytical expressions (2.19), (2.20) in tables 2.4 and 2.5 show the calculated values of the length of the levers depending on the angle α and the distance K_1K_2 . On the basis of these calculations, graphical dependences of the change in the length of the levers $l_{D'O_1}, l_{DO_1}, l_{D''O_1}$ from the increase in the angle α were obtained for various values of $K_1K_2, \Delta C_1, \Delta D_1$, which are presented in Figure 2.7. a, b.

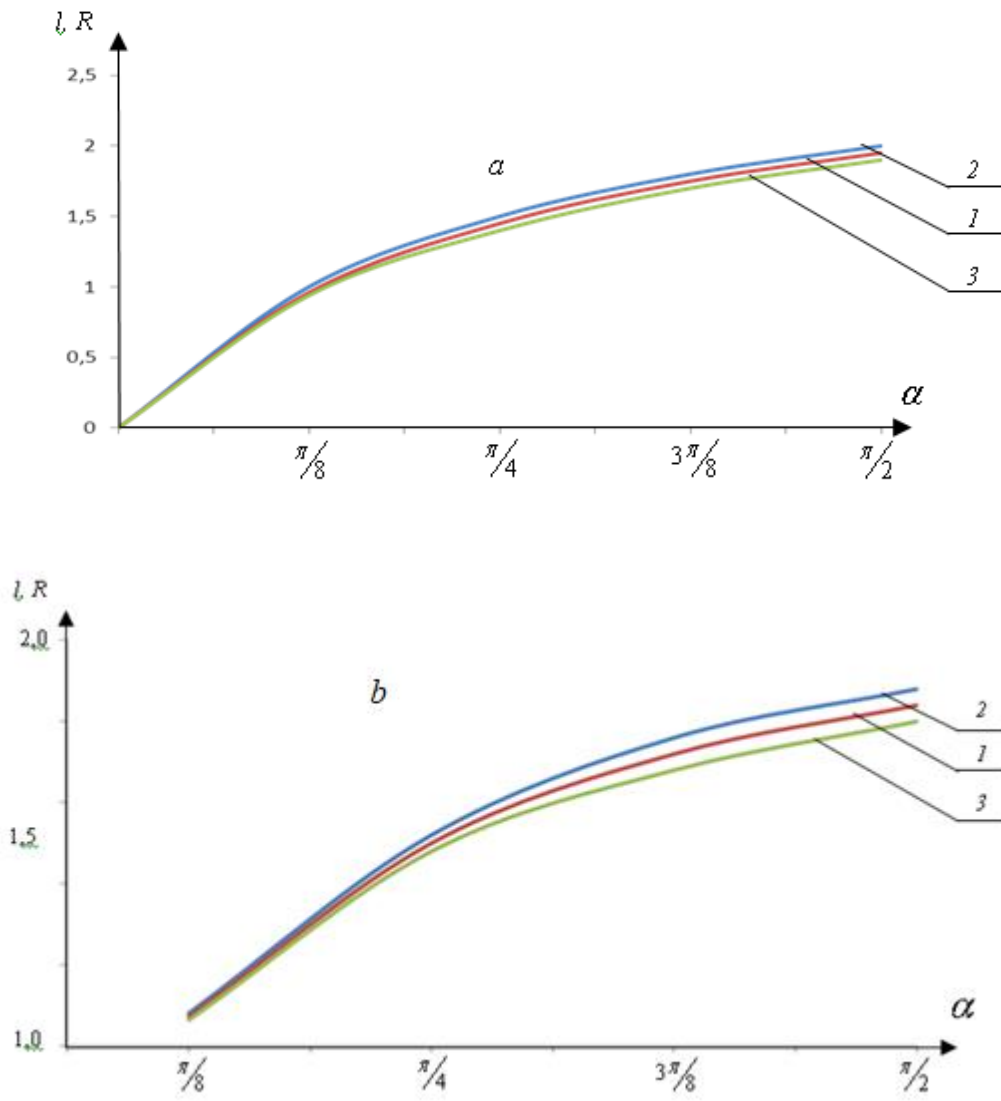


Figure 2.6. Dependences of the change in the distances between the hinges of the earrings of the driven and driving shafts, taking into account the compound hinges of the coupling.

g de, a - $K_1 K_2 = 0$;

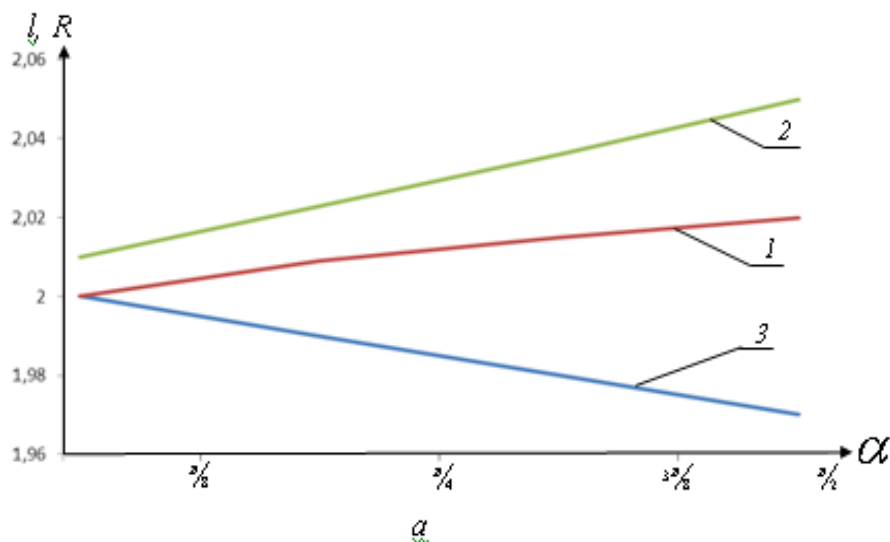
b - $K_1 K_2 \approx 0.02 R$.

Analysis of tables 2.4 and 2.5 shows that with an increase in the angle α from 0° to 90° , without taking into account deformations in hinges A and D_1 , the length $l_{C_1 D_1}$ will be equal to $2R$, and $l_{D_1 O_1}$ varies within $(2.001 \div 2.01)R$, a $l_{D_1' O_1} = (2.01 \div 2.055)R$ and $l_{D_1'' O_1} = (2.0 \div 1.95)R$ at $K_1 K_2 = 0.02 R$, $\Delta D_1 = 0, 01R$. With an increase in the values of deformation $\Delta C_1 = 0, 04 R$ and $\Delta D_1 = 0, 02 R$ and the distance $K_1 K_2 = 0.1R$ the maximum value of the lever DO_1 reaches at the

angle $\alpha = 90^\circ$, $l_{D'O_1} = 2.085R$, and the minimum value is obtained at the angle $\alpha = 90^\circ$, $l_{D''O_1} = 1.80R$. From the obtained graphs in Figure 2.7. it can be seen that with small values of deformations in the compound hinges A and D₁ and the distance $K_1 K_2$, the change in the length of the levers $l_{D'O_1}$, $l_{D'O_1}$ and $l_{D''O_1}$, from an increase in the angle α has patterns closer to linear, and with significant values of $K_1 K_1$,

Table 2.4. Estimated values of the length of the levers of the articulated coupling with composite joints

No.	α_1	α_2	$2l_{C_1D_1} = 2l_{E_1F}$	$l_{C_1O_1}$ $l_{F_1O_1}$	$\frac{\Delta C_1}{\Delta I}$	$\frac{\Delta I_1}{I_1}$	$K_1 K_2$	$l_{D''O_1}$	$l_{D'O_1}$	$l_{D'O_1}$
1.	0°	0°	2 R	0.02R _ _	0.025R _	0.01 R _	0.02R _ _	2.01 R	2.0 01R _	2.0 R
2.	15°_0	15°_0	2 R	0.27R _ _	0.025R _	0.01 R _	0.02 R _	2.015R _	2.0 02R _	1.99R _
3.	30°_0	30°_0	2 R	0.54 R _ _	0.025R _	0.01 R _	0.02R _ _	2.020R _	2.0 03 R _	1.98R _
4.	45°_0	45°_0	2 R	0.75R _ _	0.025R _	0.01 R _	0.02 R _	2.025R _	2.0 04 R _	1.97R _
5.	60°_0	60°_0	2 R	0.8 9 5R _	0.025R _	0.01 R _	0.02 R _	2.035R _	2.0 06R _	1.965R _
6.	75°_0	75°_0	2 R	0.995R _ _	0.025R _	0.01 R _	0.02 R _	2.045R _	2.0 08R _	1.96R _
7.	90°_0	90°_0	2R _	1.05R _ _	0.025R _	0.01 R _	0.02 R _	2.055R _	2.0 10R _	1.95R _



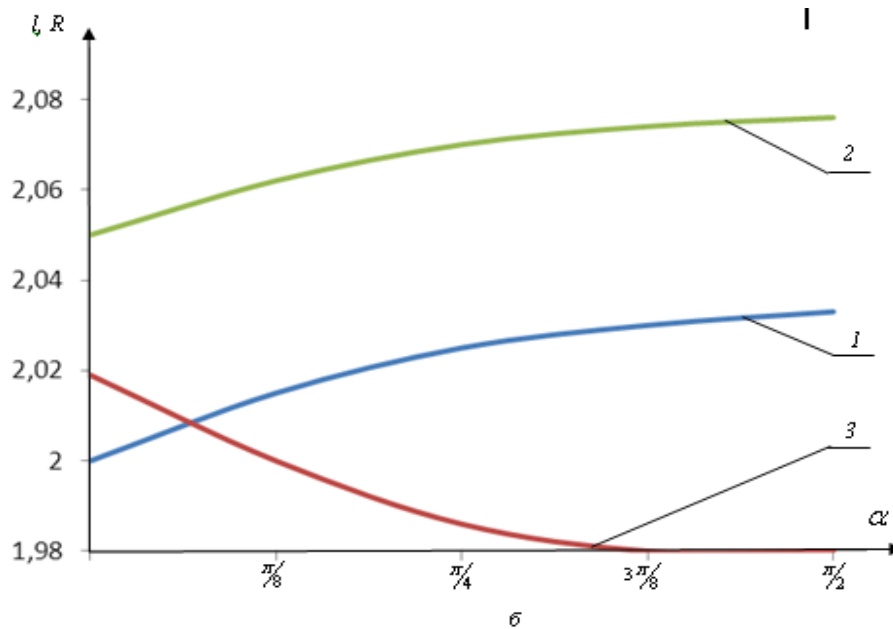


Figure 2.7. Dependences of the change in the length of the connecting rod of the articulated coupling with composite hinges with elastic elements

where a - at $K_1 K_2 = 0.02 R$; $\Delta C_1 = 0.025 R$; $\Delta D_1 = 0.01 R$

b - at $K_1 K_2 = 0, 1 R$; $\Delta C_1 = 0.04 R$; $\Delta D_1 = 0.02 R$

1- $l_{D'O_1} = f(\alpha)$; 2- $l_{D'O_1} = f(\alpha)$; 3- $l_{D'O_1} = f(\alpha)$;

Table 2.5. Estimated values of the length of the levers of the articulated coupling with composite joints

No.	α_1	α_2	$2l_{C_1D_1} = 2l_{E_1F}$	$l_{C_1O_1}$ $l_{F_1O_1}$	$\frac{\Delta C_1}{\Delta D_1}$	ΔD_1	$K_1 K_2$	$l_{D'O_1}$	$l_{D'O_1}, l_{E'O_1}$	$l_{D''O_1}$
1.	0	0	2R	0.05 R	0.0 4 R	0.02R	0.10 R	2.05 R	2.0 08R	2.0 15R
2.	15 0	15 0	2R	0.29 R	0.0 4R	0.02 R	0.10R	2,06R	2.0 11 R	2.0 1R
3.	30 0	30 0	2R	0.56R	0.0 4R	0.02 R	0.10R	2.0 65R	2.0 15R	2.00 R
4.	45 0	45 0	2 R	0.77R	0.0 4 R	0.02R	0.10R	2, 07 R	2.0 19R	1.95 R
5.	60 0	60 0	2 R	0.915 R	0.0 4 R	0.02R	0.10R	2, 0 7 5 R	2.0 22 R	1, 9 0 R
6.	75 0	75 0	2R	1, 05 R	0.0 4 R	0.02 R	0.10R	2, 08 R	2.0 22R	1,85R
7.	90 0	90 0	2 R	1.15R	0.0 4R	0.02 R	0.10 R	2.0 85R	2.0 3R	1, 8 0 R

$\Delta C_1, \Delta D_1$ these patterns are non-linear. As noted above, at the angle $\beta=0$ and $\alpha=90^\circ$, the mechanism goes into dead positions. At angles $\alpha=10^\circ \dots 75^\circ$

and angle $\beta > 0^\circ$, the articulated coupling mechanism is considered to be operational. Taking into account the deformations in the composite hinges A and D_1 , as well as the presence of the distance $K_1 K_2$ leads to an increase in length, that is, to an increase in the dimensions of the lever-articulated coupling. Therefore, in order to reduce the dimensions of the mechanism and ensure its operability, from the above conditions and analysis, it is recommended to choose the range of angle α within $10^\circ \dots 75^\circ$, $\beta > 0^\circ$, the center distance between the centers of the hinged joints of the driving and driven coupling halves with earrings $(2.08 \div 2.1)R$, the length of the levers $l_{DO_1} = l_{D_1M} = l_{EO_1} = l_{E_1m} = 2R$ at a distance $K_1 K_2 = (0.04 \div 0.1)R$ at the values of deformation $\Delta C_1 \leq 0.04R$ and $\Delta D_1 \leq 0.02R$.

From this section, the following conclusions can be drawn:

- a structural analysis of spatial lever-articulated couplings with one and two closed circuits was carried out. The technique of liquidation of redundant connections in lever-hinge couplings is determined;

- a new structural formula is recommended for determining the degree of mobility of lever-hinge couplings, taking into account excess bonds and elastic bonds in the mechanism. A technique has been developed for the elimination of redundant links in the spatial mechanisms of lever-hinge couplings, based on the inclusion of elastic links, the number of which is equal to the number of redundant links in the mechanism. It is recommended that elastic connections are established between links, hinges, and are also made in the form of composite hinges with elastic elements;

- An analytical method has been used to obtain formulas for determining the distance between the centers of the articulated joints of the driving and driven shafts with earrings in the absence of deformation in the composite hinges and the distance between the hinges in the zero dead position. Formulas are obtained for determining the maximum and minimum values of the interaxial

distance between the hinges in the presence of deformations in the composite hinges and the distance between the hinges of the levers in the dead position;

- Graphical dependences of the change in the distance between the centers of the swivel joints of the driving and driven half-coupling with earrings as a function of the angle of divergence between the shafts of the mechanism have been obtained. It was revealed that to ensure the operability of a lever-articulated coupling with composite hinges in the support of the driven shaft and between the earring and the lever at angles $\alpha = 30^\circ \dots 75^\circ$ and $K_1 K_2 = 0.02 R$, it is recommended to choose the center distance between the centers of the mechanism's earrings in within $(2.08 \div 2.1) R$, and in the absence of deformations in the hinges and $K_1 K_2 = 0$, a center distance of $2 R$ is proposed;

- Formulas were obtained for determining the length of the levers, taking into account the deformation in the compound hinges and the distance $K_1 K_2$ and without them. Graphical dependences of the change in the length of the levers as a function of the angle of divergence between the shafts of the lever-articulated coupling are constructed. It has been established that in order to reduce the dimensions of the mechanism and ensure its operability, it is recommended to choose the range of angle α within $10^\circ \dots 75^\circ$, the angle between the earring and the lever $\beta > 0^\circ$, the length of the levers to be equal to the length of the mechanism's earrings and the distance between the hinges of the earrings in the axial direction $K_1 K_2 = (0.04 \div 0.1) R$ at deformations of elastic elements of composite hinges $\Delta C_1 \leq 0.04R$ and $\Delta D_1 \leq 0.02 R$.

3. KINEMATIC AND DYNAMIC ANALYSIS OF A LINKAGE COUPLING

The articulated-lever coupling [81,82,83], without elastic elements, ensures the synchronous movement of the coupling halves. Therefore, the transfer function between the driving and driven shaft of the lever-articulated clutch is equal to one. With an increase in the angle of deviation of the axes of rotation of the shafts of the half-couplings from the horizontal axis, it leads to rapid wear of the hinged bearings. In this case, the transfer function between the shafts of the coupling halves will gradually differ from unity. This leads to a change in the speed and load changes of the drive shaft and, accordingly, the drive motor, which is undesirable.

The proposed new design of the lever-articulated clutch provides the necessary uneven speed and load in the drive shaft of the clutch due to elastic hinges [84,85]. In this case, on the driven shaft, the unevenness of the angular velocity and load changes will be large, corresponding to the patterns of external perturbation. Therefore, to ensure the necessary speed and load modes of operation of the lever-articulated clutch, kinematic and dynamic studies of the recommended lever-articulated clutch with hinges having elastic elements were carried out. The results of the research carried out allow the expansion of the theory of cardan mechanisms.

3.1. Kinematic analysis of a lever-hinge coupling with elastic elements.

3.1.1. Analysis of the positions of the links of the mechanism.

According to the results of a structural study of a lever-articulated coupling with hinges having elastic elements, it was revealed that the degree of mobility of the mechanism is equal to one.

Elastic elements make it possible to eliminate excessive connections in the mechanism. In the kinematic analysis of the recommended lever-articulated coupling, the following are determined: - the position of the fork relative to the earrings of the mechanism;

- the position of the connecting rods (levers) relative to the earrings;
- the position of the earrings and connecting rods relative to the axis of rotation of the shafts.

In this case, the initial parameters are:

the distance between the centers of the hinges of the forks of the half-couplings of the mechanism, the length of the forks, earrings and connecting rods (levers, the angle between the axes of the shafts and the horizontal line). For kinematic analysis, we use the method [86,87,88] recommended for a coupling without elastic elements. It is known that both half-couplings are symmetrical, the presence of elastic elements in the hinges of the driven half-coupling is distinctive. Therefore, the determination of the positions of the links of the lever-articulated clutch is carried out for the driven half of the mechanism. In this case, the average values of the positions of the links of the driven half-coupling will be identical to the values of the positions of the links of the leading half-coupling.

In the initial position (vertical) of the coupling at $\varphi = 0$ (see Fig. 3.1), the deviation of the driven shaft of the coupling in the XOY plane from axes $O - O$ through the angle α , leads to the rotation of the half-coupling fork by an angle ξ relative to its axis. In this case, the connecting rod, the earring and the shaft with the fork lie on different planes at an angle α . Therefore, the angle of rotation of the fork relative to its axis will also be equal to this angle. With the horizontal position of the mechanism $\varphi = \pi/2$, the connecting rod, earring, fork and half-coupling shaft are in the XOY ($\alpha=0$) plane . In this case, the angle of rotation of the fork ξ relative to its axis will be equal to zero. From Figure 3.1 it can be seen that when the elastic element of the driven shaft support is deformed, its

maximum value will be when the shaft axis is moved parallel. Then the axes $O - O$, $O_1 - O_1$ and $O_2 - O_2$ will be approximately parallel, in view of the fact that the amount of deformation will be insignificant in relation to the distance between the axes of the hinges of the half-coupling forks. In doing so, we have:

$$BB_1 = BB_2; C_1R_1 = C_2R_2 = CP; EE_1 = BB_1 + \Delta E;$$

$$EE_2 = BB_2 - \Delta E$$

where, BB_1 , BB_2 - the maximum values of the deformation of the elastic element of the support of the driven shaft of the coupling half; ΔE - maximum values of deformation of the elastic element of the hinge at point E.

The limit values for the length of the fork are determined, as noted in chapter 2 of the dissertation, we can write:

$$l_1 = BE_1 = BE + \Delta E = l_{BE} + \Delta E;$$

$$l_2 = B_2E_2 = BE - \Delta E = l_{BE} - \Delta E \quad (3.1)$$

where, l_{BE} - half the length of the fork of the driven half-coupling.

As noted above, in a vertical position $\varphi = 0$, the location of the shaft relative to the axis $O-O$ is equal to the angle of rotation of the fork around its axis $\alpha = \xi$. With the horizontal position of the coupling fork $\varphi = \pi/2$, the driven shaft with the yoke lies on the XOY plane. To determine the dependencies between the angles α , ξ and φ the condition [88] is used that in the initial vertical position of the fork of the clutch mechanism $\xi = \alpha$ and at the same time, taking into account the

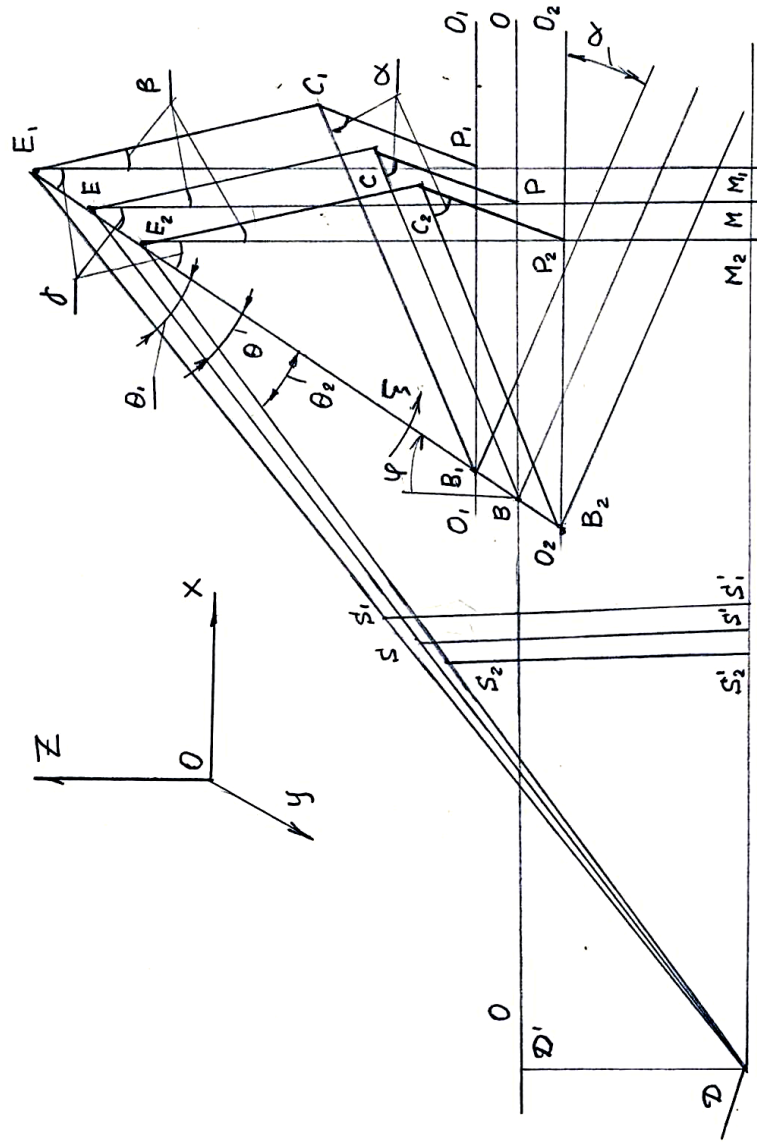


Figure. 3.1 Diagram of the driven coupling half, taking into account the elastic elements in the hinge E and the shaft support.

length of the driven shaft, it is possible to determine in the XOY plane the distance of the shaft end from the $O-O$ axis by the value, $l_e \sin \alpha$, then we have

$$\frac{l_e \sin \xi}{l_e \sin \alpha} = 1, \quad \sin \xi = \sin \alpha$$

When turning the driven shaft of the articulated coupling at an angle φ , ($\varphi = 0$), the initial position of the shackle is determined

$$l_{BE} \cos \varphi = l_{BE}; \quad \cos \varphi = 1$$

Then we have

$$\xi = \arcsin(\sin \alpha \cdot \cos \varphi) \quad (3.2)$$

into account the angular deformations of the elastic element of the driven shaft support, we can write:

$$\xi = \arcsin[\sin \alpha \cdot \cos(\varphi \pm \Delta\varphi)] \quad (3.3)$$

The obtained dependences of the angle change ξ according to (3.2) are presented in Figure 3.2. Analyzes show that at $\varphi = 0$, $\xi = \alpha$ and at $\varphi = \pi/2$, $\xi = 0$. With a full turn of the driven shaft, the angle of rotation of the fork ξ relative to the earring reaches twice the values α and 0.

Due to the deformation of the elastic element of the coupling, according to the obtained expression (3.3), it is possible to obtain graphical dependencies, which are shown in Figure 3.3. It can be seen from the graphs that for $\alpha = \pi/6$ and the phase shift $\Delta\varphi = \pi/36$ in graphs 1,2,3 is actually shifted by $\Delta\varphi$, and the nature of the change ξ remains unchanged. Therefore, the value of deformation of the elastic element allows the phase shift of the angle ξ by $\Delta\varphi$. So when $\varphi \pm \Delta\varphi = \frac{\pi}{2} \pm \frac{\pi}{36}$ in three positions $\xi \neq 0$, and when $\varphi \pm \Delta\varphi = \pi \pm \frac{\pi}{36}$, angle $\xi = \pi/6$ (see Fig.3.3). To determine the position of the earring and the connecting rod relative to the X-axis of the coupling, the values of the angles β and are required θ .

From $\triangle EPB$ we get :

$$l_{EP} = l_{EB} \cos \varphi \sqrt{1 + tg^2 \varphi \cos^2 \alpha} ; \quad \beta = \arccos \sqrt{1 + tg^2 \varphi \cos^2 \alpha} \quad (3.4)$$

Where, $l_{EC} = l_{EB} \cos \varphi$; $l_{CP} = l_{EB} \sin \varphi \cos \alpha$;

in this case, taking into account the value of the deformation of the elastic element of the coupling, we have $l_{EP} = l_{E_1P_1} = l_{E_2P_2}$.

To determine the position of the earring relative to the connecting rod from $\triangle DME$ and $\triangle BPE$, we have:

$$\sin(\theta + \gamma) = \frac{l_{MD}}{l_{ED}} = \frac{l_{SD} + l_{MS}}{l_{ED}} = \frac{1 + \sin \alpha \cdot \sin \varphi}{2}$$

$$\theta = \frac{1 + \sin \alpha \cdot \sin \varphi}{2} - \gamma \quad (3.5)$$

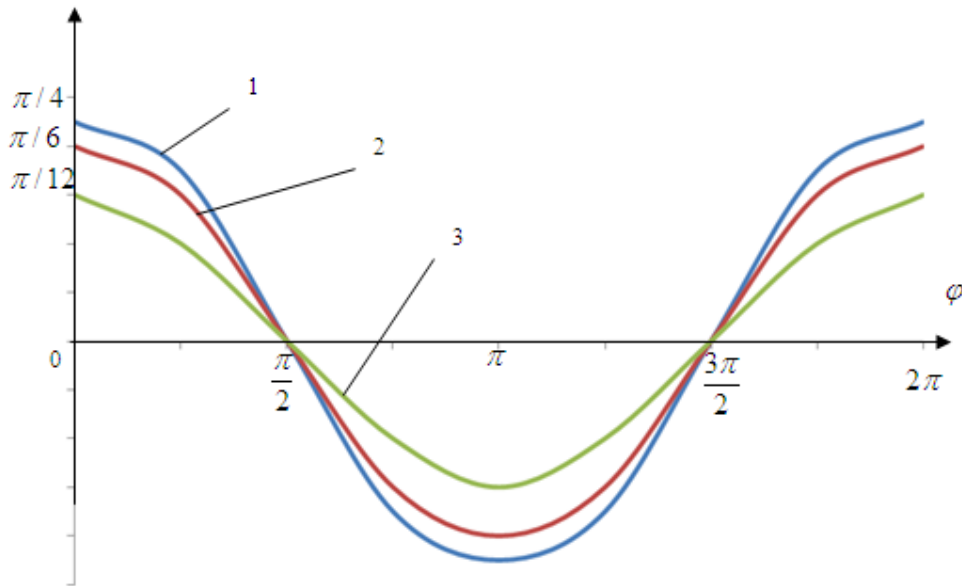
or

From fig. 3.1 it can be seen that, taking into account the deformation of the elastic element, the length DE and the angle change θ . In this case, taking into account (2.20), we have:

$$\theta = \arcsin \frac{l_{S_1D} + l_{M_1S'_1}}{l_{E_1D}} - \gamma =$$

$$= \arcsin \frac{l_{S_1D} + l_{M_1S'_1}}{\sqrt{(l_{EB} + \Delta l_{EB})^2 \cos^2 \alpha + \left((l_{EB} + \Delta l_{EB}) \sin \alpha + \frac{1}{2} (2l_{EB} \sin \alpha + K_1 K_2) \right)^2}}$$

(3.6)



Where; 1-at $\alpha = \pi/4$; 2-at $\alpha = \pi/6$; 3-for $\alpha = \pi/12$

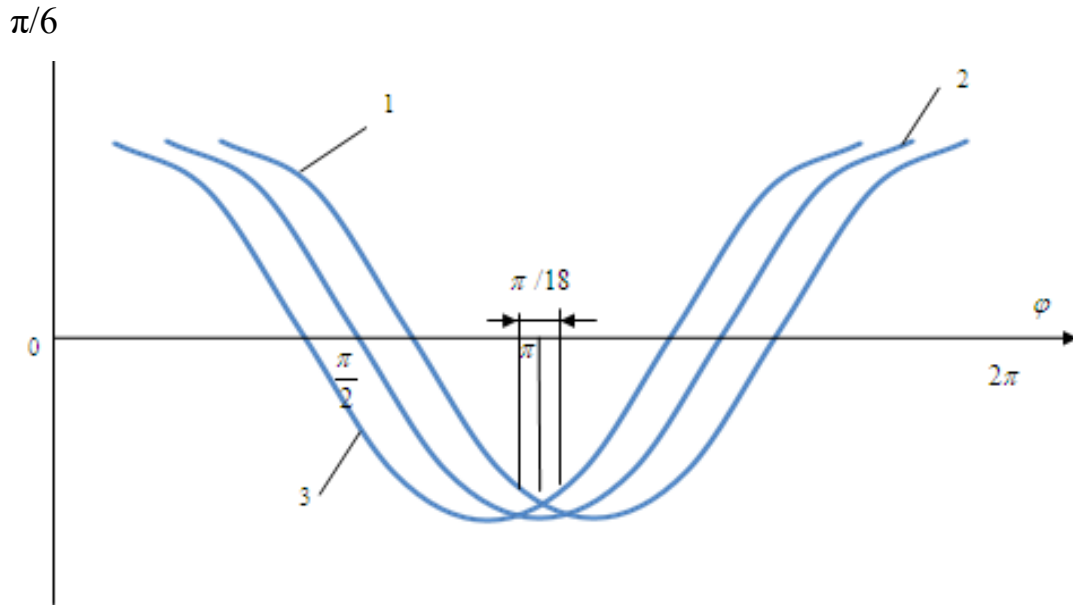
Figure 3.2 Dependences of the change in the angle of rotation of the fork as a function of the angle φ

The angle γ is determined from the expression:

$$\gamma = \arcsin \frac{l_{BP}}{l_{BE}} = \arcsin \frac{l_{BE} \sin \alpha \cdot \sin \varphi}{l_{BE}} = \arcsin(\sin \alpha \sin \varphi) \quad (3.7)$$

Then, taking into account (3.7), the expression for determining θ looks like:

$$\theta_1 = \arcsin \frac{l_{S_1D} + l_{M_1S_1'}}{\sqrt{(l_{EB} + \Delta l_{EB})^2 \cos \alpha + \left((l_{EB} + \Delta l_{EB}) \sin \alpha + \frac{1}{2} (2l_{EB} \sin \alpha + K_1 K_2) \right)^2}} - \arcsin(\sin \alpha \sin \varphi) \quad (3.8)$$



Where; 1-at $\Delta\varphi = \pi/36$; 2-at $\Delta\varphi = 0$; 3-at $\Delta\varphi = -\pi/36$ at $\alpha = \pi/6$

Figure 3.3. Dependences of the angle change ξ as a function of the angle φ , taking into account α and $\Delta\varphi$

Corner δ_1 which determines the position of the connecting rod, taking into account the deformation of the elastic element of the coupling, is determined from $\Delta DM_1 E_1$:

$$\delta_1 = \pi - (\theta_1 + \gamma)$$

or

$$\delta_1 = \pi - \gamma - \arcsin \frac{l_{S_1D} + l_{M_1S_1'}}{\sqrt{(l_{EB} + \Delta l_{EB})^2 \cos \alpha + \left[(l_{EB} + \Delta l_{EB}) \sin \alpha + \frac{1}{2} (2l_{EB} \sin \alpha + K_1 K_2) \right]^2}} +$$

$$+ 2 \arcsin(\sin \alpha \sin \varphi) \quad (3.9)$$

It is important to determine the position of the center of gravity of the connecting rod of the lever-articulated coupling. At the same time, it should be noted that due to the deformation of the elastic element in the hinge, the earrings with the connecting rod slightly affect the coordinates of the position of the center of gravity of the connecting rod.

$$\text{From figure 3.1. according } \Delta SDS \text{ to we have: } \sin \delta = \frac{l_{SS'}}{l_{SD}} = \frac{(l_{SS_2} + l_{S_2S'})}{l_{ED}};$$

Then

$$l_{SS_2} = \frac{l_{ED}}{2} \sin \gamma - l_{S_2S'} = \frac{l_{ED}}{2} \left\{ \sqrt{1 - \sin^2 \alpha \sin^2 \varphi} - \sin \left[\arccos \left(\frac{1 + \sin \alpha \sin \varphi}{2} \right) \right] \right\} \quad (3.10)$$

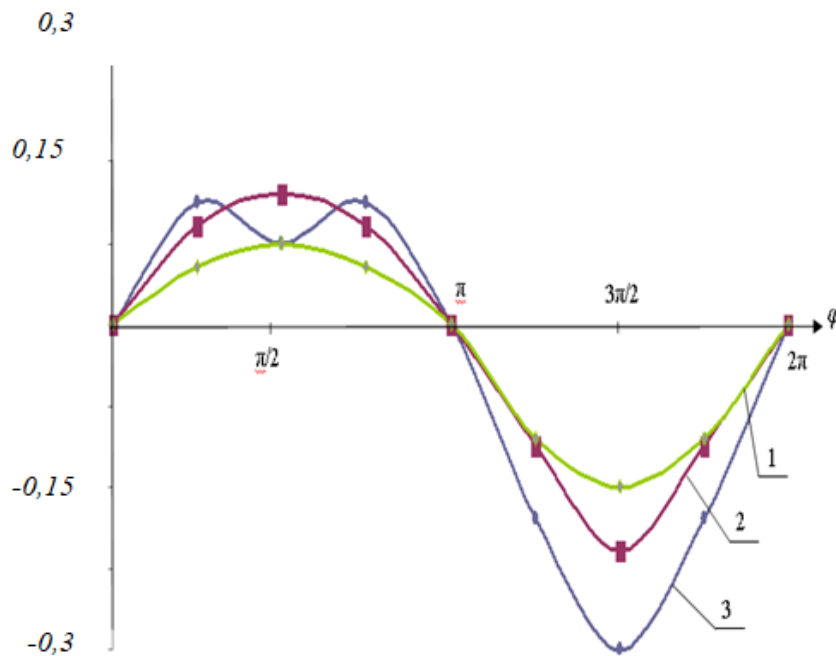
where, angle δ without taking into account the deformation of the elastic element of the coupling

$$l_{SS_2}, \left(R = \frac{l_{DE}}{2} \right)$$

$$\delta = \arccos \frac{1 + \sin \alpha \sin \varphi}{2}$$

The resulting graphical dependencies are shown in Fig.3.4. According to the above methodology, you can also determine the angles θ_2, δ_2 .

Thus, taking into account the deformation of the elastic elements of the lever-hinge coupling and the derived expressions (3.1), (3.3), (3.4), (3.7), (3.8), (3.9) and (3.10), we can determine the positions of the points of the links mechanism.



where 1 - at $\alpha = 15^0$; 2 - at $\alpha = 30^0$; 3 - at $\alpha = 45^0$;

Figure 3.4. Graphical dependences of the change in the position of the center of gravity of the connecting rod as a function of the angle φ with a variation in the angle of divergence of the shafts of the lever-articulated coupling.

3.2. Determination of the transfer function of a lever-articulated coupling, taking into account the elastic elements in the hinges of the mechanism

The transfer function of the articulated-lever coupling is determined by the ratio of the angular velocities of the driving and driven shafts. In the idle mode of movement of the articulated coupling, the pattern of change in the transfer function is mainly affected by the angle of inclination of the shafts relative to the horizontal line. The elastic elements in the hinges of the driven coupling half absorb fluctuations in the angular velocity of the driven shaft to some extent and therefore the angular velocity in the drive shaft will be smoother. In kinematic analysis, the influence of elastic elements on changes in

the angular velocity is taken into account due to deformations, thereby additional angular displacements of the links forming elastic hinges. In this case, the method for determining the angular velocities of the shafts of the articulated-lever coupling given in [32] is used. According to this work, the problem is solved using the Euler equations [91]. In the mechanism under consideration, the driven shaft is mounted on an elastic support, and the hinged connection of the earring with the connecting rod of the driven half-coupling also has an elastic element. Therefore, the point O_1 is fixed, and the point O_2 is mobile. Considering that the displacement of the point O_2 much less than the other points of the links of the half-coupling, we will also accept the point O_2 as fixed (see Fig.3.5). Points O_1 and O_2 are the centers of the forks and earrings of the coupling halves. We denote the coordinates of the points of the forks $O_1 X_{\epsilon_1} Y_{\epsilon_1} Z_{\epsilon_1}$ and $O_2 X_{\epsilon_2} Y_{\epsilon_2} Z_{\epsilon_2}$ and earrings $O_1 X_{c_1} Y_{c_1} Z_{c_1}$ and $O_2 X_{c_2} Y_{c_2} Z_{c_2}$. The coordinate axes for the leading coupling half are considered remain constant, and the axes of the driven coupling half deviate by some angles from the initial position.

From fig. 3.5 it can be seen that the axis of the drive shaft is directed vertically upwards [32], and the axis of symmetry of the earring deviates from this vertical by an angle ψ_1 . In this case, the axis $O_1 Z$ of the fixed coordinate system is directed along the axis of the shaft, and the axis $O_1 X$ is aligned with the axis of the socket *And* the forks. The third axis $O_1 Y$ is in the plane of rotation of the axis $O_1 X$. It should be noted that the movable coordinate system associated with the fork of the drive shaft of the coupling half $O_1 X_{\epsilon_1} Y_{\epsilon_1} Z_{\epsilon_1}$ is considered to coincide with the fixed coordinate system before the start of movement. Considering that the drive and driven shafts of the coupling are located at a certain angle, the plane of the earring makes a certain angle with the plane of the fork ψ_1 .

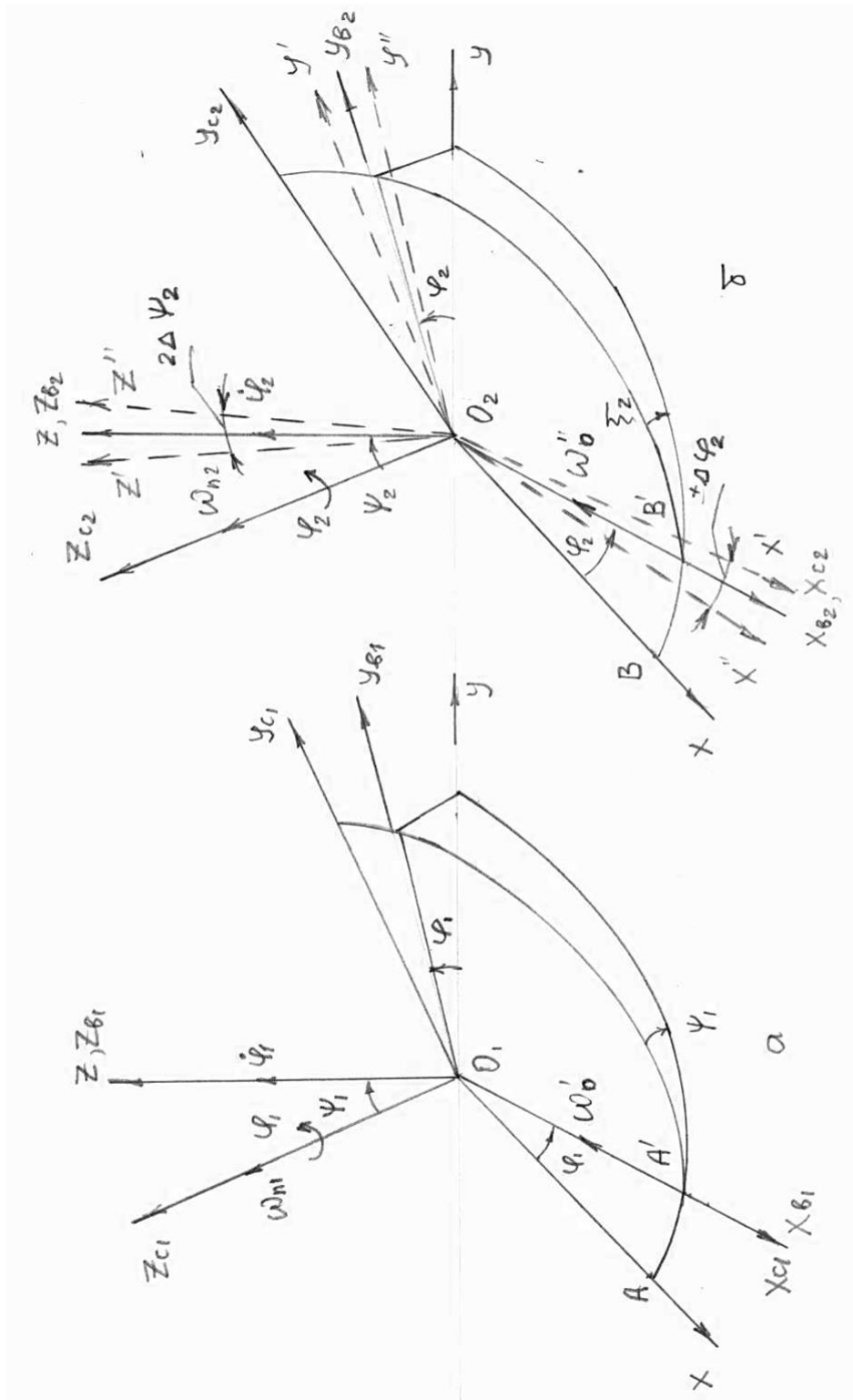


Figure 3.5. Calculation diagram of the positions of the coordinate axes of the lever-joint coupling

velocity vector ω_0^1 is directed along the axis $O_1 X_{c_1}$, which coincides with the axis $O_1 X_{c_1}$ from point A' to point O_1 in this moment of time. Because the rotation of the trunnion point A of the earring relative to the plug socket occurs counterclockwise. The portable angular velocity of the shackle ω_{n1} is equal in

value to the angular velocity of the drive shaft ω_1 of the lever-articulated clutch. The considered analysis of the angular velocity vectors for the driving coupling half corresponds to the methods given in [32]. For the driven coupling half, where it is necessary to take into account some additional angular displacements of the axes due to deformations of the elastic elements in the bearing of the driven shaft and in the hinged connection of the earring with the connecting rod, the Euler angles will be different (see Figure . 3.5 *b*). Due to the elastic support of the driven shaft, the coordinate axis of the fork $O_2 X_{e_2} Y_{e_2} Z_{e_2}$ changes its position. In this case, we assume that the origin of coordinates O_2 remains fixed. Due to the deformation of the elastic support (compression and tension), the axes are displaced by a certain angle, so the axis is $O_2 Z_{e_2}$ on $O_2 Z'$ and $O_2 Z''$, the axis is $O_2 X_{e_2}$ on $O_2 X'$ and $O_2 X''$, and also the axis $O_2 Y_{e_2}$ on $O_2 Y'$ and $O_2 Y''$. In this case, additional angles are obtained, for the angle $\psi_2, \pm\Delta\psi_2$, for the angle $\varphi_2, \pm\Delta\varphi_2$. The determination of the instantaneous angular velocities of the earrings of the leading and driven coupling halves ω_{c1} is ω_{c2} carried out by vector equations. The vector equations of the resulting movements of the earrings of the driving and driven shafts of the lever-articulated clutch according to the scheme, in Figure 3.5 *b* are obtained:

$$\bar{\omega}_{c1} = \bar{\omega}_1 + \bar{\omega}_{n1} + \bar{\omega}_{o1}; \quad \bar{\omega}_{c2} = \bar{\omega}_2 + \bar{\omega}_{n2} + \bar{\omega}_{o2} \quad (3.10)$$

where, $\bar{\omega}_1, \bar{\omega}_2$ - are the angular velocity vectors of the driving and driven shafts of the lever-articulated clutch; n_1, n_2 vectors of portable angular velocities of the earrings in the coupling half; $\bar{\omega}_{o1}, \bar{\omega}_{o2}$ - vectors of relative angular velocities of coupling halves.

To determine $\bar{\omega}_{c1}, \bar{\omega}_{c2}$ the obtained (3.11), we project onto the axes of the fixed coordinate systems O, XYZ :

$$\begin{aligned}
\omega_{c1}^x &= \omega_1^x + \omega_{n1}^x + \omega_{o1}^x; \quad \omega_{c2}^x = \omega_2^x + \omega_{n2}^x + \omega_{o2}^x; \\
\omega_{c1}^y &= \omega_1^y + \omega_{n1}^y + \omega_{o1}^y; \quad \omega_{c2}^y = \omega_2^y + \omega_{n2}^y + \omega_{o2}^y; \\
\omega_{c1}^z &= \omega_1^z + \omega_{n1}^z + \omega_{o1}^z; \quad \omega_{c2}^z = \omega_2^z + \omega_{n2}^z + \omega_{o2}^z;
\end{aligned} \tag{3.11}$$

According to the scheme shown in Fig. 3.5 *a* and *b*, we determine the corresponding projections of the angular velocities of the driving and driven coupling halves:

$$\begin{aligned}
\omega_{c1}^x &= \omega_{n1} \sin\psi_1 \sin\varphi_1 + \omega_{o1} \cos\varphi_1; \\
\omega_{c2}^x &= \omega_{n2} \sin(\psi_2 \pm \Delta\psi_2) \sin(\varphi_2 \pm \Delta\varphi_2) + \omega_{o2} \cos(\varphi_2 \pm \Delta\varphi_2) \\
&\quad \omega_2 \sin(\pm\Delta\psi_2) \sin(\pm\Delta\varphi_2); \\
\omega_{c1}^y &= -\omega_{n1} \sin\psi_1 \cos\varphi_1 + \omega_{o1} \sin\varphi_1 \quad ; \\
\omega_{c2}^y &= \omega_2 \sin(\pm\Delta\psi_2) \cos(\pm\Delta\varphi_2) - \omega_{n2}; \omega_2 \sin(\psi_2 \pm \Delta\psi_2) \cdot \\
&\quad \cdot \cos(\varphi_2 \pm \Delta\varphi_2) + \omega_{o2} \sin(\varphi_2 \pm \Delta\varphi_2); \\
\omega_{c1}^z &= -\omega_{n1} \cos\psi_1 + \omega_1 \\
\omega_{c2}^z &= \omega_2 + \omega_2 \cos(\pm\Delta\psi_2) + \omega_{n2} \cos(\psi_2 \pm \Delta\psi_2) + \omega_{o2} \sin(\pm\Delta\varphi_2) \sin(\pm\Delta\psi_2)
\end{aligned}$$

The resulting angular velocities of the earrings of the driving and driven coupling halves are determined from the expressions

$$\begin{aligned}
\omega_{c1} &= \sqrt{(\omega_{n1} \sin\psi_1 \sin\varphi_1 + \omega_{o1} \cos\varphi_1)^2 + (\omega_{o1} \sin\varphi_1 - \omega_{n1} \sin\varphi_1 \cos\varphi_1)^2 + (\omega_1 + \omega_{n1} \cos\psi_1)^2}; \\
\omega_{c2} &= \sqrt{[\omega_2 \sin(\pm\Delta\psi_2) \sin(\pm\Delta\varphi_2) + \omega_{n2} \sin(\psi_2 \pm \Delta\psi_2) \cdot \sin(\varphi_2 \pm \Delta\varphi_2) + \\
&\quad + \omega_{o2} \cos(\varphi_2 \pm \Delta\varphi_2)]^2 + [\omega_2 \sin(\pm\Delta\psi_2) \cdot \cos(\pm\Delta\varphi_2) - \omega_{n2} \sin(\psi_2 \pm \Delta\psi_2) \cdot \cos(\varphi_2 \pm \Delta\varphi_2) + \\
&\quad + \omega_{o2} \sin(\varphi_2 \pm \Delta\varphi_2)]^2 + [\omega_2 + \omega_2 \cos(\pm\Delta\psi_2) + \omega_{n2} \cos(\psi_2 \pm \Delta\psi_2) + \omega_{o2} \sin(\pm\Delta\varphi_2) \sin(\pm\Delta\psi_2)]^2}
\end{aligned} \tag{3.12}$$

As noted above, the portable angular velocities ω_{n1} and ω_{02} are numerically equal to the corresponding angular velocities of the corresponding shafts, and the relative angular velocities ω_{01} and ω_{n2} .

It should be noted that angles ψ_1 and ψ_2 are respectively equal to the angles α_1 and α_2 and subject to the implementation of the lever-articulated coupling $\alpha = \alpha_2 = \alpha_1$. Additional angle deviations $\Delta\varphi_2, \Delta\psi_2$ are determined from the expressions:

$$\Delta\varphi_2 = \arcsin \frac{\Delta_2}{l_{c2}}; \quad \Delta\psi = \Delta\alpha = \arcsin \frac{\Delta'_2}{l_2} \quad (3.13)$$

where, l_{c2}, l_2 - respectively, the length of the earring and the shaft of the driven half-coupling, Δ_2 - the value of the linear deformation of the elastic element in the hinge between the earring and the connecting rod of the driven half-coupling, Δ'_2 - the value of the linear deformation elastic element of the bearing of the driven shaft of the coupling half.

Considering the above, taking into account (3.13) and a number of transformations (3.12), we obtain:

$$\omega_{c1} = \omega_1 \sqrt{\frac{\sin^2 \alpha (1 - 2 \cos 2\varphi_1) + \cos^2 \alpha}{\cos^2 \varphi_1 (1 - 2 \sin^2 \alpha) + \sin^2 \varphi_1}};$$

$$\omega_{c2} = \omega_2 \sqrt{\frac{\sin^2(\alpha + \arcsin \frac{\Delta'_2}{l_2}) [\sin(\arcsin \frac{\Delta'_2}{l_2}) - \cos^2(\varphi_2 + \arcsin \frac{\Delta_2}{l_{c2}})]}{\cos^2(\varphi_2 + \arcsin \frac{\Delta'_2}{l_{c2}}) \cdot \{\sin(\arcsin \frac{\Delta'_2}{l_2}) - \sin^2(\alpha + \arcsin \frac{\Delta'_2}{l_2})\}}}$$

$$\frac{\sin^2(\varphi_2 + \arcsin \frac{\Delta_2}{l_{c2}}) + \cos^2(\arcsin \frac{\Delta_2}{l_{c2}}) \cos^2(\alpha + \arcsin \frac{\Delta'_2}{l_2})}{\cos(\arcsin \frac{\Delta'_2}{l_2}) + \sin(\varphi_2 + \arcsin \frac{\Delta_2}{l_{c2}}) \sin(\arcsin \frac{\Delta'_2}{l_2})}$$

(3.14)

The change in the angular velocity of the shackle of the leading coupling half depends on the position angle of the driving shaft and the angle of the shaft axis relative to the horizontal line. In the initial position $\varphi_1 = 0^0$, $\varphi_1 = 180^0$ and $\varphi_1 = 360^0$, $\omega_{C1} = \omega_1$. As the angle increases, α the peak values ω_{C1} are given at $\varphi_1 = \frac{\pi}{2}$ and $\frac{3\pi}{2}$. For values $\varphi_1 = \frac{\pi}{4}$, $\omega_{C1} = (1 - 0,5 \sin^2 \alpha)^{-1/2}$. Figure 3.6 shows graphical dependences of the change in the angular velocity of the leading half-coupling earring as a function of the angular displacement of the driving shaft. The dependences obtained are harmonic in nature and the magnitude of the oscillation amplitude depends on the angle α . So at $\alpha = 10^0$, the amplitude of oscillations ω_{C1} reaches $0.185\omega_1$, and at $\alpha = 30^0$, the amplitude of oscillations of the angular velocity of the leading earring

coupling half reaches $0,029\omega_1$. The greater the angle between the axis of the drive shaft of the lever-articulated coupling relative to the horizontal axis, the greater the amplitude of the oscillations of the angular velocity of the linkage of the leading half-coupling. At the angle $\alpha = 0$, $\omega_{C1} = \omega_1$ remains constant.

Figure 3.7 shows graphical dependences of the change in the angular velocity of the driven half-coupling shackle depending on the angular displacement of the driven shaft of the lever-articulated coupling at various values and angle α .

where, 1 - $\alpha = 10^0$; 2 - $\alpha = 20^0$; 3 - $\alpha = 30^0$;

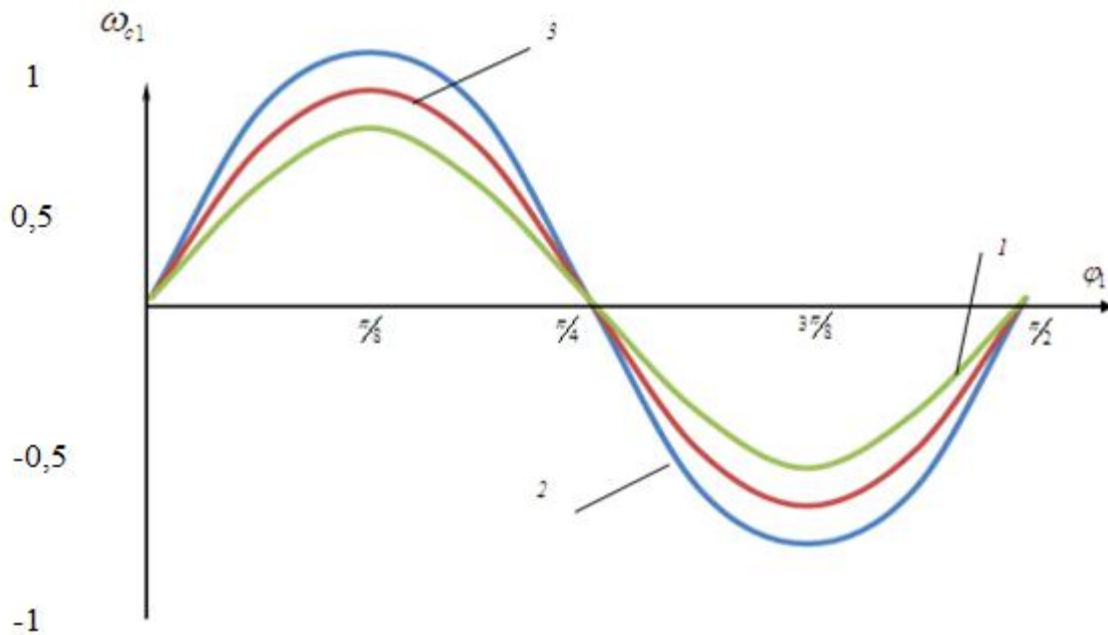


Figure. 3.6 . Dependences of the change in the angular velocity of the shackle of the leading coupling half as a function of its angular displacement

It should be noted that the dependences of the change in the angular velocity of the driven half-coupling earring also have a harmonic character, but it has some distortions and a phase shift, that is, additional small speed fluctuations are visible that are 6–8 times higher in frequency and the amplitude of oscillations reaches 5%: These oscillations occur due to the presence of $\Delta\varphi_2$ and $\Delta\alpha$, which depend respectively on the values of $\Delta_2, \Delta_2', l_{c2} u l_2$. So when the value $\Delta_2 = 0,05l_{c2} u \Delta_2' = 0,05l_2$ of the amplitude of the oscillations of the angular velocity ω_{c2} reaches $0,205\omega_2$ at $\alpha=10^\circ$. at $\alpha=30^\circ$ the amplitude of oscillations of the angular velocity ω_{c2} reaches $0,31 \cdot \omega_2$. The amplitude of small fluctuations in the angular velocity of the driven coupling half will vary within $\pm(0,045-0,055)\omega_2$.

The difference between the angular velocities ω_{c1} and ω_{c2} is insignificant. In the absence of elastic elements in the support of the driven shaft and in the hinge between the driven earring and the connecting rod, $\omega_{L1} = \omega_{C2}$

. The deformation of the elastic element in the support of the driven shaft of the articulated-lever coupling actually has little effect on the difference between the angular velocities.

$$\Delta\omega_C = |\omega_{C1} - \omega_{C2}| \quad (3.15)$$

The value $\Delta\omega_C$ is mainly affected by the deformation of the elastic element in the hinge between the driven earring and the connecting rod. In principle, the elastic elements were included in order to reduce load fluctuations from the working body connected to the driven shaft of the lever-articulated coupling, which is transmitted to the driven shaft, and are damped by the elastic elements. In this case, the angular velocity and torque on the drive shaft will be more uniform, that is, the angular speeds of the shackles of the drive and driven shafts will be close in magnitude.

Taking into account the foregoing and dividing the first equation by the second equation (3.14), taking into account (3.13), we obtain an expression for determining the transfer function of a lever-articulated clutch in the following form:

$$U_{12} = \sqrt{\frac{\left[\cos \varphi_1 \cos^2 \alpha + \sin^2 \varphi_1 \right] \cdot \sin^2 (\alpha + \Delta\alpha) \left[\sin \Delta\alpha - \cos^2 (\varphi_2 + \Delta\varphi_2) \right]}{\left[\sin^2 \alpha (1 - 2 \cos 2\varphi_1) + \cos^2 \alpha \right] \cdot \cos^2 (\varphi_2 + \Delta\varphi_2) \cdot \left[\sin \Delta\alpha_2 - \sin^2 (\alpha + \Delta\alpha) \right]}} \cdot \frac{\sin^2 (\varphi_2 + \Delta\varphi_2) + \cos \Delta\varphi_2 \cdot \cos^2 (\alpha + \Delta\alpha)}{\cos \Delta\alpha + \sin (\varphi_2 + \Delta\varphi_2) \cdot \sin \Delta\alpha}; \quad (3.16)$$

Analysis (3.16) shows that the transfer function of a lever-articulated coupling, taking into account the values of deformation of the elastic elements, depends on the following parameters: $\alpha, \varphi_1, \varphi_2, \Delta\varphi_2, \Delta\alpha$. In calculations, changes in φ_1 and φ_2 were carried out within $0^\circ - 2\pi$, identical limits. In this case, the fluctuations of the function U_{12} , which depend on the values of $\alpha, \Delta\alpha$ and $\Delta\varphi_2$

are special . Figure 3.7 shows graphical dependences of the change in the amplitude of oscillations of the transfer function of the considered lever-articulated clutch from the change in angles $\Delta\alpha$ and $\Delta\varphi_2$. It can be seen from them that with an increase in the angle, α the amplitude of the oscillations of the transfer function increases according to a non-linear pattern. But, the larger the angle α , the less the intensity of the increase ΔU_{12} . This is because the value ΔU_{12} is also affected by the value $\Delta\alpha$ u $\Delta\varphi_2$. In this case, as the angle α increases, the values $\Delta\alpha$ u $\Delta\varphi_2$ remain constant.

where, $1 - \Delta H_{12} = f(\alpha)$ at $\frac{\Delta 2}{l_2} = 0,03; \frac{\Delta_2^I}{l_{c2}} = 0,03$; $2 - \Delta U_{12} = f(\alpha)$ at $\frac{\Delta 2}{l_2} = 0,05; \frac{\Delta_2^I}{l_{c2}} = 0,05$; $3 - \Delta U_{12} = f(\frac{\Delta_2}{l_2})$ at $\alpha = 20^\circ$; $4 - \Delta U_{12} = f(\frac{\Delta_2^I}{l_{c2}})$ at $\alpha = 20^\circ$.

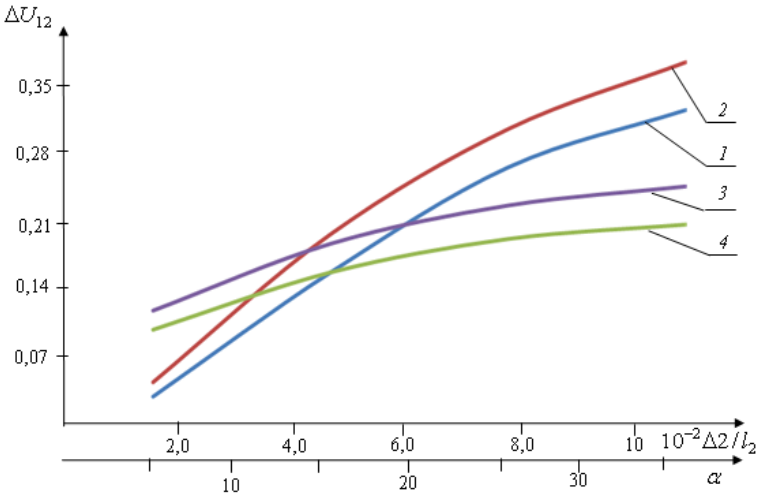


Figure . 3.7. Dependences of the change in the amplitude of oscillations of the transfer function of the lever-articulated clutch as a function of the angle $\alpha, \frac{\Delta_2}{l_2}$ and $\frac{\Delta_2^I}{l_{c2}}$

So at $\alpha = 5^\circ$, the amplitude of oscillations of the transfer function of the lever-articulated clutch is 0.065 at $\frac{\Delta_2}{l_2} = 0,03$, and with an increase in the angle α

to 30° at $\frac{\Delta_2}{l_2} = 0,05$, the value of the amplitude of the oscillations of the transfer function reaches 0.34. The influence of values Δ_2 , Δ_2^I also leads to an increase in values ΔU_{12} in a non-linear pattern. At the same time, it has a more significant effect Δ_2 than Δ_2^I . So at $\frac{\Delta_2}{l_2} = 0,02$ the amplitude of oscillations of the transfer function $\Delta U_{12} = 0,139$ at $\alpha = 20^\circ$, and with an increase $\frac{\Delta_2}{l_2}$ to 0.09, the amplitude of the transfer function increases to 0.264. Accordingly, with an increase $\frac{\Delta_2^I}{l_{c2}}$ from 0.02 to 0.09, the transfer function increases from 0.136 to 0.231. So, the impact on the change ΔU_{12} has values $\frac{\Delta_2}{l_2}$ rather than $\frac{\Delta_2^I}{l_{c2}}$. Therefore, for the necessary adjustment of the amplitude of oscillations of the transfer function of a lever-articulated clutch, it is advisable to increase the amount of deformation of the elastic element in the support of the driven shaft of the clutch [89,90].

3.3. Dynamics of the machine unit of a lever-articulated coupling with elastic elements.

3.3.1 Calculation scheme and mathematical model of the machine unit of the lever-articulated coupling.

The developed design of the lever-articulated coupling is intended for use in cardan mechanisms of the vehicle drive system. The main task of dynamic research of a lever-articulated clutch is to determine the patterns of angular velocities, angular accelerations and loading of the drive and driven shafts of the coupling, taking into account external loads on the driven shaft, the mechanical characteristics of the drive, as well as the justification of the main parameters of

the coupling, elastic - dissipative characteristics of the elastic elements of the driven support . shaft and hinge between the earring and the connecting rod of the driven coupling half.

When choosing the design scheme of the machine unit , it was taken into account that the elastic elements in the support of the driven pulley and in the hinge of the earring with the connecting rod make it possible to smooth the movement of the drive shaft. Figure 3.9 shows the design diagram of the machine unit.

Drawing up the equations of motion of the driving and driven shafts of the lever-articulated coupling is carried out using the Lagrange equations of the II - kind [91,92].

$$\frac{d}{dt} \left[\frac{\partial T}{\partial \dot{\varphi}_i} \right] - \frac{\partial T}{\partial \varphi_i} + \frac{\partial \Pi}{\partial \varphi_i} + \frac{\partial \Phi}{\partial \dot{\varphi}_i} = M_i(\varphi_i) \quad (3.17)$$

where, φ_i are the angular displacements of the i mass system, T is the kinetic energy of the i mass system; P - potential energy of the i mass system, Φ - Rayleigh dissipative function, $M_i(\varphi_i)$ - torques of external forces acting on the i mass system.

According to the design scheme, Figure 3.9. expressions for kinetic and potential energy will be:

$$T = \frac{1}{2} \left[I_{n1} \left(\frac{d\varphi_1}{dt} \right)^2 + I_{n2} \left(\frac{d\varphi_2}{dt} \right)^2 \right] \quad (3.18)$$

$$\Pi = \frac{1}{2} C_y (\varphi_1 - U_{12} \varphi_2)^2$$

The derivatives of (3.18) have the form:

$$\frac{d}{dt} \left(\frac{\partial T}{\partial \dot{\varphi}_1} \right) = I_{n1} \frac{d^2 \varphi_1}{dt^2}; \quad \frac{\partial}{\partial t} \left(\frac{\partial T}{\partial \dot{\varphi}_2} \right) = I_{n2} \frac{d^2 \varphi_2}{dt^2};$$

$$\frac{d\Pi}{d\varphi_1} = C_y (\varphi_1 - U_{12} \varphi_2) \left(1 - \frac{\partial U_{12}}{\partial \varphi_1} \varphi_2 \right) \quad (3.19)$$

$$\frac{d\Pi}{d\varphi_2} = -C_y(\varphi_1 - U_{12}\varphi_2)(U_{12} + \frac{\partial U_{12}}{\partial \varphi_1} \varphi_2)$$

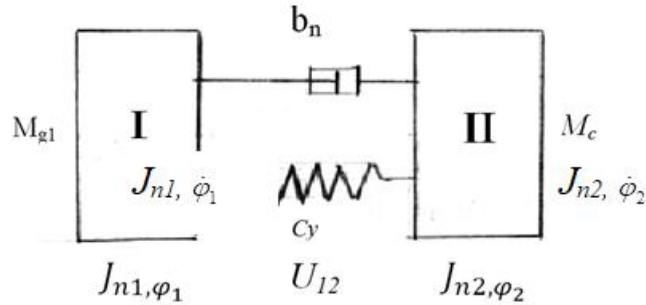


Figure 3.8. Calculation scheme of the machine unit of the lever-articulated clutch.

The dissipative Rayleigh function and its derivative will be:

$$\Phi = \frac{1}{2} \epsilon_y \left(\frac{d\varphi_1}{dt} - U_{12} \frac{d\varphi_2}{dt} \right)^2 ;$$

$$\frac{\partial \Phi}{\partial \dot{\varphi}_1} = \epsilon_y \left(\frac{d\varphi_1}{dt} - U_{12} \frac{d\varphi_2}{dt} \right) ; \quad (3.20)$$

$$\frac{\partial \Phi}{\partial \dot{\varphi}_2} = U_{12} \epsilon_y \left(\frac{d\varphi_1}{dt} - U_{12} \frac{d\varphi_2}{dt} \right)$$

where, I_{n1}, I_{n2} - reduced moments of inertia to the driving and driven shafts of the lever-articulated coupling ; φ_1, φ_2 - angular displacements of the driving and driven shafts of the coupling, U_{12} - transfer function between the shafts; c_y, ϵ_y - the reduced coefficients of stiffness and dissipation of the elastic elements of the coupling.

Moments of generalized forces in the machine unit:

$$M_1(\varphi_1) = M_g ; M_2(\varphi_2) = -M_c \quad (3.21)$$

where, M_g - driving moment on the drive shaft of the coupling; M_s is the moment of resistance on the driven shaft of the coupling.

Lever-elastic couplings are installed in the cardan shaft of the vehicle. In this case, the movement to the cardan shaft is transmitted from the internal

combustion engine. Therefore, the mechanical characteristic of the drive shaft of the lever-articulated clutch will be similar to the mechanical characteristic of the internal combustion engine.

For the base machine, the mechanical characteristic of the internal combustion engine is expressed [93] :

$$M_g = f\left(\frac{d\varphi_g}{dt}\right) \quad (3.22)$$

The mechanical characteristic according to [94,95] is described in the form of static and dynamic characteristics. These characteristics consider the start-up modes, steady-state motion modes and the process of stopping the internal combustion engine. In the steady state of the machine, changes in the angular velocity of the crankshaft and torque change depending on the external resistance . Figure 3.10 shows a graphical dependence of the mechanical static characteristic of the internal combustion engine. The operating mode of the engine is carried out in zone AB. Therefore, the operation of the lever-articulated coupling will also be considered in the steady operating mode. In this case, the mechanical characteristic of the drive shaft of the lever-articulated clutch, which directly receives movement from the drive of the internal combustion engine of the machine, we will consider the corresponding zone AB (see Figure 3.10 *a*). In Figure 3.10. *b* shows the mechanical characteristics of the drive shaft of the lever-articulated clutch for the operating mode of the machine (corresponding to a vehicle speed of 3.4 gears) [94]. Therefore, for the operating mode, this characteristic is taken as a straight line, which corresponds to the zone AB of the mechanical characteristic of the internal combustion engine (see Figure 3.10. *a*). Then we write the mechanical characteristic of the coupling drive shaft:

$$M_{g1} = M_1 - K_1 \frac{d\varphi_1}{dt} \quad (3.23)$$

where, M_{I-} is the value of the initial moment on the drive shaft of the lever-articulated clutch, K_1 is the slope coefficient of the mechanical characteristic of the drive shaft of the coupling for the operating mode, $K_1 =$

$$tg\alpha_1 = \frac{M_1}{\Delta\dot{\varphi}_1}.$$

Certain terms of the Lagrangian equations for the drive and driven shafts of the coupling (3.19), (3.20), (3.21), taking into account (3.23) and (3.22), we obtain a system of differential equations for a machine unit of a lever-hinge coupling with elastic elements:

$$M_{g1} = M_1 - K_1 \frac{d\varphi_1}{dt};$$

$$I_{n1} = \frac{d^2\varphi_1}{dt^2} = M_{g1} - \epsilon_y \left(\frac{d\varphi_1}{dt} - U_{12} \frac{d\varphi_2}{dt} \right) - c_y (\varphi_1 - U_{12}\varphi_2) \left(1 - \frac{\partial U_{12}}{\partial \varphi_1} \varphi_2 \right); \quad (3.26)$$

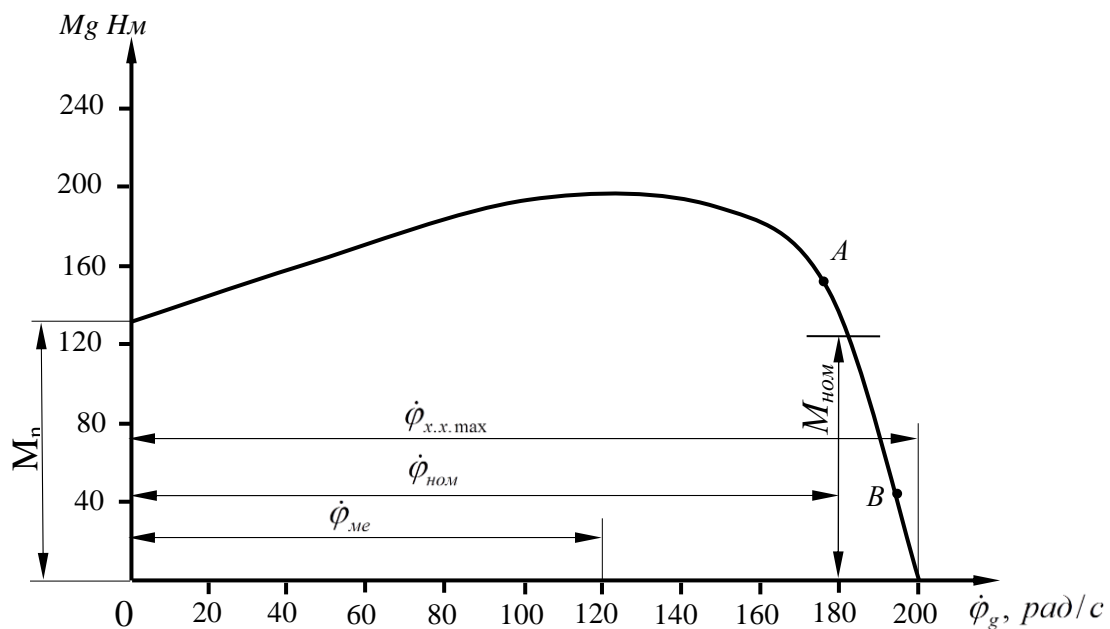


Figure 3.9 Mechanical static characteristic of the internal combustion engine of the machine.

where, $\dot{\varphi}_{ю.з}$ is the angular speed of idling; $\dot{\varphi}_н$ - nominal angular velocity; M_r - starting moment; $M_н$ - nominal moment.

here,

$$U_{12} = \sqrt{\frac{\left[\cos \varphi_1 \cos^2 \alpha + \sin^2 \varphi_1 \right] \cdot \sin^2 (\alpha + \Delta \alpha) \left[\sin \Delta \alpha - \cos^2 (\varphi_2 + \Delta \varphi_2) \right] \cdot \left[\sin^2 \alpha (1 - 2 \cos 2\varphi_1) + \cos^2 \alpha \right] \cdot \cos^2 (\varphi_2 + \Delta \varphi_2) \cdot \left[\sin \Delta \alpha_2 - \sin^2 (\alpha + \Delta \alpha) \right] \cdot \sin^2 (\varphi_2 + \Delta \varphi_2) + \cos \Delta \varphi_2 \cdot \cos^2 (\alpha + \Delta \alpha)}{\left[\cos \Delta \alpha + \sin (\varphi_2 + \Delta \varphi_2) \cdot \sin \Delta \alpha \right]}}$$

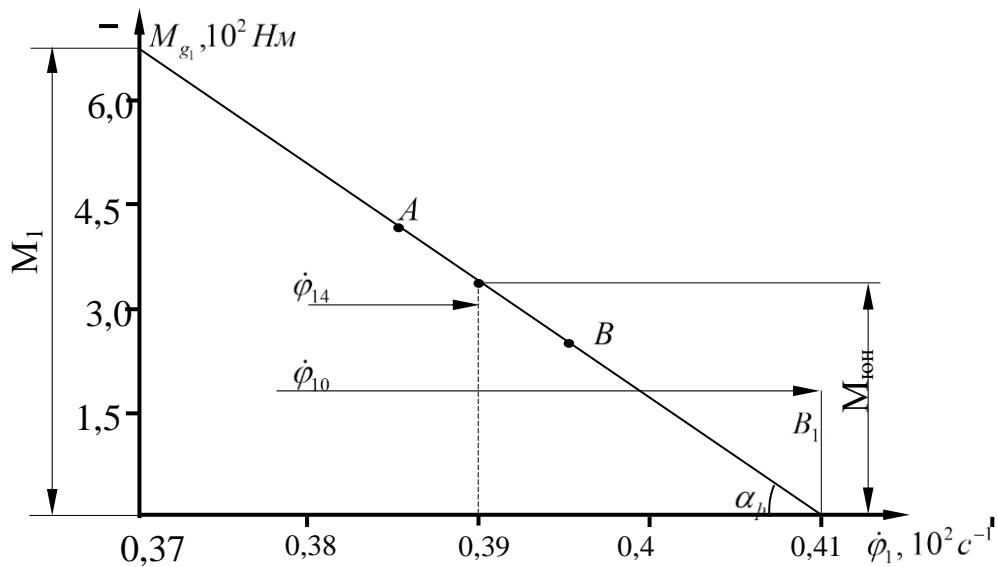


Figure. 3.10 Mechanical characteristics of the drive shaft of the lever-articulated clutch.

The solution of the system of differential equations (3.26) is carried out by the numerical method Mathcad on a PC.

The calculation of the reduced moments of inertia of the masses is determined by the well-known method according to [96]. For each mass element, the following formula was used [96]:

$$I = \frac{\gamma}{g} \cdot \frac{\pi}{32} l d^4 \quad (3.27)$$

where, g - is the acceleration due to gravity, γ is the relative weight of the element, l and d is the length and diameter of the element.

The calculation of cylindrical elements is carried out according to (3.27), and the moments of inertia of elements with complex shapes (rods, etc.) were

calculated taking into account the tables and data given in [96,97]. The calculation of the reduced stiffness of the elastic elements in the support of the driven shaft and in the hinge of the earring with the connecting rod is determined in the methodology of the given work [98]:

$$c_y = 6,25K_{dyn} H_w \frac{1}{d_{max}^3} \quad (3.28)$$

where, K_{dyn} - dynamic coefficient of rubber (for rubber grade 7V-14MVS. $K_{dyn} = 1.78$) ;

H_w - hardness of rubber according to Shore [99], for rubber grade 7V-14MVS $H_w = 75 \div 80$; d_{max} is the diameter of the location of the elastic element relative to the axis of rotation.

The damping coefficient of the elastic elements of the coupling according to [98] is determined from the expression:

$$\epsilon_y = \frac{\psi_y \cdot c_y \cdot T_m}{2\pi^2} \quad (3.29)$$

where, T_m - is the oscillation period, c_y is the reduced stiffness coefficient, ψ_y - the energy dissipation coefficient.

The moment of technological resistance is determined experimentally by strain measurement. Resistance is a random function

$$M_c = M_m \pm \delta M_m \quad (3.30)$$

where, M_m - mathematical expectation (average value) of the moment of resistance on the driven shaft of the coupling; δM_m - random component of the moment of resistance.

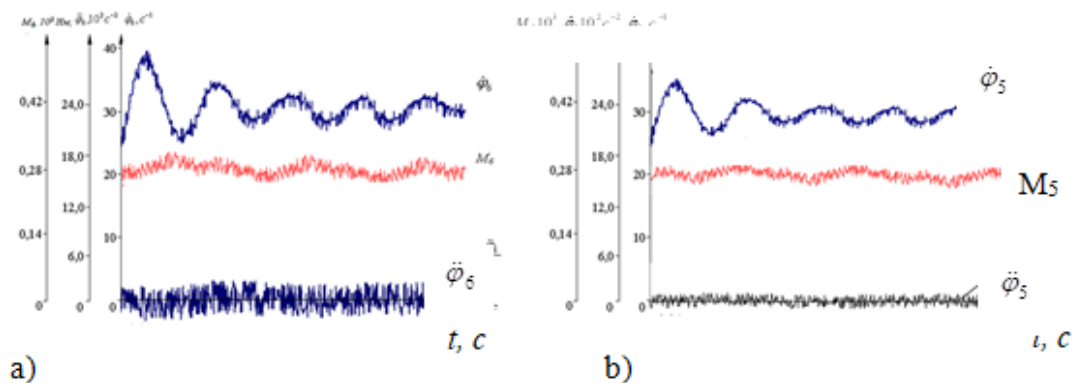
At the same time, the calculated values of the parameters of the machine unit for a vehicle of the KAVZ-685 brand: $I_{n1} = 0,128 Hmc^2$; $I_{n2} = 0,161 Hmc^2$; $M_1 = 6,23 \cdot 10^2 HM$; $\epsilon_y = 6,35 \cdot Hmc / pa\partial$; $c_y = 715,4 \cdot HM / pa\partial$; $M_m = 107,5 HM$; $\delta M = \pm 8,8 HM$; $g = 9,81 M / c^2$; $H_w = 75 \div 80$; $K_{dyn} = 1,78$.

3.3.2. Solution of the problem and analysis of results

When solving the problem, we used the results of experimental studies of the loading of a lever-hinge coupling installed in the cardan drive of a KaVZ-685 type machine. The solution was carried out taking into account the following initial conditions: at $t = 0$, $\dot{\varphi}_{10} = 0,39 \cdot 10^2 \text{ c}^{-1}$; $M_1 = 6,23 \cdot 10^2 \text{ Hm}$.

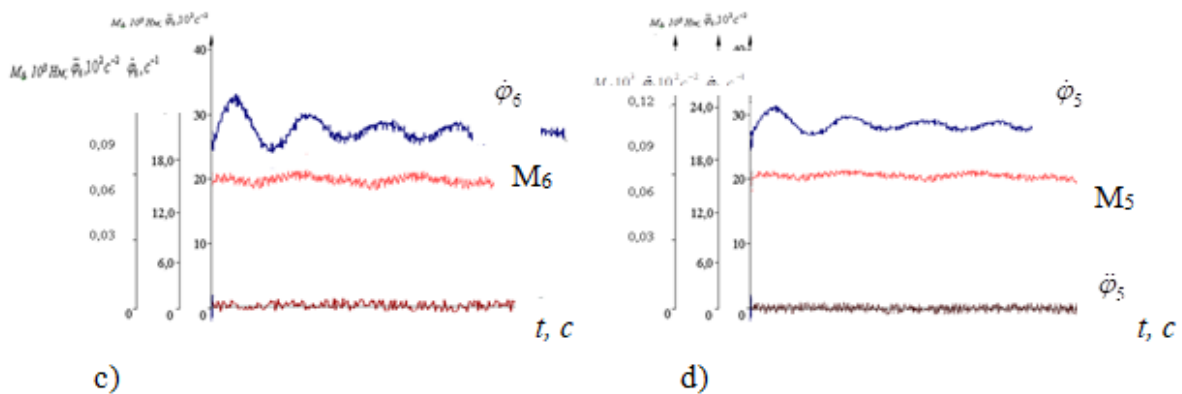
In studies with the aim of a more accurate assessment of the parameters of elastic elements and geometric parameters to reduce the unevenness of the angular velocities and torques of the coupling shafts.

Moments of friction forces in the supports were not taken into account due to their smallness. The problem was solved using the numerical method Mathcad



at $M_s = 107.5 \pm 8.8 \text{ Nm}$

at $M_s = 107.5 \pm 8.8 \text{ Nm}$



at $M_s = 107.5 \pm 8.8 \text{ Nm}$

at $M_s = 107.5 \pm 8.8 \text{ Nm}$

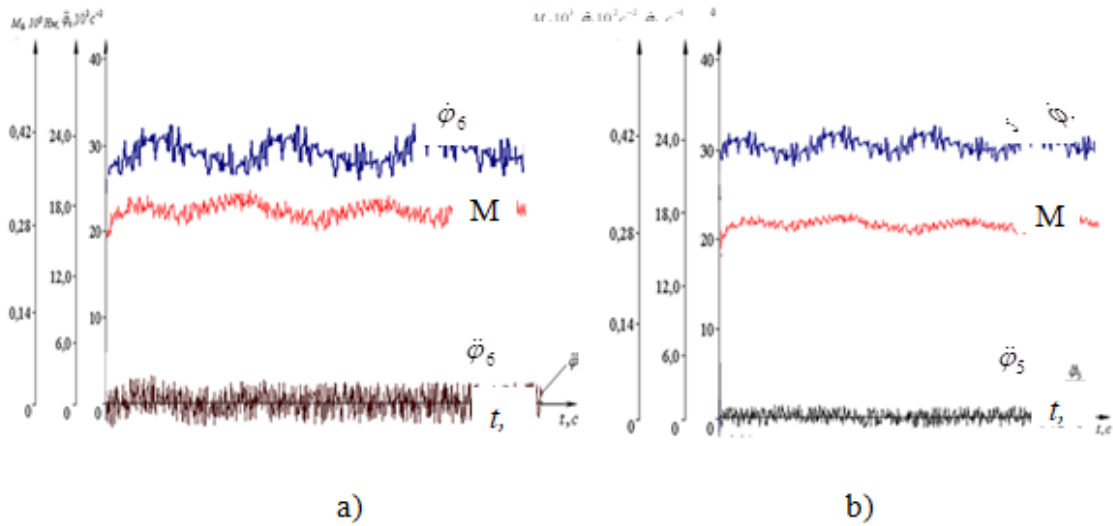
where, a, b - for the driven shaft c, d for the drive shaft

Figure. 3.11. Patterns of changes in angular velocities and torque on the driving and driven shafts of the lever-articulated clutch.

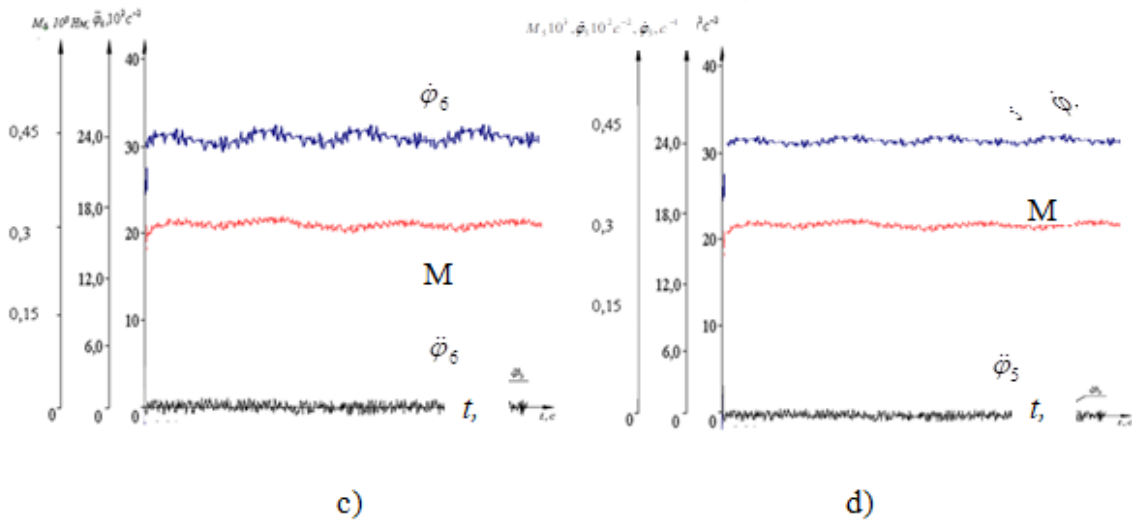
Based on the solution of the problem, the regularities of changes in angular velocities, accelerations and torques on the driving and driven shafts of the articulated-lever coupling are obtained. The patterns of change $\dot{\varphi}_1, \ddot{\varphi}_1, M_1$ and $\dot{\varphi}_2, \ddot{\varphi}_2, M_2$ were obtained at a technological load of $107.5 \pm 8.8 \text{ Nm}$ (see Figure 3.11. *a, b*) and at $225.4 \pm 18.3 \text{ Nm}$ (see Figure 3.11. *c, d*). As can be seen from the patterns obtained, with an increase in the technological load, the amplitude of fluctuations in angular velocities, accelerations and torque on the drive and driven shafts of the coupling increases significantly. It should be noted that it is obvious that the amplitude of oscillations $\dot{\varphi}_1, \ddot{\varphi}_1, u M_1$ of the drive shaft decreases rather than the amplitude of oscillations $\dot{\varphi}_2, \ddot{\varphi}_2, u M_2$. This is due to the presence of elastic elements in the lever-hinge coupling. An increase in MS leads to a decrease in the average value $\dot{\varphi}_1 u \dot{\varphi}_2$ and an increase in M_1 and M_2 . In fact, the average values $\dot{\varphi}_1 u \dot{\varphi}_2$ and also M_1 and M_2 coincide with each other, only the oscillation amplitudes are distinctive. In this case, the oscillation frequency of the random component $\dot{\varphi}_1 u \dot{\varphi}_2$ also coincides.

On figure 3.12 shows the patterns of changes in the angular velocities, accelerations and torques of the shafts with a variation in the stiffness coefficient c_y . and in fig. 3.13 when varying the dissipation coefficient of the elastic element b_y . On figure 3.14 shows the patterns of change $\dot{\varphi}_1, \dot{\varphi}_2, \ddot{\varphi}_1, \ddot{\varphi}_2, M_1$ and M_2 when varying the angle of divergence of the shafts α of the lever-articulated coupling.

On the basis of the results obtained, graphical dependences of the oscillation amplitude $A_1, A_2, A_1', A_2' u A_{M1}, A_{M2}$ on the change in technological resistance are constructed, which are shown in Figure 3.15. It should be noted that fluctuations in angular velocities, angular accelerations and



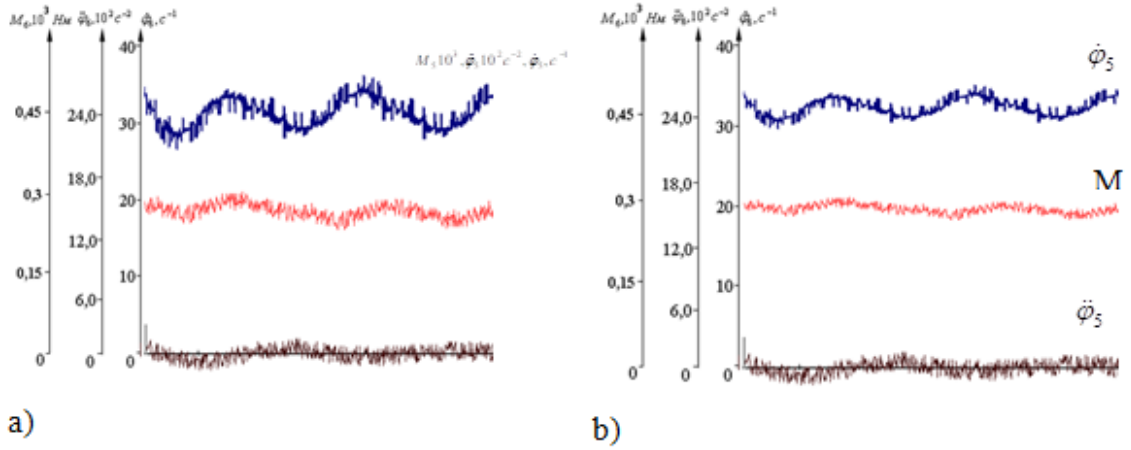
at $c_n = 450 \text{ nm/rad}$



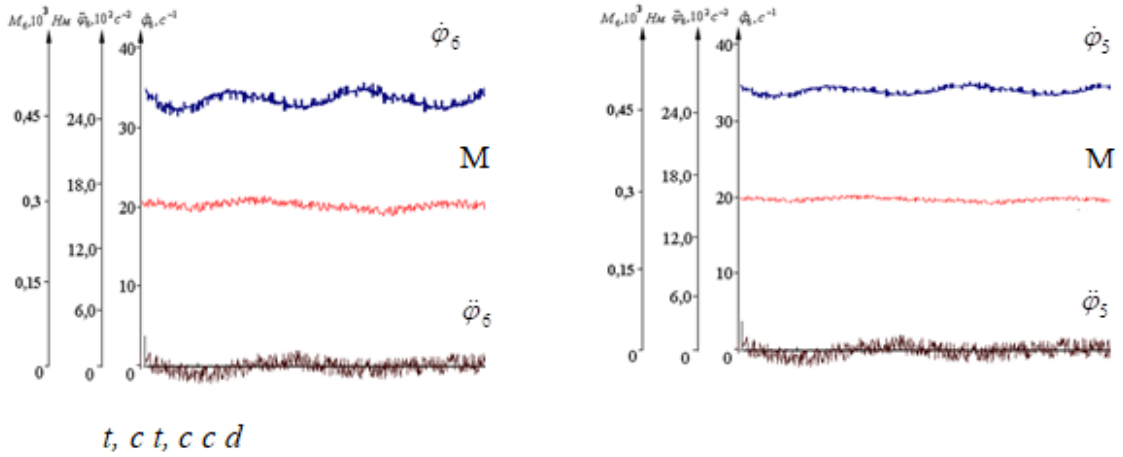
at $C_n = 850 \text{ Nm / rad}$

where a, b - for the driven shaft , c, d for the drive shaft

Figure 3.12 Patterns of change in angular velocities and torque on the drive and driven shafts of a lever-articulated clutch with a variation in the rigidity of the elastic elements of the system.



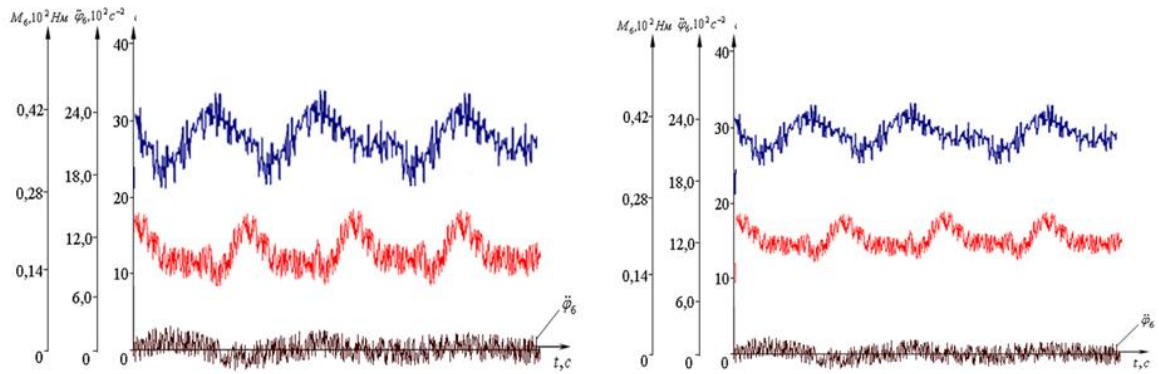
At $n = 4.5 \text{ Nms / rad}$, $t = 0.35$



At $n = 4.5 \text{ Nms / rad}$, $t = 0.35$

where, a, b - for the driven shaft, c, d for the drive shaft.

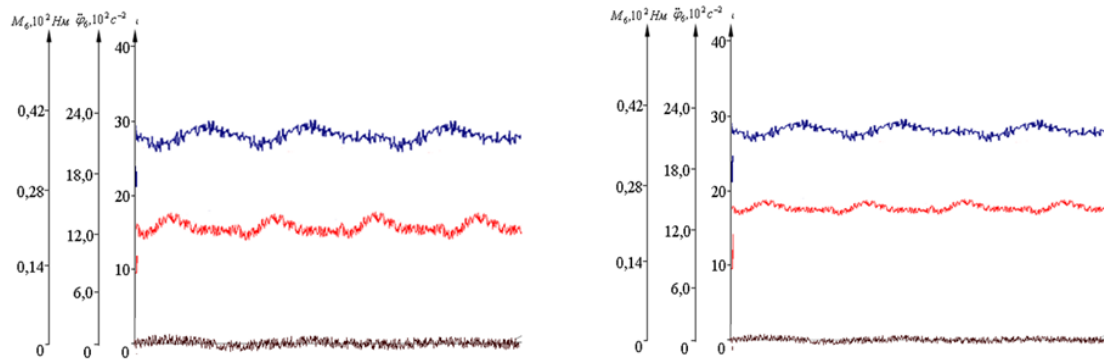
Figure 3.13. Patterns of change in angular velocities of accelerated and torque of the driving and driven shafts of the lever-articulated coupling when varying the dissipation coefficient of the elastic elements.



a)

b)

at $\alpha=30^\circ$



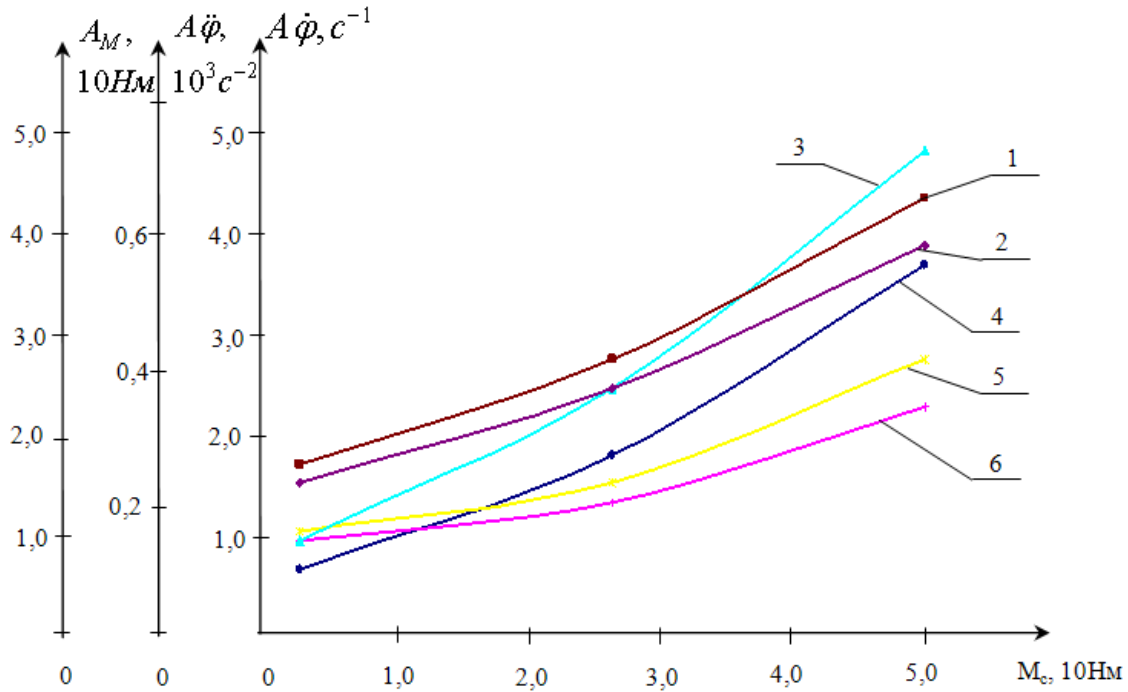
c)

d)

at $\alpha=5^\circ$

where, a, b - for the driven shaft, c, d for the drive shaft.

Figure 3.14 Patterns of change of angular velocities and torque on the driving and driven shafts of the lever-articulated coupling with varying the angle of α inclination of the shafts.



Where, $1 - M_{cp} = f(M_c)$; $1 - \dot{\phi}_{cp} = f(M_c)$; $1 - M_{cp} = f(I_{n2})$ at $\alpha = 15^\circ$

Figure 3.15. Graphic dependences of the change in the amplitudes of oscillations of the angular velocity, acceleration and torque of the driving and driven shafts of the articulated lever coupling.

torques on the driving and driven shafts arise not only due to changes in the transfer function of the coupling and the angle α divergence of shafts, but also by the influence of external technological load on the driven shaft. This resistance takes into account the load and unevenness of the road, the load in the vehicle, etc. Therefore, in this regard, the technological load is decisive. From Fig. 3.15 it can be seen that with an increase in M_c oscillation amplitudes $\dot{\phi}_1, \dot{\phi}_2, \ddot{\phi}_1, \ddot{\phi}_2, M_1$ and M_2 increase in a non-linear pattern. When the resistance M_c changes from $100 \pm 8.8 \text{ Nm}$ to $500 \pm 21.9 \text{ Nm}$, the amplitude of the angular velocity of the drive shaft increases from 0.65 s^{-1} to 3.94 s^{-1} , and the angular velocity of the driven shaft from 0.92 s^{-1} to 5.18 s^{-1} . In this case, the greater the technological load, the greater the difference between the amplitudes of oscillations of the angular velocities of the shafts. The amplitudes of oscillations

of angular accelerations and torques of the shafts also change with a similar regularity. Yes, at $M_c = 150 \pm 11.5 \text{ Nm}$ and $\alpha = 15^\circ$ amplitude of oscillations of the acceleration of the drive shaft $0.18 \cdot 10^3 \text{ c}^{-2}$, and the driven shaft $0.21 \cdot 10^3 \text{ c}^{-2}$, and at $M_c = 500 \pm 21.3 \text{ Nm}$, the amplitudes $A \ddot{\varphi}$ increase, respectively, of the driven shaft of the coupling up to $0.51 \cdot 10^3 \text{ c}^{-2}$, and the drive shaft up to $0.38 \cdot 10^3 \text{ c}^{-2}$, it must be taken into account that an increase in the angle of α divergence of the shafts of the articulated

- lever coupling, respectively leads to an increase in the amplitude of oscillations of angular velocities, accelerations and torques of the shafts. At $\alpha = 15^\circ$ and $M_c = 500 \pm 21.3 \text{ Nm}$ oscillation amplitude A_{m2} increases to 49.4 Nm , and A_{m1} of the drive shaft reaches 43.2 Nm . At the same time, the influence of the random component of technological resistance is important δM_c . From fig. 3.11 and 3.15 it can be seen that the influence of the random component of the load is greatest for changing the oscillations of the angular accelerations of the driving and driven shafts of the lever-articulated coupling.

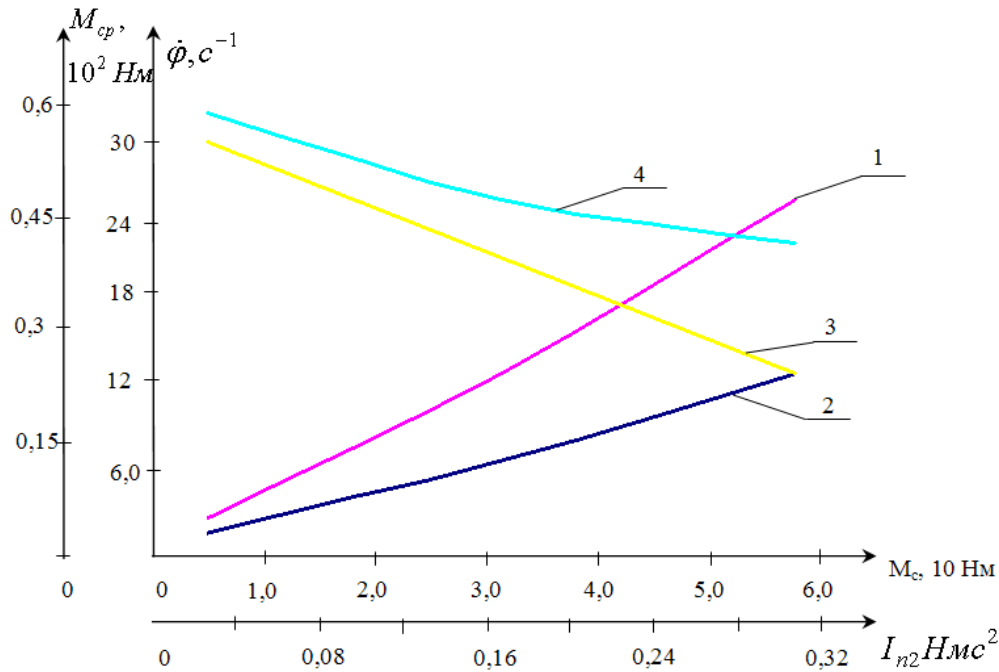
It is known from the general theory of machines and mechanisms [79,80] that with an increase in the load on the rotating shaft of the system, the average value of the angular velocity decreases, and the average value of the torque increases.

In addition, the greater the moment of inertia of the shaft, the less the unevenness of the angular velocity. But, in this case, the average value of the angular velocity decreases, and the torque increases. For the considered machine unit with a articulated-lever coupling in figure 3.16 shows graphical dependences of the change in the average values $\dot{\varphi}_{cp}$ and M_{cp} of the shafts as a function of the technological external load and the reduced moment of inertia of the driven shaft of the lever-articulated coupling. With an increase in load from 100 ± 8.8 to $550 \pm 24.1 \text{ Nm}$, the average value of the angular velocities of the coupling shafts decreases from 37.2 c^{-1} to 23.4 c^{-1} , the average value of the

torque increases from 78 Nm to 484 Nm according to a non-linear pattern. At the same time, to ensure the average angular velocity of the coupling shafts, according to the mechanical characteristic for the operating mode, M_s should not exceed the value $(450 \div 550)$ Nm with a random component up to $\pm(20 \div 22.5)$ Nm. Then the average angular velocity varies within $\pm(0.24 \div 2.55) c^{-1}$.

The influence of the values of the reduced moment of inertia of the driven shaft slightly affects the value $\dot{\varphi}_{cp}$ and M_{cf} , than the influence of M_s . So with an increase in the moment of inertia I_{n2} from 0.08 Nms^2 to 0.30 Nms^2 the average angular velocity of the coupling shafts decreases from 3 to $33.9 c^{-1}$, and the average torque on the shafts increases from 720 Nm to 281.0 Nm according to a non-linear pattern. This is explained by the fact that with an increase in the moment of inertia I_{n2} , the mass of the system increases, this leads to an increase in the load, thereby reducing the angular velocity $\dot{\varphi}_{cp}$. The recommended values are $I_{n2} = 0.14 \div 0.15 \text{ Nms}^2$ and $I_{n2} = 0.52 \div 0.13 \text{ Nms}^2$.

The use of elastic elements in the articulated-lever coupling is aimed at reducing the amplitudes of fluctuations in the angular velocity, acceleration and torque on the drive shaft, which allows increasing reliability and efficiency. operation of the transport system.



Where, $1 - M_{cp} = f(M_c)$; $2 - \dot{\varphi}_{cp} = f(M_c)$; $3 - M_{cp} = f(I_{n2})$ at $\alpha = 15^\circ$

Figure 3.16. Graphic dependences of the change in the average angular velocity and torque on the shafts of the articulated-lever coupling on the technological load and the reduced moment of inertia of the driven shaft.

The degree of influence of elastic elements on the nature of the movement of the drive shaft mainly depends on the elastic-dissipative characteristics of the rubber brand used as elastic elements in the coupling. Figure 3.17 shows the dependences of changes in the differences in the amplitude of oscillations of angular velocities, accelerations and torques of the driving and driven shafts on changes in the reduced stiffness coefficients and dissipation of the elastic elements of the lever-articulated coupling. As noted above, it is important to reduce the oscillation amplitudes $A\dot{\varphi}_1, A\ddot{\varphi}_1 u A M_1$ of the drive shaft. Therefore, to assess the mixing of the oscillations of the drive shaft, the values of the difference in the amplitudes of the oscillations were studied:

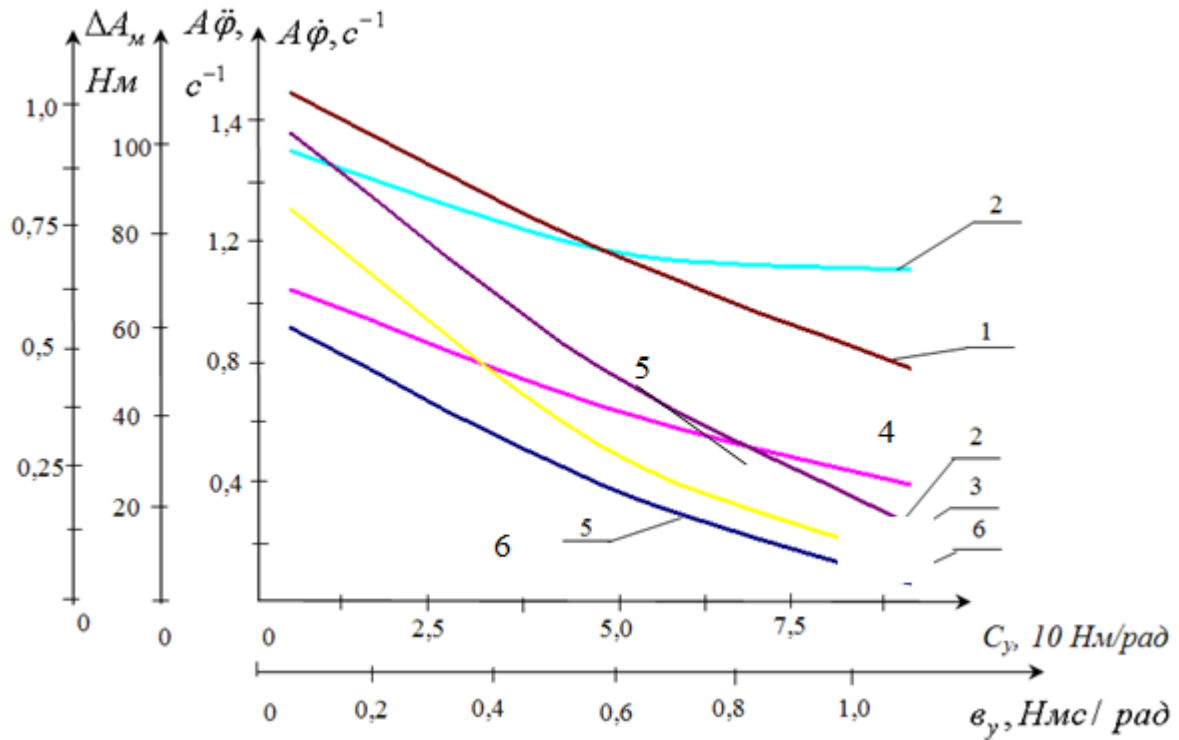


Figure 3.17. Dependences of the change in the difference in the amplitudes of oscillations of speeds, accelerations and torques of the driving and driven shafts as a function of the reduced coefficients of rigidity and dissipation of the elastic elements of the lever-articulated coupling.

Where, $1 - \Delta A\dot{\phi} = f(C_y)$; $2 - \Delta A\dot{\phi} = f(C_y)$; $3 - \Delta A_M = f(C_y)$; $4 - \Delta A\ddot{\phi} = f(\epsilon_y)$;
 $5 - \Delta A\dot{\phi} = f(\epsilon_y)$; $6 - \Delta A_M = f(\epsilon_y)$; at $\alpha = 15^\circ$; $M_c = 150 \pm 11 \text{ HM}$;

$$\Delta A_{\dot{\phi}_1} = A_{\dot{\phi}_2} - A_{\dot{\phi}_1} = \frac{\dot{\phi}_{2\max} - \dot{\phi}_{2\min}}{2} - \frac{\dot{\phi}_{1\max} - \dot{\phi}_{1\min}}{2};$$

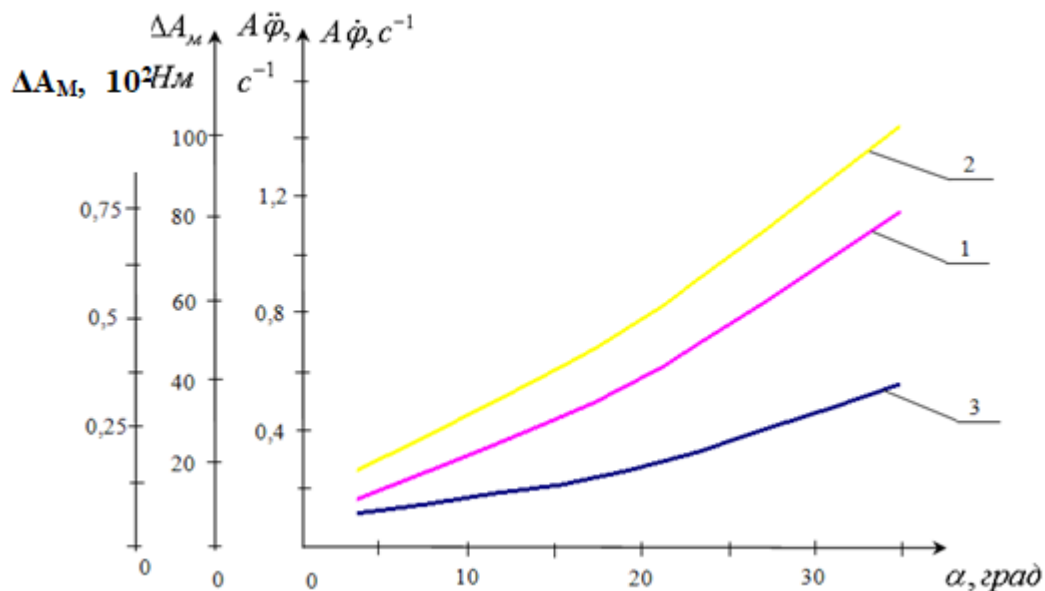
$$\Delta A_{\ddot{\phi}_1} = A_{\ddot{\phi}_2} - A_{\ddot{\phi}_1} = \frac{\ddot{\phi}_{2\max} - \ddot{\phi}_{2\min}}{2} - \frac{\ddot{\phi}_{1\max} - \ddot{\phi}_{1\min}}{2};$$

$$\Delta A_M = A_{M1} - A_{M2} = \frac{M_{2\max} - M_{2\min}}{2} - \frac{M_{1\max} - M_{1\min}}{2}$$

where, $A_{\dot{\phi}_1}, A_{\dot{\phi}_2}, A_{\ddot{\phi}_1}, A_{\ddot{\phi}_2}, A_{M1}, A_{M2}$ is the amplitude of oscillations of the angular velocity, the angular acceleration of the torque, respectively, on the driving and driven shafts of the coupling; $\dot{\phi}_{1\max}, \dot{\phi}_{1\min}, \dot{\phi}_{2\max}, \dot{\phi}_{2\min}, \ddot{\phi}_{1\max}, \ddot{\phi}_{1\min}, \ddot{\phi}_{2\max}, \ddot{\phi}_{2\min}$ - minimum and maximum angular velocities and accelerations of the coupling

shafts; $M_{1\max}, M_{1\min}, M_{2\max}, M_{2\min}$ - maximum and minimum torque values of the coupling shafts.

From figure 3.17 it can be seen that with an increase in the reduced stiffness coefficient, the decrease in the difference in the amplitudes of oscillations of angular velocities and accelerations and torques is carried out according to a non-linear pattern. With an increase in the stiffness coefficient from $2.0 \cdot 10^2 \text{ HM} / \text{pad}$ to $8.2 \cdot 10^2 \text{ Nm} / \text{rad}$ at $\alpha = 15^\circ$ the difference between the amplitudes of oscillations of the angular velocities of the driving and driven shafts of the coupling decreases from 1.26 c^{-1} to 0.78 c^{-1} . In this case, $\Delta A\ddot{\varphi}$ it decreases from 980 s^{-2} to 395 s^{-2} , and the difference in the amplitudes of oscillations of torques on the shafts decreases from 7.1 Nm to 13.2 Nm .



Where, 1 - $\Delta A\dot{\varphi} = f(\alpha)$; 2 - $\Delta A\ddot{\varphi} = f(\alpha)$; 3 - $\Delta A_M = f(\alpha)$; 4 - $\Delta A\ddot{\varphi} = f(\epsilon_y)$; at

$$M_c = 150 \pm 11 \text{ HM};$$

Figure 3.18. Graphic dependence of the change in the difference in the amplitudes of oscillations of angular velocities, angular accelerations and torques as a function of the angle of inclination of the driving and driven shafts of the lever-articulated coupling.

It should be noted that with an increase in the rigidity of the elastic elements, the average value of the torque on the shafts increases. This is

explained by the fact that with an increase in the rigidity of the elastic elements, the system becomes a single, massive one. Increasing the dissipation factor also leads to an increase in the average torque value. But, at the same time, the difference in the amplitudes of oscillations of angular velocities, accelerations and torques on the shafts decreases (see Figure 3.17, curves 4,5,6). An increase \mathcal{E}_y to 10 Nms/rad leads to a decrease ΔA_m to 12.8 Nm , $\Delta A_{\ddot{\varphi}}$ to 128 s^{-2} and a decrease in $\Delta A_{\dot{\varphi}} = 0,38c^{-1}$. The most acceptable values for the recommended articulated coupling are values with $y = 710 \div 850 \text{ Nm/rad}$, in $y = 6.4 \div 8.5 \text{ Nm/rad}$ [100-103].

Important are the studies of the dynamics of the movement of the shafts of the coupling, which is when the angle of divergence of the axes of the shafts of the articulated-lever coupling varies α (see Figure 3.14). The resulting graphical dependencies with angle variation α are shown in Figure 3.18. It can be seen from them that with an increase in the angle of divergence of the shafts, α the difference in the amplitudes of oscillations of angular velocities, angular accelerations and torques increase according to a non-linear pattern. When the angle increases α from 10° to 35° , the difference in the amplitudes of oscillations of the angular velocities of the driven and driving shafts of the coupling increases within $(0.28 \div 1.37)\text{s}^{-1}$, and $\Delta A_{\ddot{\varphi}}$ increases from $(225 \div 98)\text{s}^{-2}$. In this case, the increase ΔA_m is obtained within $(11.0 \div 56.0) \text{ Nm}$. An increase in the angle of divergence α of the shafts mainly affects the fluctuation of the transfer function of the articulated-lever coupling, which in turn leads to changes $\Delta A_{\dot{\varphi}}, A_{\ddot{\varphi}}$ in and ΔA_m . Analysis of the graphs in fig. 3.18 shows that the increase $\Delta A_m, \Delta A_{\dot{\varphi}}, \Delta A_{\ddot{\varphi}}$ become intense with increasing angle α , the axis is larger at values $\alpha = 20^\circ \div 25^\circ$. Therefore, the recommended values are $\alpha = 10^\circ \div 25^\circ$, at which the minimum values of oscillations of the angular velocity, acceleration and torque of the drive shaft of the articulated-lever coupling are provided. It should

be noted that the operating mode $\dot{\varphi}_1 = 33 \div 37 c^{-1}$ allows small values of the incoming forces of the coupling halves at small mismatch angles. Therefore, the mismatch angle of the shaft axes α should not exceed the value of $20^\circ \div 25^\circ$. The following conclusions can be drawn from this section:

- obtained formulas for calculating the angles that determine the positions of the link and connecting rods, taking into account the angle of divergence of the shafts and deformations of the elastic elements of the coupling. The graphical regularities of the change in angles are determined, which determine the positions of the link and the connecting rod as a function of the angular displacement of the coupling shaft at various values of the angle. Discrepancies between the driving and driven shafts;

- using the method of moving coordinates and vector equations, formulas were obtained for determining the angular velocities of the coupling half shackles, taking into account the angle of divergence of the shaft axes and the deformation of the elastic elements of the driven shaft support and the shackle hinge with the connecting rod. Graphic dependences of the change in the angular velocities of the coupling halves as a function of the angular displacements of the driving and driven shafts are obtained, taking into account the angle of their divergence;

- a formula has been derived for determining the transfer function between the drive and driven shafts of the articulated-lever coupling, taking into account the angle of divergence of the shaft axes and the deformation of the elastic elements. The dependences of the change in the amplitude of oscillations of the transfer function of the articulated-lever coupling on the change in the angle of divergence of the axes of the shafts and deformations of the elastic elements are obtained;

- dynamic and mathematical models of a machine unit with a lever-articulated clutch are left, taking into account the mechanical characteristics of the drive, the variability of the transfer function of the clutch, the elastic-

dissipative properties of the elastic elements, the characteristics of the technological load of the vehicle of the KAVZ-685 type.

Based on the solution of the problem of the dynamics of the machine unit by the numerical method Mathcad, the laws of change of angular velocities, angular accelerations and torques for various values of the technological load, the moments of inertia of the shafts, the angle of their divergence, the characteristics of elastic elements are obtained;

- the dependences of the change in the amplitude of oscillations of the angular velocities, accelerations and torques of the coupling shafts on the change in the technological load, the reduced stiffness coefficient, the dissipation coefficient and the angle of divergence of the axes of the driving and driven shafts are obtained. Recommended parameter values: $I_{n1} = 0,12 \div 0,13 Hm c^2$;
 $I_{n2} = 0,14 \div 0,15 Hm c^2$; $M_c = (450 \div 550) Hm$; $\delta M_c = \pm(20 \div 22,5) Hm$;
 $C_y = (710 \pm 850) Hm / pa \partial$; $B_y = (6,4 \div 8,5) Hm c / pa \partial$, $\alpha \leq (10^\circ \div 25^\circ)$

4. EXPERIMENTAL INVESTIGATIONS OF A LEVER - HINGED COUPLING WITH ELASTIC ELEMENTS

4.1. Experimental methodology

The developed design of the lever-articulated coupling is recommended for use in the cardan mechanism of a motor vehicle of the KAVZ-685 type. In this case, fluctuations in load and angular velocity on the driven shaft of the cardan mechanism will be reduced due to the elastic elements of the lever-articulated clutch, thereby increasing the reliability of the drive and internal combustion engine of the machine.

The main objective of experimental studies is to determine the speed and load characteristics of the drive and driven shafts of the lever-hinge coupling in the cardan mechanism of the KAVZ-685 machine at different angles of divergence of the shaft axes and technological load on the output shaft. In this case, it is considered appropriate to determine the elastic - dissipative properties of elastic elements rubber bushings on the modes of operation of the mechanism, thereby substantiating the recommended brand of rubber for a lever-articulated clutch, which should provide a reduction to the required values of torque fluctuations and angular velocity on the clutch drive shaft.

It is important to compare the results of theoretical studies with the results of experiments carried out on the KAVZ-685 machine.

To conduct experimental studies, a prototype of a lever-articulated coupling was made with the possibility of varying rubber bushings in the driven shaft support and in the hinge of the link and connecting rod of the driven half-coupling of the cardan mechanism. For the manufacture of elastic bushings, a special matrix was made. When installing rubber bushings in the support and the hinge, a special glue "leukanat" was used [104]. For the experiments, the following rubber brand options were chosen:

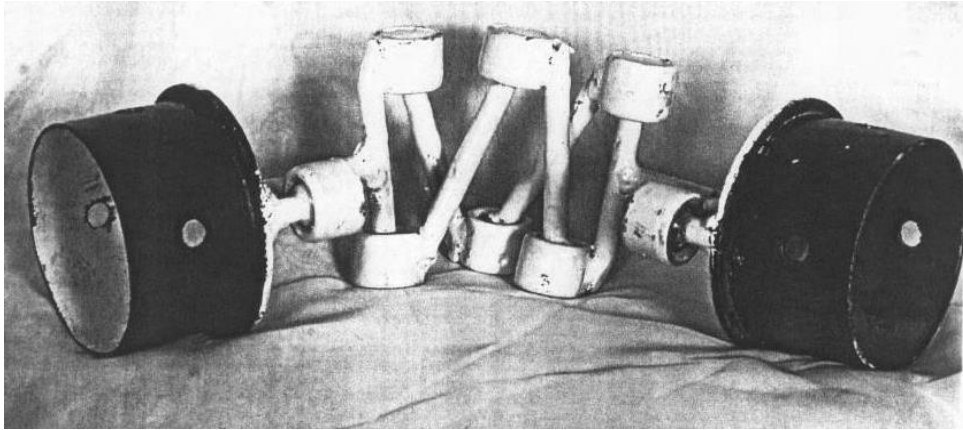
825 MBCS , 3826 M B C , 1338, 1847, 7 B - 14 MBS, 7 IRP 13-46, 7 IRP 13-48. Technological characteristics [99,104] of the considered variants of the rubber brand are presented in Table 4.1.

Table 4.1. Technological characteristics of the brand of rubber

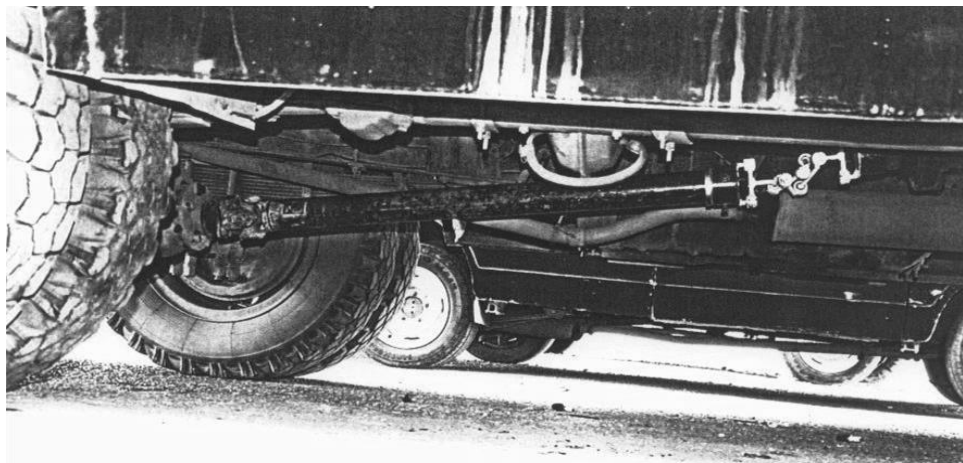
No.	Tire brand	Relative extension at break	Shore Hardness	Strength kg / cm ²	Coefficient. hardness, N/m
1.	3826MVS	25-300	60-75	80.0	$0.25 \cdot 10^{-4}$
2.	1338	360	70-75	85.0	$0.28 \cdot 10^{-4}$
3.	1847	550	80-85	75-80	$0.45 \cdot 10^{-4}$
4.	3825MVS S	120	85 - 90	80 -90	$0.33 \cdot 10^{-4}$
5.	7B-54 MVS	1 30	75 - 80	9 0.0	$0.4 2 \cdot 10^{-4}$
6.	7 IRP 13-46	300-350	70-75	75-80	$0.25 \cdot 10^{-4}$
7.	7IRP 13-48	150-200	90-95	90-95	$0.51 \cdot 10^{-4}$

In the process of operation of the cardan mechanism of motor vehicles KAVZ-685 rubber work in cyclic loading with random components and in a dusty environment. Elastic bushings are made on a press unit at a temperature of 135-145 ° C for 40 minutes with a gradual increase in load. The experiments were carried out on a motor vehicle in the conditions of the base of the vehicle fleet of JSC "Kyzylkiya" PATP. Kyrgyz Republic. On fig. 4.1a shows a general view of the developed design of a lever-articulated coupling with elastic elements, and in fig . 4.1 b shows a side view of the installed design of the lever-articulated coupling in the cardan mechanism of a KAVZ-685 car. To highlight the design of the clutch, its levers are painted white.

The torques on the driving and driven shafts of the coupling were produced by the method of electrotension measurement [105,106]. In this case, 6÷10 cycles of loading of the coupling shafts were measured. According to this technique, the torques on the shafts were measured. The shaft rotation frequency was measured by magnetoelectric sensors [107]. The choice of strain gauges, the method of gluing on the surface of the shafts, the measurement is carried out according to the work of elastic elements. [106].



a



b

Figure. 4.1.

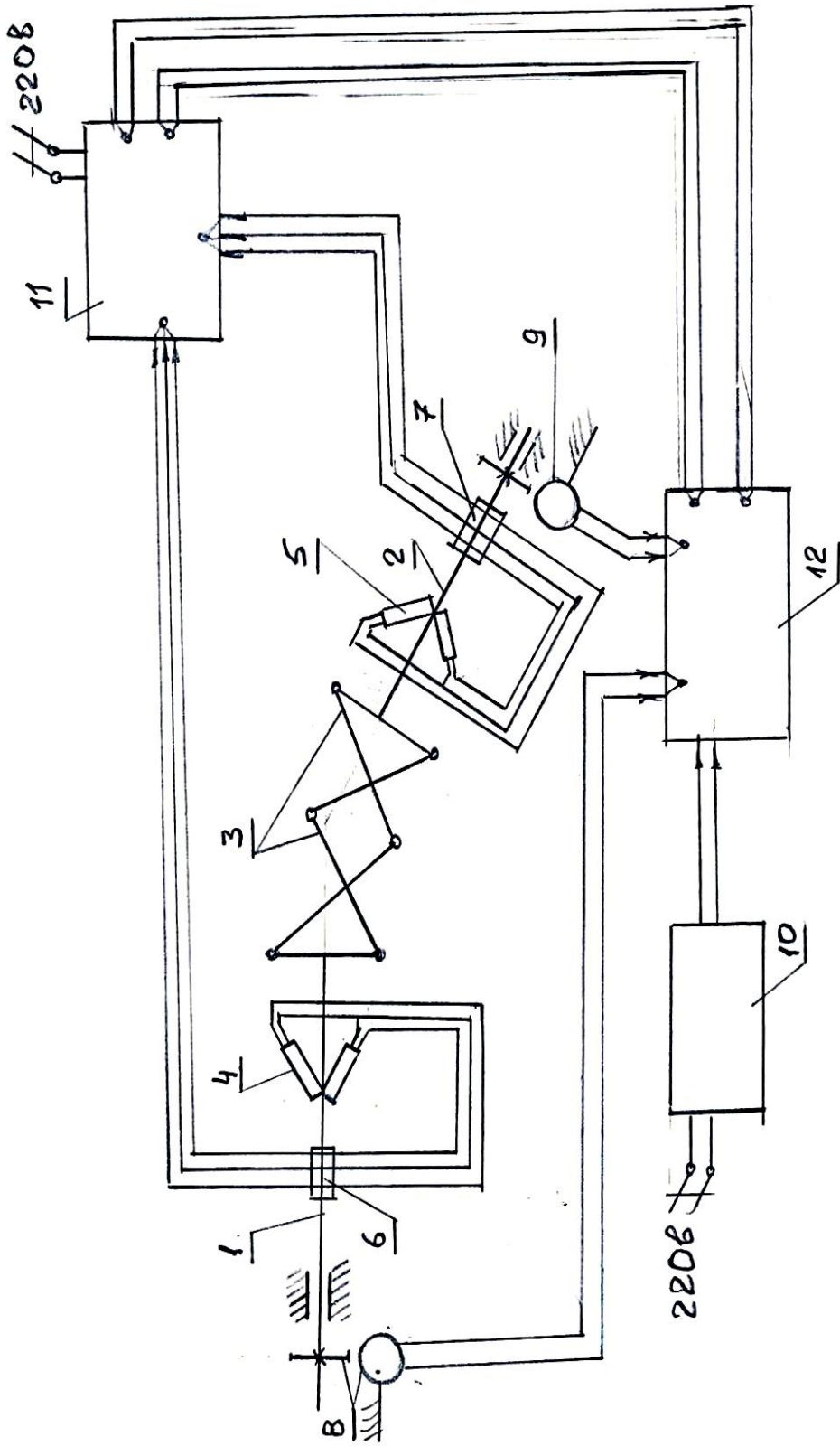
a - general view of the recommended lever-articulated coupling with elastic elements;

b - side view of the KAVZ-685 car with a developed design of a lever-articulated clutch installed in the cardan mechanism with

On fig. Figure 4.2 shows a diagram of electrostrain measurement of a cardan mechanism with a recommended lever-articulated clutch in a car, and Figure 4.3 *a* shows a photograph of a cardan mechanism with a lever-articulated clutch with strain gauges on the shafts, *b* - bottom view of the lever-articulated clutch. According to the strain measurement scheme, strain gauges 4, current collectors 6 and a magnetoelectric sensor 8 are installed in the drive shaft 1, and strain gauges 5, current collectors 7 and a magnetoelectric sensor 9 are also

glued on the driven shaft 2 of the coupling half. A recommended lever-articulated coupling 3 is installed between shafts 1 and 2. 4 and 5 are connected in a half-bridge circuit according to [106], which are connected to amplifier 11 through current collectors 6 and 7. Amplifier 11 is powered by a 220V power source. The amplified signals from amplifier 11 are transmitted to oscilloscope 12, which is powered by current rectifier 10. Rectifier 10 is powered by a 220 V source. At the ends of shafts 1 and 2, magnetolectric sensors 8 and 9 are installed, the signals from which are directly transmitted to the oscilloscope 12. At the same time, one of the teeth of the sensor sprocket 8 and 9 is cut off, and therefore, when these short teeth pass in front of the sensors, each revolution of shafts 1 and 2 is recorded. Magnetolectric sensors 8 and 9 receive signals with a frequency within 6.3 MHz-3.4 MHz. The signals are transmitted to the H-115 oscilloscope, galvanometers, which, by reflecting light from a halogen lamp, implement signals on the screen of the oscilloscope 12. These signals were recorded on oscillographic paper. On fig. 4.4. *a* - a photograph of the magnetolectric sensor 8 is shown, and in figure. 4.4. *b* - used equipment.

To measure the torques in the coupling shafts, sensors of the 2PKB-20-200GV brand with a base of 20 mm were used. The recording of torques and circular frequency of the driving and driven shafts of the lever-articulated coupling was recorded on an oscilloscope with photo paper of the UV type. Strain gauges on the cleaned surfaces of the shafts were glued with BF-3 glue



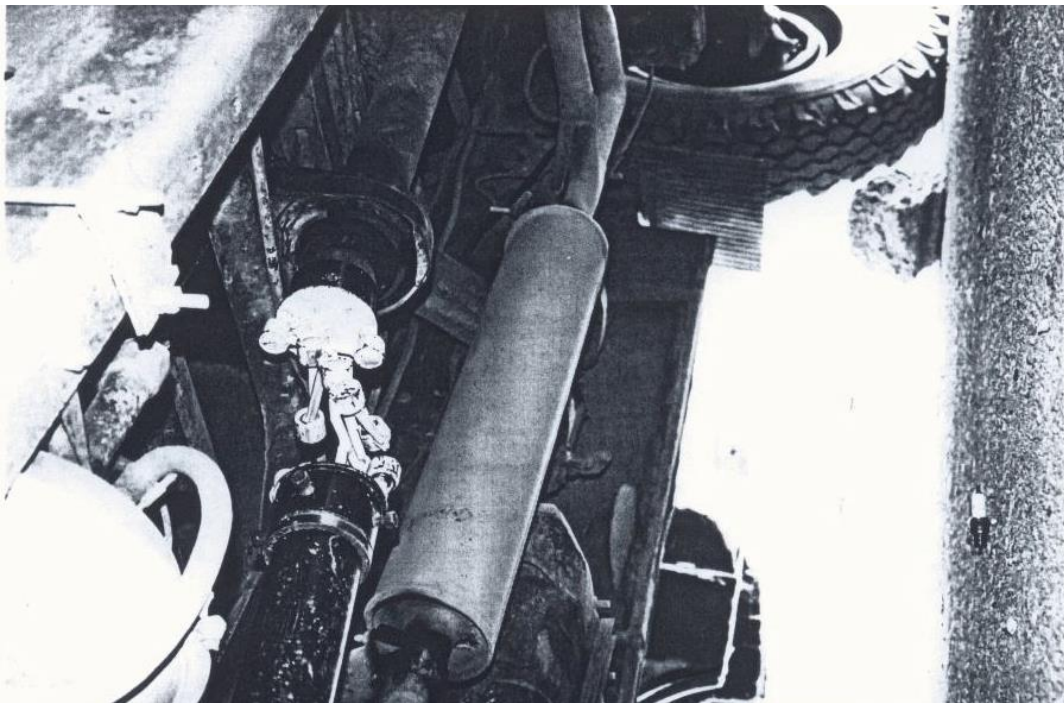
where, 1-drive shaft of the cardan mechanism; 2 driven shaft; 3-lever coupling; 4-drive shaft load cells; 5-strain gauges on the driven shaft; 6,7-current collectors; 8,9-magnetolectric sensors;

10-strain amplifier; 11-rectifier; 12-oscilloscope.

Fig.. 4.2. Scheme of electrical strain gauging of a cardan mechanism with a lever-articulated coupling



a



b

Figure. 4.3.

a - view of the cardan mechanism with a lever-articulated clutch with strain gauges;

b - bottom view of the lever-articulated coupling of the cardan mechanism



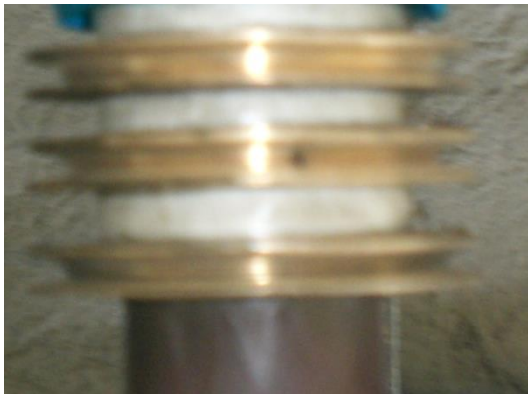
A



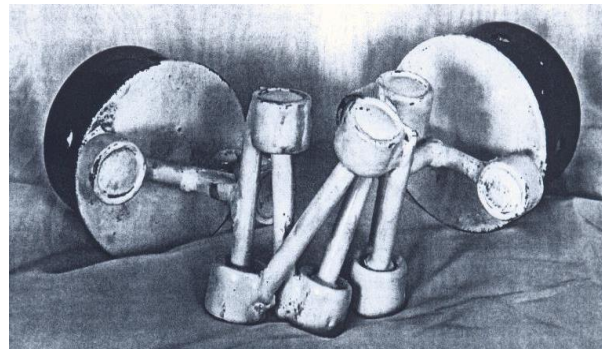
b

Figure.4.4.

a - magnetoelectric sensor; *b* - strain gauge.



A



b

Figure.4.5.

a - current collector;

b - lever-articulated coupling in the position of the maximum angle of divergence of the shafts.

half-bridge scheme, at an angle 45° to the axis of the shafts. The torques were recorded in an oscilloscope with galvanometers of the M₀₀₄ type with a frequency of 400 Hz. Recording was carried out at a cassette rotation speed of 50 mm/s. Recording was carried out in triplicate. Calibration was carried out

with a special lever, weights (20÷400) kg according to the prepared technique [106], calibration graphs were built.

4.2. Processing and analysis of experimental results

To conduct experimental research on the KAVZ-685 car bushings were made from various grades of rubber (see table 4.1) for installation in a lever-articulated coupling. The technological load in the driven shaft of the coupling was regulated by a special brake unit. As a result of the experiments, a number of oscillograms were obtained, in which the moments and angular frequencies of rotation of the driving and driven shafts of the lever-articulated clutch were recorded.

The processing of oscillograms was carried out according to the methodology given in the works of G.V. Vedenyapin and R. Manly [108,109].

On fig. 4.6 shows an oscillogram, which shows the transitional start-up of the system corresponding to the mechanical characteristics of the coupling drive shaft. It can be seen from the oscillogram that the drive shaft reaches the steady state in 0.42 s. In this case $\dot{\varphi}_1 = 39,0c^{-1}$, it should be noted that the angular frequency of the driven shaft $\dot{\varphi}_2 = 39,0c^{-1}$, but between the rotations of the shafts in terms of angular velocity, there is some phase shift (see Figure 4.6).

In this case, $M_c = 0$, therefore, M_1 of the characteristic fluctuates near the zero line. With an increase in the angle of divergence of the driving and driven shafts (measured using a special device), the amplitude of the moment oscillations increases sharply.

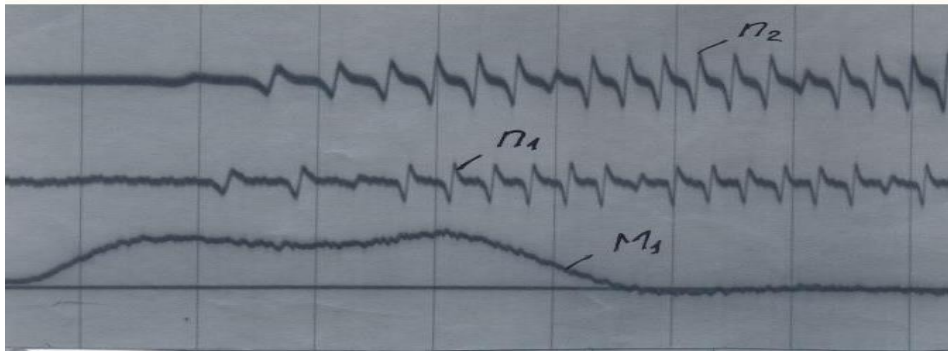
On figure 4.6. b shows an oscillogram, where the amplitude of the torque oscillations on the drive shaft reaches $15 \div 40$ Nm, with a technological load $M_c = 350 \pm 21$ Nm, and an angle of divergence of the shafts of 16° . It should be noted that with an increase in the angle of divergence of the coupling shafts, the amplitude of the transfer function oscillations increases. Elastic bushings in the

support of the driven shaft and in the hinge of the earring with the connecting rod to some extent reduce the amplitude of the oscillations of the drive shaft. This can be seen from the waveform shown in Figure 4.6 in. From where it can be seen that the moment M_2 on the driven shaft of the lever-articulated coupling of the cardan mechanism of the car fluctuates according to a harmonic law corresponding to the rotational speed of the driven shaft 35.6 s^{-1} . At the same time, the high-frequency component of the torque oscillations on the driven shaft of the clutch is within $415 \div 425 \text{ s}^{-1}$. As can be seen from the obtained regularity of the change in the torque M_1 on the drive shaft of the lever-articulated clutch due to the elastic elements, it has a smoother character. The oscillation amplitude is 25-30 % less than the amplitude of the moment M_2 oscillations on the driven shaft. In addition, the oscillation amplitude of the random component of the moment M_1 decreased by 3-4.5 times than the amplitude of the oscillations of the random component of the moment M_2 . On the oscillogram in Figure 4.6. in the average values of M_1 and M_2 are equal to each other (zero line of the moment M_1 moved up).

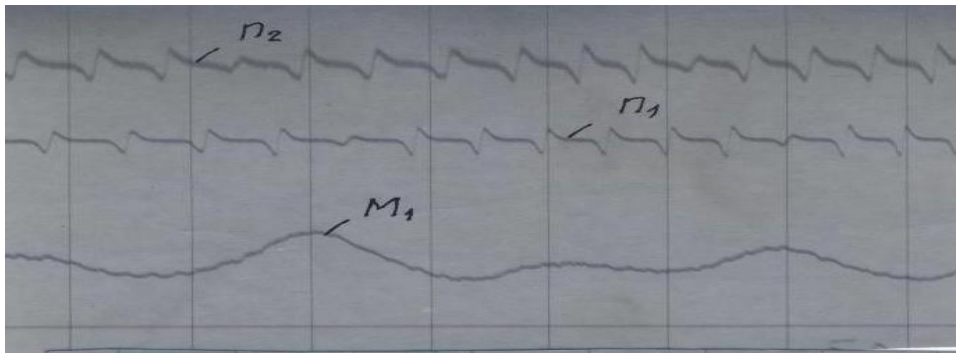
With a decrease in the angle of divergence between the driving and driven shafts, the amplitude of the oscillations of the moments M_1 and M_2 are also decreasing. But at the same time, the influence of elastic-dissipative characteristics on the laws of change of M_1 and M_2 .

M_1 and M_2 is more important, which directly affects the reliability of the car drive. On fig. 4.7 shows the obtained oscillograms, which show the patterns of change in M_1 , M_2 , n_1 and n_2 when using various grades of rubber as elastic elements of a lever-articulated coupling.

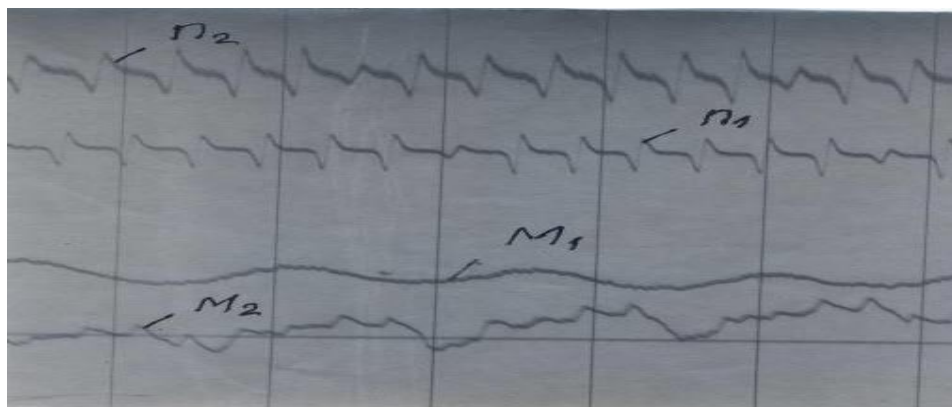
When using the rubber brand 7I P P 13-48 with a torsional stiffness of $\div 1200-1400 \text{ Nm / rad}$, the vibration amplitude M_1 reaches 15-32



a



b



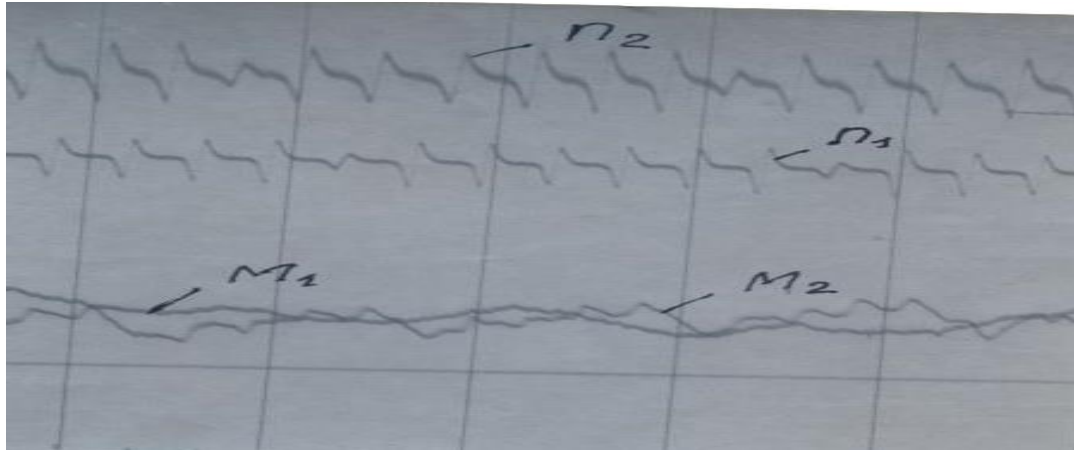
v

Figure 4.6.

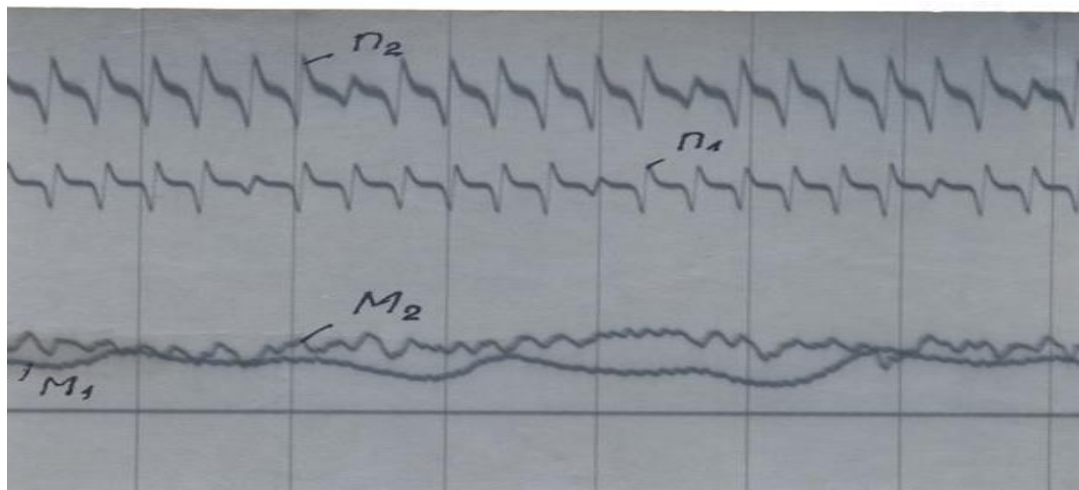
a - Oscillogram characterizing the output to the steady state of the drive shaft of the lever-articulated clutch. $n_1 = 374.8$ rpm, $n_2 = 372.6$ rpm ;

b - patterns of change in torque on the drive shaft and patterns n_1 and n_2 ;
at $M_c \approx 350 \pm 21$ Nm, $\alpha = 16^\circ$

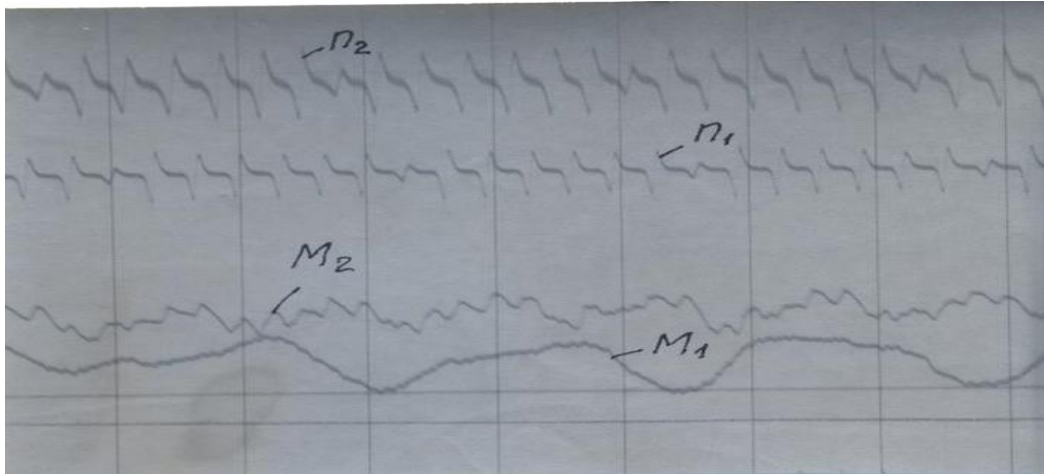
v - load and frequency of rotation of the coupling shafts when using rubber grade 3826 MVS.



a



b



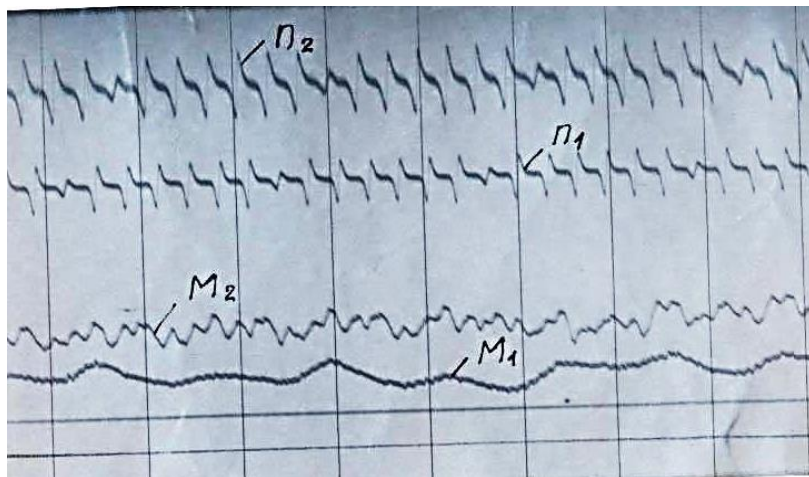
v

Figure.4.7. Oscillograms of the patterns of change in M_1 and M_2 , n_1 n_2 at use in couplings of rubbers of various grades

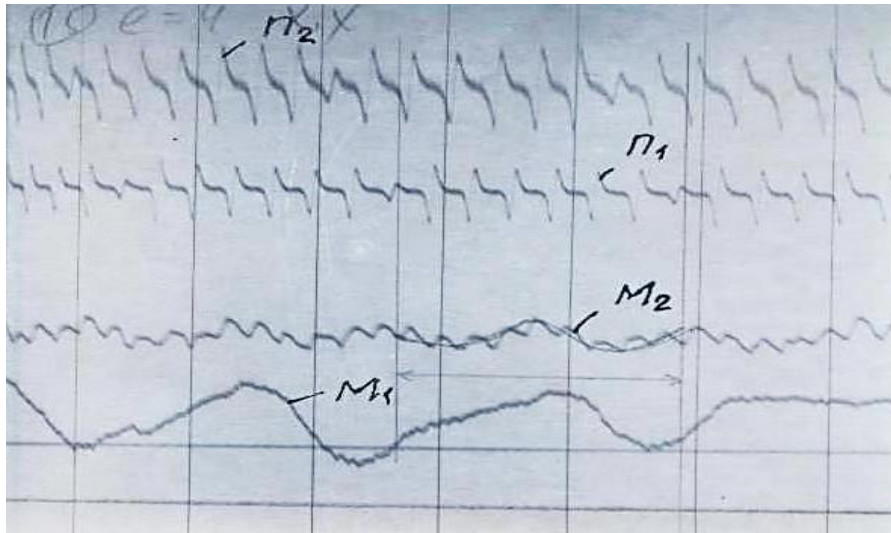
a - rubber grade 7IRP 13-48 (1200 Nm / rad);

b - brand of rubber 7V -14 MVS (750 Nm / rad)

v - brand of rubber 1847 (650 Nm/rad)



g



d

Figure.4.7. (Continuation)

g - brand of rubber 17IRP 13-46 (900 Nm / rad);

d - brand of rubber 3826 MVS (450 Nm / rad)

Nm, at $M_c = 250 \pm 15.0$ Nm and $\alpha = 5^\circ$ (see Fig. 4.7.a). The use of rubber grade 7V-14MVS with a torsional rigidity of 850 Nm / rad, the difference in vibrations between M_1 and M_2 is significantly reduced (see Figure 4.7. b). This is explained by the fact that with an increase in rigidity, the system becomes, as it were, a single, massive one. In addition, with a large torsional terrain of the elastic elements of the lever-articulated coupling, the amplitudes of the oscillations of the moments decrease to $9.0-15.0 \pm$ Nm. In this case, the random component of torque fluctuations is only sufficiently absorbed. There is a phase shift between M_1 and M_2 and also between the frequencies of rotation of the shafts n_1 and n_2 up to $0.03 \div 0.04 \pi$. This is due to the deformation of the elastic elements in the coupling. The greater the value of deformation of the elastic elements, the greater the phase shift between M_1 , M_2 and n_1 , n_2 . With a decrease in the torsional rigidity of the elastic elements of the coupling, the vibration amplitudes M_1 and M_2 (rubber grade 1847). When using rubber grade 382 MVS with a torsional rigidity of $450 \div 550$ Nm / rad, the amplitude of vibrations M_1 reaches $51 \div 64$ Nm, and the phase shift between them will

increase to $0.07 \div 0.1 \pi$, which negatively affects the operation of the car's cardan mechanism (see Fig. . 4.7 r. d .). Tables 4.2, 4.3, 4.4, 4.5, 4.6 show the results of M_1 values from the corresponding oscillograms, as well as in tables 4.7÷4.11. M_2 values .

Analysis of the data given in Table 4.2 shows that when using the rubber brand 7IRP 13-48 as an elastic element, the average value of the torque on the drive shaft is in the range of $199.1 \div 252.4$ Nm, that is, the oscillation amplitude reaches 26.5 Nm (at $\alpha = 16^\circ$). With a decrease in the angle of divergence of the shafts to 5° , the amplitude of the oscillations of the torque M_1 decreases to $8.0 \div 12.0$ Nm.

In this case, respectively, the amplitude of oscillations of the torque on the driven shaft of the coupling of the cardan mechanism is within $14-18 \div$ Nm (see Table 4.7). So when using the specified brand of rubber, the peak torque values are reduced to 6.0 Nm. When using rubber with lower torsional stiffness, this value becomes significant. So when using rubber grade 7V-14MVS in a lever-articulated clutch (see tables 4.3 and 4.8), the torque of the driven shaft varies within $172.1 \div 268.1$ Nm, and the moment M_1 varies within $185 \div 262$ Nm.

Table 4.2

No.	Angle of rotation of the drive shaft, degree	The value of the moment on the drive shaft of the muff when using rubber brand 7 IRP-13-48, 10 Nm						Average value Torque, M_1 , 10 Nm
		1 cycle	2 cycle	3 cycle	4 cycle	5 cycle	6 cycle	
1	0.360	22.3	23.1	20.5	19.8	18.9	21.6	20.75
2	thirty	19.4	19.9	20.2	20.5	19.7	20.7	19.68
3	60	20.7	21.6	22.8	21.3	20.5	19.9	20.85
4	90	25.4	26.2	22.9	21.9	19.6	22.1	23.61
5	120	26.1	25.6	25.5	24.2	24.2	25.2	25.32
6	150	22.1	22.2	27.1	26.2	25.1	26.3	25.24
7	180	20.3	23.1	24.3	25.5	26.4	24.8	24.46
8	210	19.9	19.6	23.3	25.2	23.3	21.9	22.85
9	240	18.7	20.7	20.0	23.8	22.2	19.4	20.80
10	270	20.1	20.1	18.5	20.2	20.4	21.5	20.05
eleven	300	20.8	19.9	19.9	19.0	18.9	19.2	19.91
12	330	21.4	20.4	18.6	18.2	19.6	20.0	19.93

Table 4.3

No.	Angle of rotation of the drive shaft, φ_1 degree	The value of the torque on the drive shaft of the coupling when using rubber brand 7V-14MVS, 10 Nm						Average value
		1 cycle	2 cycle	3 cycle	4 cycle	5 cycle	6 cycle	Torque, M_j , 10 Nm
1	0.360	18.3	17.9	18.6	17.8	19.2	18.7	18.5
2	thirty	20.2	19.7	20.4	19.6	19.58	20.9	19.9
3	60	19.4	18.8	19.7	18.4	20.1	19.2	19.4
4	90	23.5	20.6	22.9	20.2	22.6	20.8	22.5
5	120	24.8	22.8	23.8	21.9	25.21	24.5	24.2
6	150	26.4	26.9	26.6	26.8	26.1	26.8	26.2
7	180	25.2	26.0	25.4	25.9	26.2	26.1	26.1
8	210	24.1	24.6	24.2	24.4	25.3	24.6	24.5
9	240	20.9	20.2	20.6	19.9	22.3	20.4	20.7
10	270	19.4	19.3	19.1	18.7	20.6	20.1	19.5
eleven	300	20.5	18.7	20.2	19.6	19.2	19.6	19.3
12	330	18.9	17.9	18.8	18.7	19.6	19.1	18.6

Table 4.4

No.	Angle of rotation of the drive shaft, φ_1 degree	The value of the torque on the drive shaft of the coupling when using rubber brand 1338, 10 Nm						Average value
		1 cycle	2 cycle	3 cycle	4 cycle	5 cycle	6 cycle	$M_{1,10Nm}$
1	0.360	16.1	17.3	16.0	16.3	17.1	16.0	16.5
2	thirty	21.2	20.8	22.2	21.6	20.9	22.4	21.6
3	60	20.8	21.7	20.9	22.6	23.5	23.1	22.1
4	90	25.3	22.9	25.6	24.8	25.1	24.8	24.0
5	120	26.8	27.3	28.1	27.3	27.4	27.6	27.3
6	150	28.2	29.1	29.0	28.8	28.9	29.3	28.6
7	180	27.3	28.2	28.1	27.8	27.5	28.6	27.9
8	210	26.23	26.9	25.9	26.1	25.4	26.5	26.4
9	240	22.1	22.4	22.9	24.1	23.9	24.2	23.1
10	270	21.5	21.3	20.9	22.5	22.4	23.1	21.9
eleven	300	19.5	18.25	17.8	19.6	19.4	20.2	19.3
12	330	17.4	16.9	16.8	18.1	17.4	16.7	17.2

Table 4.5

No.	Angle of rotation of the drive shaft, φ_1 degree	The value of the torque on the drive shaft of the coupling when using rubber brand 1897, 10 Nm						Average value
		1 cycle	2 cycle	3 cycle	4 cycle	5 cycle	6 cycle	$M_{1,10Nm}$
1	0.360	18.4	18.0	18.2	17.7	19.4	18.5	18.3

2	thirty	19.9	20.1	20.5	19.4	19.9	21.0	19.6
3	60	19.2	18.5	19.4	18.1	20.2	19.6	19.5
4	90	22.6	21.2	22.8	20.4	23.1	20.4	22.4
5	120	24.9	22.9	23.7	22.4	25.4	24.1	24.5
6	150	26.8	26.9	26.8	26.9	26.7	26.6	26.8
7	180	25.6	26.32	25.4	26.1	27.1	26.4	26.4
8	210	24.3	24.2	23.9	23.8	25.34	25.1	24.7
9	240	20.4	20.4	21.0	20.4	22.1	20.3	20.9
10	270	19.1	19.4	18.9	18.6	19.9	20.1	19.3
eleven	300	20.1	18.3	17.9	19.4	18.9	18.8	19.1
12	330	19.1	17.9	18.1	18.2	18.5	18.0	18.3

Table 4.6

No.	Angle of rotation of the drive shaft, φ_1 degree	The value of the moment on the drive shaft of the coupling using rubber grade 3826 MVS, 10 Nm						Average value $M_{1,10Nm}$
		1 cycle	2 cycle	3 cycle	4 cycle	5 cycle	6 cycle	
1	0.360	22.1	23.2	20.4	19.6	19.1	21.4	20.6
2	thirty	19.7	21.1	21.4	20.6	20.2	21.1	20.15
3	60	20.4	20.3	23.1	21.9	20.9	22.4	21.23
4	90	24.9	25.7	24.6	24.3	19.3	23.5	24.36
5	120	27.3	26.5	27.3	26.5	25.4	28.1	26.74
6	150	23.3	24.6	27.4	28.1	26.0	26.6	27.17
7	180	20.4	23.5	25.1	25.2	26.8	24.3	24.53
8	210	19.7	19.9	22.9	24.1	22.9	22.3	22.2
9	240	18.2	20.4	20.1	21.7	20.9	19.9	20.74
10	270	20.4	21.5	18.9	19.9	20.1	20.9	20.25
eleven	300	16.4	18.6	17.7	17.2	17.8	17.1	17.22
12	330	20.9	20.3	20.1	18.1	19.9	18.9	19.51

Table 4.7

No.	Angle of rotation of the driven shaft, φ_2 degree	The value of the moment on the driven shaft of the coupling using rubber grade 7IRP 13-48, 10 Nm						Average value $M_{2,10Nm}$
		1 cycle	2 cycle	3 cycle	4 cycle	5 cycle	6 cycle	
1	0.360	22.4	23.3	20.3	19.7	18.6	21.8	20.66
2	thirty	19.2	19.6	19.6	20.7	19.9	20.4	19.71
3	60	20.8	21.7	22.8	21.1	20.7	18.9	20.73
4	90	25.5	26.4	23.5	20.9	18.9	22.4	23.15
5	120	26.3	25.9	25.4	24.5	23.7	25.8	25.22
6	150	22.3	26.2	26.6	26.7	26.1	23.6	25.91
7	180	20.1	22.2	24.2	24.9	25.9	25.7	24.16
8	210	19.7	23.5	23.1	25.7	23.4	24.6	23.49
9	240	18.5	19.4	20.4	22.9	22.1	21.7	20.33

10	270	20.3	20.8	18.2	20.6	19.8	19.2	19.88
eleven	300	21.1	19.3	20.1	18.9	21.1	21.3	20.84
12	330	20.7	20.5	18.7	20.1	18.7	18.9	19.41

Table 4.8

No.	Angle of rotation of the driven shaft, $\dot{\phi}_2$ degree	The value of the moment on the driven shaft of the coupling using rubber grade 7-14, MVS, 10 Nm						Average value
		1 cycle	2 cycle	3 cycle	4 cycle	5 cycle	6 cycle	$M_{2,10Nm}$
1	0.360	17.0	17.6	17.3	17.2	18.0	17.1	17.21
2	thirty	20.4	19.8	20.7	20.1	19.9	20.6	20.34
3	60	19.1	18.4	19.3	18.1	20.4	18.9	19.22
4	90	23.4	20.9	22.4	20.5	19.2	21.4	21.86
5	120	25.1	22.9	24.3	21.8	23.8	24.4	24.12
6	150	25.3	26.7	26.8	25.9	26.1	26.8	26.81
7	180	26.2	24.8	25.1	24.9	25.2	24.9	25.32
8	210	24.3	24.1	23.9	26.1	26.1	25.7	24.96
9	240	20.7	20.1	20.2	20.8	21.8	22.2	20.63
10	270	19.2	18.9	18.8	18.3	19.1	18.8	18.95
eleven	300	21.1	20.1	20.6	20.2	17.9	20.3	20.1
12	330	18.7	17.5	18.2	18.1	18.5	18.4	18.31

Table 4.9

No.	Angle of rotation of the driven shaft, $\dot{\phi}_2$ degree	The value of the moment on the driven shaft of the coupling using rubber grade 1338, 10 Nm						Average value
		1 cycle	2 cycle	3 cycle	4 cycle	5 cycle	6 cycle	$M_{2,10Nm}$
1	0.360	17.2	16.9	16.6	16.1	15.9	16.2	16.46
2	thirty	20.8	20.5	18.3	19.4	17.8	19.3	19.37
3	60	19.3	21.8	20.2	21.5	19.9	21.5	20.64
4	90	24.5	19.1	18.9	19.1	21.7	23.1	22.47
5	120	26.4	24.6	24.2	23.9	24.6	25.5	25.05
6	150	24.9	26.9	28.6	27.8	28.1	28.2	27.71
7	180	27.1	28.8	29.1	29.2	28.5	29.1	28.59
8	210	25.8	25.8	26.3	25.9	26.1	27.2	26.52
9	240	23.9	26.4	23.9	22.8	23.3	24.4	24.61
10	270	20.2	22.1	21.6	20.2	20.3	20.1	21.12
eleven	300	21.3	18.9	19.3	18,7	18.2	19.1	19.36
12	330	18.2	20.5	17.3	16.4	16.5	16.7	17.81

Table 4.10

No.	Angle of rotation of the driven shaft, $\dot{\phi}_2$ degree	The value of the moment on the driven shaft of the coupling using rubber grade 1338, 10 Nm						Average value
		1 cycle	2 cycle	3 cycle	4 cycle	5 cycle	6 cycle	$M_{2,10Nm}$
1	0.360	18.1	17.8	17.9	17.5	18.4	17.7	17.91
2	thirty	19.7	20.4	20.6	19.6	20.2	20.5	20.36
3	60	18.9	18.2	18.9	17.9	20.9	19.1	18.97
4	90	22.7	21.5	22.8	19.7	24.1	23.8	22.84
5	120	25.2	23.4	24.1	23.2	22.8	21.6	23.49
6	150	26.7	26.8	26.5	26.2	26.1	25.9	26.36
7	180	25.1	25.5	24.6	24.7	25.2	26.2	25.42
8	210	24.0	24.1	22.3	25.1	23.7	24.0	24.18
9	240	21.0	20.2	20.5	21.3	21.9	21.5	21.17
10	270	18.9	19.3	18.7	19.5	18.6	18.3	18.89
eleven	300	20.3	20.5	19.9	18.3	19.4	19.8	19.68
12	330	18.8	18.2	18.4	19.1	18.2	17.9	18.37

Table 4.11

No.	Angle of rotation of the driven shaft, $\dot{\phi}_2$ degree	The value of the moment on the driven shaft of the coupling using rubber grade 3826 MVS, 10 Nm						Average value
		1 cycle	2 cycle	3 cycle	4 cycle	5 cycle	6 cycle	$M_2, 10Nm$
1	0.360	19.4	21.3	20.3	19.5	19.2	20.6	20.18
2	thirty	22.2	18.7	21.2	20.4	20.4	21.5	20.46
3	60	18.9	20.8	23.3	21.6	21.1	22.7	21.65
4	90	20.5	22.5	24.4	24.2	19.5	20.9	22.71
5	120	25.2	26.1	26.2	26.5	24.8	26.1	25.86
6	150	27.1	25.6	26.7	27.2	25.8	24.9	26.21
7	180	24.2	24.1	25.0	25.4	24.9	26.2	25.11
8	210	22.8	19.9	23.1	24.6	22.9	22.8	22.83
9	240	24.1	20.4	20.4	21.2	23.3	20.9	22.19
10	270	19.7	21.6	19.2	19.3	20.5	20.1	19.73
eleven	300	20.6	19.4	18.6	20.1	18.9	19.1	19.38
12	330	18.9	20.4	19.8	18.9	19.6	20.2	19.66

In this case, the difference in the amplitudes of oscillations of the moments M_2 and M_1 is $8.2 \div 12.9$ Nm at $\alpha = 5^\circ$, and with an increase in the angle of divergence to $1, 5^\circ$ this difference reaches $13.0 \div 15.0$ Nm.

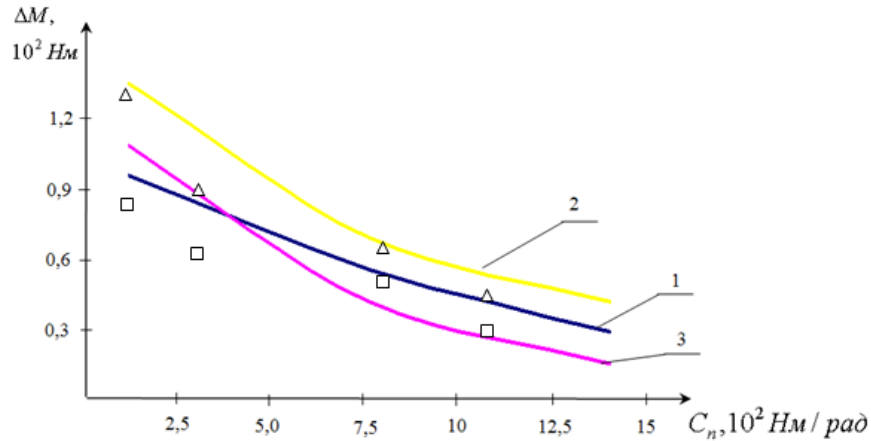
When using rubber grades 1338 (tables 4.4 and 4.9) and 3826 MBC (tables 4.6 and 4.11), the range of torque fluctuations on the drive shaft is $58.0 \div 112.5$ Nm, and on the driven shaft $92.7 \div 126.2$ Nm. It can be seen from them that when using rubber grades with lower torsional rigidity, the decrease in vibration amplitudes on the drive shaft occurs insignificantly, the influence of the elastic element on the operation of the lever-articulated clutch becomes ineffective.

From this point of view, 7V-14MVS rubber with a torsional rigidity of 710-850 Nm/rad is the most suitable for reducing the amplitudes of torque oscillations on the drive shaft of a lever-articulated clutch.

Figure 4.8 shows graphical dependences of the change in the average values of the range of torque fluctuations on the driving and driven shafts of the lever-articulated clutch on the variation of the reduced torsional stiffness of the elastic elements of the coupling of the cardan mechanism.

The analyzes have established that an increase in the reduced torsional stiffness of the elastic elements leads to a decrease in the average values of the range of torque oscillations on the driving and driven shafts according to a non-linear pattern. Moreover, with an increase in the stiffness coefficient C_n , the difference between ΔM_1 and ΔM_2 decreases. So at $C_n \approx 450$ Nm / rad and $M_c \approx 380 \pm 15$ Nm, the difference between ΔM_1 and ΔM_2 is on average 24.3 Nm, and at $C_n \approx 1250$ Nm / rad, this difference decreases to 8.8 Nm, that is, three times. With an increase in the angle of divergence of the axes between the driving and driven shafts of the coupling, this difference becomes negative. Therefore, it is expedient to choose the coefficients of the reduced stiffness of the elastic elements of the lever-hinge coupling in the range of 820-875 Nm/rad, which corresponds to the rubber grade 7V-14MVS.

Where in where, 1- $M_{1cp} = f(C_n)$, 2- $M_{2cp} = f(C_n)$; 3- $M_{cp} = f(C)$



1,2-experimental curves, 3-theoretical curves

Figure 4.8. Dependence of the change in the average values of the range of torque fluctuations on the driving and driven shafts of the lever-articulated coupling of the cardan mechanism as a function of the reduced stiffness coefficient of the elastic elements

the range of torque fluctuations on the drive shaft is reduced by $13.0 \div 15.0 \text{ Nm}$ at $M_c = 350 \pm 15 \text{ Nm}$ and $\alpha = 1.5^\circ$. It should be noted that the patterns of change $\Delta M_1, \Delta M_2$ obtained experimentally sufficiently coincide with the curve obtained by theoretical studies (see. Figure 4.8, curves 1,2,3). The difference between the theoretical and experimental curves when using rubber grade 7V-14MVS is $6.5-8.5 \pm \%$. Taking into account, $\dot{\varphi}_1 = \pi n_1 / 30, \dot{\varphi}_2 = \pi n_2 / 30$, the obtained results of the unevenness of the drive and driven shafts of the lever-articulated clutch of the transmission of the KAVZ-685 vehicle were calculated.

Figure 4.9 shows graphical dependences of the change in the unevenness of the angular velocities of the drive and driven shafts of the lever-articulated clutch on the change in the reduced coefficient of torsional stiffness of the elastic elements of the coupling in the cardan mechanism. It can be seen from them that the increase in C_n will lead to a decrease $\delta_1 u \delta_2$ in a non-linear pattern. Moreover, as the difference increases, the difference $\delta_1 u \delta_2$ decreases. So at $C_n = 450 \text{ Nm/rad}$, the unevenness of the angular velocities of the shafts $\delta_2 =$ is 0.165

and $\delta_1 = 0.141$, and at $C_n = 1250 \text{ Nm/rad}$, the unevenness $\delta_2 = 0.088$ and $\delta_1 = 0.056$. As C_n increases, the difference between δ_1 and δ_2 decreases to 0.032. With the recommended brand of rubber 7V-14MVS, $\delta_1 \leq 0.075 \div 0.11$ and is provided $\delta_2 \leq 0.12 \div 0.15$.

The analysis of the conducted experiments shows that the elastic elements in the lever-articulated coupling make it possible to reduce the amplitudes of the oscillations of the torque M_1 and the unevenness of the angular velocity $\dot{\varphi}_1$ of the drive shaft relative to M_2 and $\ddot{\varphi}_2$. But, at the same time, the main pattern of fluctuations M_1 and $\dot{\varphi}_1$ decrease to a lesser extent from changes in the transfer function U_{12} and angle α . Elastic elements mainly reduce vibrations arising from

where, 1,2- $\delta = f(C_n)$ - experimental curves; 3- $\delta = f(C_n)$ theoretical curve.

$$1 - \delta_1 = f(C_n); 2 - \delta_2 = f(C_n); 3 - \delta_{cp} = f(C_n)$$

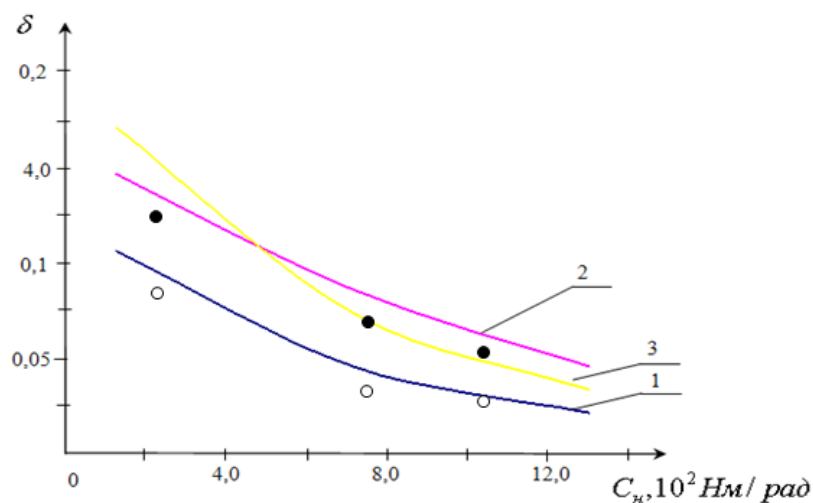
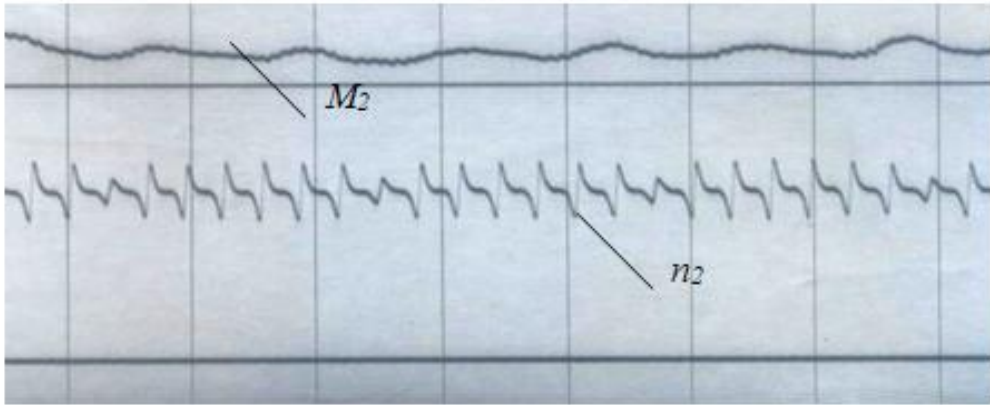


Figure .4.9. Graphic dependences of the change in the coefficient of unevenness of the angular velocities of the driving and driven shafts of the lever-articulated coupling as a function of the torsion of the reduced stiffness coefficient of the elastic elements

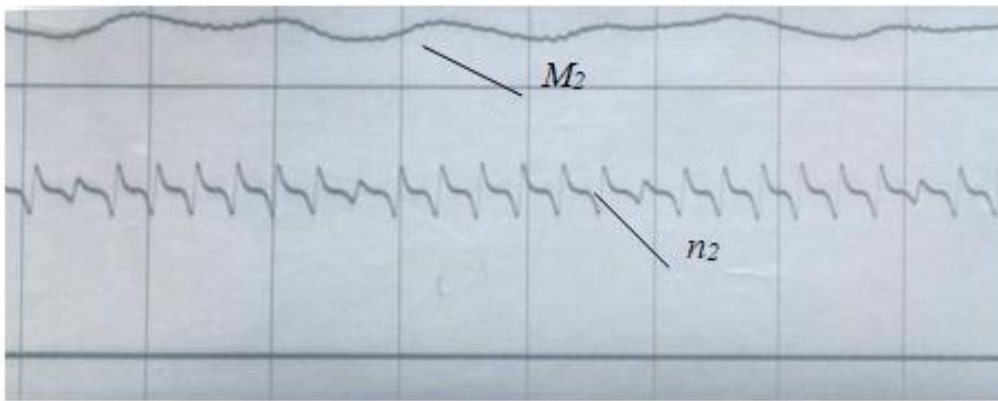
technological load. Therefore, when conducting experiments, it is important to study the influence of elastic elements on the decrease in the amplitude of vibrations M_1 and $\dot{\varphi}_1$ at various values of technological resistance on the driven shaft of the lever-articulated coupling of the cardan mechanism of a motor vehicle. KaV3-685.

On figure 4.10 shows oscillograms characterizing M_2 and n_2 ($\dot{\varphi}_2$) with a variation in the moment of resistance M_s . On osc. 1 (Figure . 4. 10) the amplitude of oscillations A_{M_2} reaches $32 \div 34.2$ Nm at $M_c \approx 320 \pm 12$ Nm and $\alpha = 5^\circ$ using rubber grade 7V-14 MVS. With an increase in the technological load M_{with} up to 420 ± 15 Nm and $\alpha = 5^\circ$, in fact, the amplitude of oscillations A_{M_2} increases slightly, up to $35.4 \div 46.1$ Nm. In this case, the angular velocity decreases from 37.8 rad/s to 35.3 rad/s. A further increase in the technological load on the driven shaft of a lever-articulated coupling leads to a significant increase in torque on the driven and driving shafts of the coupling. So at $M_c = 450 \pm 21.5$ Nm and $\alpha = 15^\circ$ the amplitude of oscillations A_{m_2} reaches $54.3 \div 68.1$ Nm (see Figure. 4.10, osc. 3), and the angular velocity decreases to 33.6 rad / s. Therefore, at large angles α discrepancies between the axes of the driving and driven shafts lever-articulated coupling, it is considered expedient to reduce the moment of technological resistance in the transmission of a car.

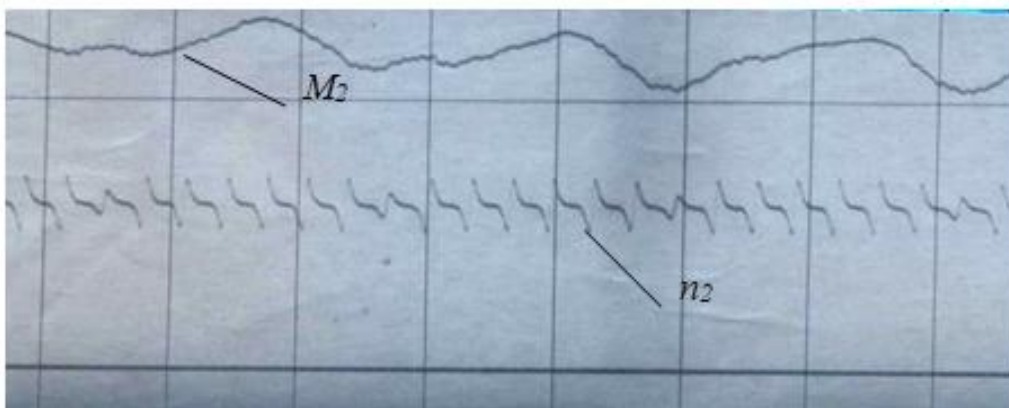
On fig. 4.11 shows oscillograms characterizing the patterns of M_1 and n_2 ($\dot{\varphi}_1$) of the drive shaft of the lever-articulated coupling of the cardan mechanism of the KAVZ - 685 machine. It can be seen from them that at $\alpha = 0$ and a technological load of 65.4 ± 5.3 Nm, the moment on the coupling drive shaft does not change significantly, the amplitude of oscillations A_{M_1} reaches $6.3 \div 8.1$ Nm. With an increase in the moment of resistance M with up to 320 ± 12 Nm and $\alpha \approx 0^\circ$, amplitude of oscillations of the moment M_1 actually increases slightly, up to $7.5 \div 9.1$ Nm. With an increase in M_s to 450 ± 21.5 Nm at $\alpha \approx 5^\circ$, the amplitude



1



2



3

Figure 4.10. Oscillograms of records of patterns of change in torque and speed of rotation of the driven shaft of the lever-articulated clutch of the cardan mechanism of the car vibrations A_{M1} increases to $30.1 \div 39.3$ Nm.

where, 1 – at $M_s = 320 \pm 12$ Nm and $\alpha = 5^0$; 2 – at $M_s = 410 \pm 15$ Nm and $\alpha = 5^0$; 3 - at $M_s = 450 \pm 21.5$ Nm and $\alpha = 15^0$.

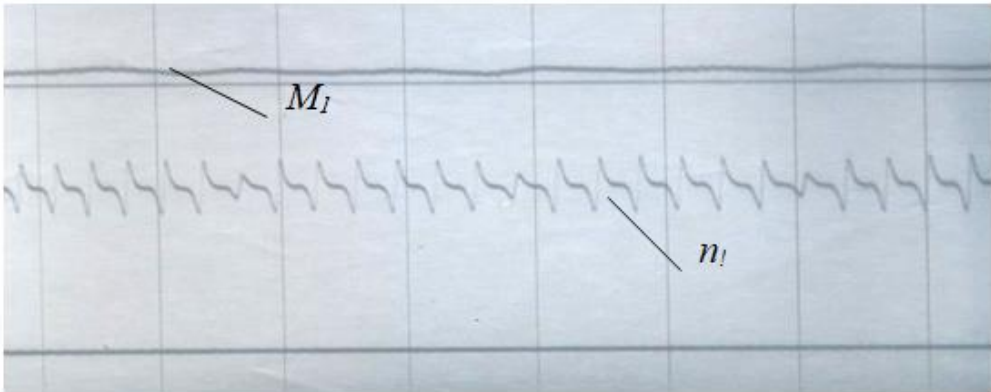
It should be noted here that in order to reduce the amplitude of A_{M1} , it is necessary to take into account the influence of the elastic-dissipative characteristics of the elastic bushings used in the lever-articulated coupling of the cardan mechanism of the machine.

On fig. 4.12 shows the constructed graphical dependences of the change in the amplitude of torque oscillations in the driving and driven shafts of the coupling. From the graphs in Figure 4.12. it can be seen that with an increase in M_c from 65.4 ± 5.3 Nm to 450 ± 21.5 Nm, the difference between A_{M1} and A_{M2} increases from 3.5 Nm to 9.46 Nm at $\alpha = 0$ and at $\alpha = 5^0$, this the difference does not actually change. In addition, it should be noted that a comparison of the results of theoretical and experimental studies shows their necessary agreement, the difference between curves 3 and 5 (see Figure. 4.12) does not exceed 5.2 8.1%, and between ÷ curves 6 and 4 this difference is 5 .4 ÷ 7.6%. According to the analysis, for the considered transmission of the KAVZ -685 car, the use of a lever-articulated clutch with elastic elements is considered appropriate $\alpha \leq 5.0 \div 10^0$;; $M_s \leq 420 \div 450$ Nm at $\delta M_s \leq (0.05 \div 0.1) M_s$; $C_n \backslash u003d 700 \div 850$ Nm / rad; $\delta_1 \leq 0.075 \div 0.11$; $\delta_1 \leq 0.12 \div 0.15$.

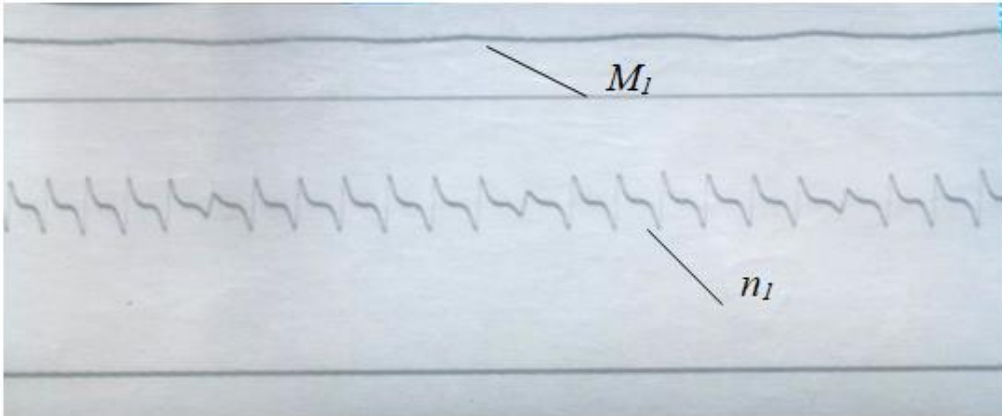
4.3. Harmonic Analysis of Torque on the Driven Shaft of a Lever-Hinge Clutch

To analyze the speed-loaded characteristics of the vehicle transmission elements, in particular the cardan mechanism with a lever-articulated clutch, it is important to determine the angle and the nature of technological and external loads. This load is mainly formed from the unevenness of the ground, the coefficient of friction of the tire of the machine with the ground, the force of the

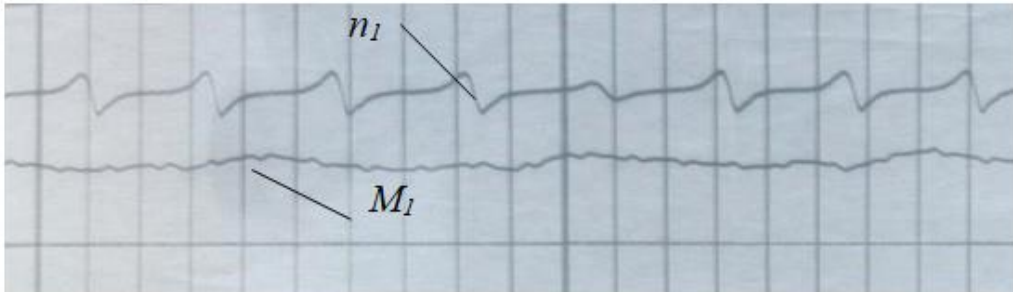
weight of the load in the machine, and also from the efficiency gears in the transmission, etc.



1



2



3

Figure. 4.11. Oscillograms of recording the patterns of torque of the rotation frequency of the drive shaft of the lever-articulated clutch of the transmission of the KAVZ -685 car.

The characteristics and values of technological resistance in the transmission of the car are determined by processing where: 1 - at $M_c = 65.4 \pm 5.3 \text{ Nm}$ and $\alpha = 0$; 2 - at $M_c = 320 \pm 12 \text{ Nm}$ and $\alpha = 0$; 3 - at $M_c = 450 \pm 21.5 \text{ Nm}$ and $\alpha = 5^\circ$;

Where:

1, 2, 3, 4 – experimental curves; 5, 6 - theoretical curves

1 - $A_{M2} = f(M_c)$, 2 - $A_{M1} = f(M_c)$ at $\alpha = 0^\circ$;

3 - $A_{M2} = f(M_c)$, 4 - $A_{M1} = f(M_c)$ at $\alpha = 5^\circ$;

5 - $A_{M2} = f(M_c)$, 6 - $A_{M1} = f(M_c)$

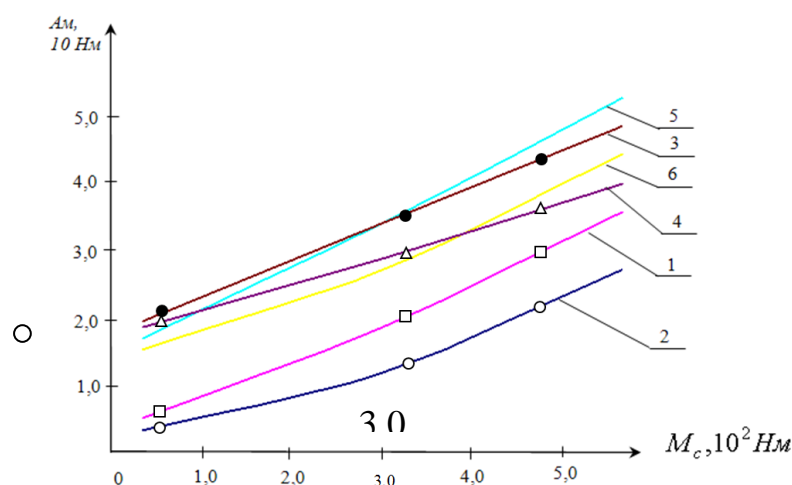


Figure. 4.12. Dependences of the change in the amplitude of oscillations of torques on the drive and driven shafts of the lever-articulated clutch on the change in the moment of technological resistance in the transmission of a car of the KAVZ -685 type.

experimentally obtained data (oscillograms) According to the obtained oscillograms (see Figure 4.6, 4.7), the curves of torque changes on the driving and driven shafts of the articulated linkage of the cardan mechanism have a periodic nature with random high-frequency components. To process the curves of the moments of the resistance forces, which are curves of periodic functions, the methods of harmonic analysis are used [110,111]. According to the well-known technique, it can be argued that any periodic function $M = f(\varphi)$ with a

period 2π that satisfies the Dirichlet condition is described by a trigonometric Fourier series in the form:

$$\begin{aligned}
 M &= \frac{M_{cp}}{2} + A_1 \cos \varphi + A_2 \cos 2\varphi + \dots + A_{n-1} \cos(n-1)\varphi + \\
 &+ A_n \cos n\varphi + B_1 \sin \varphi + B_2 \sin 2\varphi \dots + B_{n-1} \sin(n-1)\varphi + B_n \sin \varphi = \\
 &= \sum_{n=1}^{\infty} (A_n \cos n\varphi + B_n \sin n\varphi) + \frac{M_{cp}}{2}
 \end{aligned} \tag{4.1}$$

where, M_{cp} is the average value of the torque for the period under consideration; $A_1, A_2, \dots, A_n, B_1, B_2, \dots, B_n$, are constant harmonic coefficients.

As noted above, the considered function $M(\varphi)$ of technological resistance is presented in the form of oscillogram curves. In this case, the constant harmonic coefficients are determined approximately according to [110] in the form:

$$A_n \approx \frac{2}{m} \sum_{i=1}^{i=m} M_i \cos\left(\frac{2\pi n}{m} i\right); \quad B_n \approx \frac{2}{m} \sum_{i=1}^{i=m} M_i \sin\left(\frac{2\pi n}{m} i\right) \tag{4.2}$$

where, m -is the number of equal parts into which the period of oscillation of torques on the shafts of the vehicle's transmission is divided; M_i - ordinates corresponding to the indicated divisions; n - the order of the harmonics of the technological resistance curves. For the period under consideration, the average value of the moment of technological resistance is determined from the expression:

$$M_{cp} = \frac{1}{m} \sum_{i=1}^m M_i \tag{4.3}$$

The processing of torque oscillograms on the driving and driven shafts of the lever-hinge coupling was carried out as follows [110].

- the resulting torque curves on the coupling shafts for a period of 2π were

divided into equal 12 parts, that is, for each $\frac{\pi}{6}$ rotation of the shafts;

- measured the ordinates of the point of intersection of the drawn lines with the torque curves and, taking into account the calibration graphs, obtained the real values M_1 and M_2 , which are presented in tables 4.2÷4.11;

- the obtained torque values are entered into the Fourier series.

According to the processing of the oscillograms, we write the torque values, taking into account the first five harmonics, in the following form:

$$\begin{aligned}
 M_1(\varphi_1) = & M_{1cp} + a_1 \cos \varphi_1 + a_2 \cos 2\varphi_1 + a_3 \cos 3\varphi_1 + a_4 \cos 4\varphi_1 + \\
 & + a_5 \cos 5\varphi_1 + a_6 \cos 6\varphi_1 + \epsilon_3 \sin \varphi_1 + \epsilon_2 \sin 2\varphi_1 + \\
 & + \epsilon_3 \sin 3\varphi_1 + \epsilon_4 \sin 4\varphi_1 + \epsilon_5 \sin 5\varphi_1; \\
 M_2(\varphi_2) = & M_{2cp} + a'_1 \cos \varphi_2 + a'_2 \cos 2\varphi_2 + a'_3 \cos 3\varphi_2 + a'_4 \cos 4\varphi_2 + \\
 & + a'_5 \cos 5\varphi_2 + a'_6 \cos 6\varphi_2 + \epsilon'_1 \sin \varphi_2 + \epsilon'_2 \sin 2\varphi_2 + \\
 & + \epsilon'_3 \sin 3\varphi_2 + \epsilon'_4 \sin 4\varphi_2 + \epsilon'_5 \sin 5\varphi_2; \quad (4.4)
 \end{aligned}$$

Odds $a_1, a_2, a_3, a_4, a_5, a_6, a'_1, a'_2, a'_3, a'_4, a'_5, a'_6,$

$\epsilon_1, \epsilon_2, \epsilon_3, \epsilon_4, \epsilon_5, \epsilon'_1, \epsilon'_2, \epsilon'_3, \epsilon'_4, \epsilon'_5$, as well as the angular value was calculated according to the methodology given in [110], which are given in tables 4.12 and 4.13.

For five harmonics, we determine the amplitudes and phases for torques on the leading driven shafts of the lever-articulated coupling of the cardan mechanism:

$$A_1 = \sqrt{a_1^2 + \epsilon_1^2} = 8,124; \quad \operatorname{tg} \varphi_{11} \frac{a_1}{\epsilon_1} = -0,91; \quad \varphi_1 = 317^0 42';$$

The values of the coefficients for the torque of the drive shaft of the coupling

Table 4.12

cle number	M_{lsr}	a_1	a_2	a_3	a_4	a_5
1	237.15	-5.492	7.124	0.556	-3.912	0.9314
2	243.4	6.212	8.15	-0.915	0.991	0.2524
3	241.3	-4.451	4.312	-0.8219	-2.415	-1.174
4	229.7	-3.976	-4.655	-1.218	1.167	-0.866
5	229.4	-5.384	-3.473	-2.661	-2.667	-1.115
6	223.1	4.021	3.373	-1.972	-3.116	-3.928
cycle number	a_6	in_1	at_2	at_3	at_4	at_5

1	2.033	6.016	-2.446	-2.667	-1.772	1.169
2	3.853	-4.339	-6.726	-0.145	-2.276	1.138
3	9.125	-12.017	9.517	3.214	6.150	-0.523
4	-1.625	2.931	-3.238	-4.376	0.188	-1.101
5	-0.817	16.123	3.015	-0.467	-3.437	-0.550
6	-1.413	-8.064	0.2546	-1.476	-0.256	0.328

cycle number	M_{2sr}	a'_1	a'_2	a'_3	a'_4	a'_5
1	243.29	-18.48	6.817	-2.441	-4.646	3.119
2	246.17	-15.30	4.558	0.885	3.736	-0.664
3	238.16	-6.769	7.178	-1.216	1.923	-3.553
4	229.91	4.705	-8.918	-0.716	2.765	-2.941
5	239.88	-4.338	-4.851	-3.516	-4.911	-0.126
6	233.39	8.495	3.367	-1.718	6.316	1.157
cycle number	a'_6	e'_1	e'_2	e'_3	e'_4	e'_5
1	4.025	-5.621	-2.018	-4.645	1.793	1.178
2	13.528	-4.216	6.092	1.653	-0.561	1.123
3	8.312	-14.372	4.328	-0.442	-4.819	-0.623
4	1.134	2.716	-0.613	6.312	3.273	-1.103
5	-4.416	12.83	-6.254	-8.154	-0.256	-0.650
6	-0.567	-10.62	-4.205	-1.472	-3.437	3.328

$$A_2 = \sqrt{a_2^2 + e_2^2} = 7,53; \quad tg \varphi_{12} \frac{a_2}{e_2} = -2,91; \quad \varphi_2 = 288^0 54';$$

$$A_3 = \sqrt{a_3^2 + e_3^2} = 2,72; \quad tg \varphi_{13} \frac{a_3}{e_3} = -0,22; \quad \varphi_3 = 347^0 36';$$

$$A_4 = \sqrt{a_4^2 + e_4^2} = 4,29; \quad tg \varphi_{14} \frac{a_4}{e_4} = -2,21; \quad \varphi_4 = 65^0 42';$$

$$A_5 = \sqrt{a_5^2 + e_5^2} = 1,49; \quad tg \varphi_{15} \frac{a_5}{e_5} = 0,79; \quad \varphi_5 = 38^0 16';$$

$$A'_1 = \sqrt{(a'_1)^2 + (e'_1)^2} = 19,29; \quad \operatorname{tg} \varphi_{21} = \frac{a'_1}{e'_1} = -3,29; \quad \varphi_{21} = 73^{\circ} 5'$$

$$A'_2 = \sqrt{(a'_2)^2 + (e'_2)^2} = 7,11; \quad \operatorname{tg} \varphi_{22} = \frac{a'_2}{e'_2} = -3,37; \quad \varphi_{22} = 286^{\circ} 30';$$

$$A'_3 = \sqrt{(a'_3)^2 + (e'_3)^2} = 5,247; \quad \operatorname{tg} \varphi_{23} = \frac{a'_3}{e'_3} = 0,53; \quad \varphi_{23} = 28^{\circ} 52';$$

$$A'_4 = \sqrt{(a'_4)^2 + (e'_4)^2} = 4,98; \quad \operatorname{tg} \varphi_{24} = \frac{a'_4}{e'_4} = -2,41; \quad \varphi_{24} = 292^{\circ} 38';$$

$$A'_5 = \sqrt{(a'_5)^2 + (e'_5)^2} = 3,334; \quad \operatorname{tg} \varphi_{25} = \frac{a'_5}{e'_5} = 2,65; \quad \varphi_{25} = 68^{\circ} 12'.$$

According to (4.4) for the first cycle of changing torques $M_1(\varphi_1)$ and $M_2(\varphi_2)$ can be written.

$$\begin{aligned} M_1(\varphi_1) &= 237,15 - 5,492 \cos \varphi_1 + 7,124 \cos 2\varphi_1 + 0,556 \cos 3\varphi_1 - 3,912 \cos 4\varphi_1 + \\ &+ 0,931 \cos 5\varphi_1 + 2,033 \cos 6\varphi_1 + 6,016 \sin \varphi_1 - 2,446 \sin 2\varphi_1 - \\ &- 2,667 \sin 3\varphi_1 + 1,772 \cos 4\varphi_1 + 1,169 \cos 5\varphi_1; \\ M_2(\varphi_2) &= 243,29 - 18,48 \cos \varphi_2 + 6,817 \cos 2\varphi_2 - 2,441 \cos 3\varphi_2 - 4,646 \cos 4\varphi_2 + \\ &+ 3,119 \cos 5\varphi_2 + 4,025 \cos 6\varphi_2 - 5,62 \sin \varphi_2 - 2,018 \sin 2\varphi_2 - \\ &- 4,645 \sin 3\varphi_2 + 1,793 \sin 4\varphi_2 + 1,178 \sin 5\varphi_2; \end{aligned} \quad (4.5)$$

The results obtained were used in the course of theoretical studies of the dynamics of the machine unit of the cardan mechanism with a lever-articulated clutch of the KAVZ-685 automobile.

4.4. The results of production tests of the lever-articulated coupling of the cardan mechanism in the vehicle KAVZ-685

A prototype of a lever-hinge coupling with elastic elements was installed on the cardan mechanism of the KAVZ-685 transmission at Kyzylkiya JSC of the PATP of the Republic of Kyrgyzstan. The tests were carried out from 2.08.2010 to 21.10.2010

On fig. 4.13 *a* , *b* shows a general view of a prototype lever-articulated coupling with the hinges of the connecting rods in vertical (*a*) and horizontal (*b*) positions. On fig. 4.14 shows a general view of the installation of a prototype of the recommended lever-articulated clutch in the cardan transmission mechanism of the KAVZ-685 vehicle.

The results of comparative tests are summarized in Table 4.14. To evaluate the quality indicators of the recommended lever-articulated coupling with elastic elements, parallel experiments were carried out on another KaVZ-685 machine with the existing cardan transmission mechanism under the same conditions

Table 4.14

No. n/n	Road type	Mileage (km) at average speed, m/s		Failures due to transmission, pcs.		Compare fuel consumption in %		k.p.d _	
		16.67	11.10	Ex.	Rec.	Ex.	Rec.	Ex.	Rec.
1.	unpaved	122	153	4	-	100	94.8	0.82	0.882
2.	Asphalt	218	259	2	-	100	92.3	0.86	0.901

The tests were carried out for 67 days on dirt and asphalt roads at average speeds of 11.10 m/s and 16.67 m/s of vehicle movement. On a dirt road, the average mileage is for both cars 122 км(at a speed of 16.67 m/s) and 153 км(at a speed of 11.10 m/s), and for , the mileage is 218 км, 259 кмfor the corresponding speeds (see paragraph 4.14). During the test period in a vehicle with an existing transmission failures.



Figure. 4.13. General view of the prototype lever-articulated coupling

where, 1 - vertical position of the connecting rods; 2 - horizontal position of the connecting rods.



1



2

Figure. 4.14. General view of the cardan mechanism with a lever-articulated clutch of the cardan mechanism of the transmission of the KAVZ-685 car

where, 1 - installation and adjustment of the cardan mechanism;

2 - the moment of checking the rotation of the coupling shafts.

are 6, and in the recommended variant, there was no failure due to the car's transmission . It should be noted that due to the smoothing of peak loads in the transmission, the drive of the machine with the recommended clutch worked

silently and without shock loads. Due to this, the internal combustion engine of the car worked in normal mode.

At the same time, the relative fuel consumption is 5.2÷7.7% less in the recommended variant relative to the existing efficiency. In a dirt road by 10÷15%, and in an asphalt road by 8.0÷12% were higher than in the existing version [100,102]. Comparative tests revealed that the use of a lever-articulated clutch in the cardan transmission mechanism of the KAVZ-685 vehicle increases its service life by an average of 10–15%.

Thus, on the basis of the results of theoretical and experimental studies, the parameters [112] of the recommended lever-hinge coupling are substantiated.

The main conclusions for the section:

- experimental studies using the strain gauge method obtained patterns of change in torques on the drive and driven shafts of the lever-articulated coupling of the cardan mechanism with a change in the angle of divergence of the axes of the shafts, technological resistance when using different grades of rubber;

- comparative dependences of the change in the average values of the range of torque oscillations on the driving and driven shafts of the coupling were obtained as a function of the reduced stiffness coefficient of the elastic elements of the coupling. It was revealed that an increase in the rigidity of the elastic elements of the coupling leads to a decrease in the range of oscillations of the shaft torques according to a non-linear pattern. The difference between theoretical and experimental studies is 6.5÷8.5%. As the elastic elements of the coupling, the most acceptable is the use of rubber brand 7V-14MVS, with a hardness of 820-875 Nm / rad, at which $\delta_1 \leq 0.075 \div 0.11$ and $\delta_2 \leq 0.12 \div 0.15$ are provided;

- graphic dependences of the change in the amplitude of oscillations of torques on the driving and driven shafts of the lever-articulated clutch as a function of the moment of resistance in the transmission of the KAVZ-685

vehicle were obtained. It has been established that with an increase in the moment of resistance, the difference between the amplitudes of the values of the torques of the shafts increases. Recommended parameter values are: $\alpha \leq 5^{\circ} \div 10^{\circ}$; $M_s \leq 420 \div 450 \text{ Nm}$ at $\delta M_2 \leq (0.05 \div 0.1) M_s$; $C_p = 700 \div 850 \text{ Nm /rad}$;

- by the method of harmonic analysis, analytical forms of patterns of changes in torques on the driving and driven shafts of a lever-articulated clutch with elastic elements were obtained;

- comparative tests revealed that the use of a lever-articulated coupling with elastic elements in the cardan transmission mechanism of the KAVZ-685 car made it possible, compared with the existing design:

 - reduction of fuel consumption by $5.2 \div 7.7\%$;

 - increase in efficiency . in a dirt road by $10 \div 15\%$, and in an asphalt road by $8.0 \div 12\%$;

 - transmission resource increases by $10 \div 15\%$;

 - decreased failures of the car due to the reliability of the transmission;

 - of a KAVZ-685 car, the annual economic effect will be 1020 thousand ohms per car for Kyzylkiya JSC PATP .

CONCLUSION

Based on the research results, the following conclusions can be drawn:

A new design scheme of articulated-lever couplings with improved kinematic and operational characteristics has been developed. A design of a hinged-lever clutch with shock-absorbing properties of reactions in the kinematic pairs of the mechanism is proposed. A new classification of articulated couplings in cardan mechanisms has been developed, taking into account design, geometric and kinematic features.

Structural analysis of spatial lever-hinge couplings with one and two closed circuits has been carried out. The method of elimination of excessive connections in lever-hinge couplings is determined. A new structural formula is recommended for determining the degree of mobility of lever-hinge couplings, taking into account excess bonds and elastic bonds in the mechanism. A methodology has been developed for the elimination of redundant links in the spatial mechanisms of lever-hinge couplings, based on the inclusion of elastic links, the number of which is equal to the number of redundant links in the mechanism. It is recommended that elastic connections are established between links, hinges, and are also made in the form of composite hinges with elastic elements.

Analytically obtained formulas for determining the distance between the centers of the hinged connections of the driving and driven shafts with earrings in the absence of deformation in the composite hinges and the distance between the hinges in the zero dead position. Formulas are obtained for determining the maximum and minimum values of the interaxial distance between the hinges in the presence of deformations in the composite hinges and the distance between the hinges of the levers in the dead position.

Graphic dependences of the change in the distance between the centers of the hinged joints of the driving and driven coupling halves with earrings as a

function of the angle of divergence between the shafts of the mechanism are obtained. It was revealed that to ensure the operability of a lever-articulated coupling with composite hinges in the support of the driven shaft and between the earring and the lever at angles $\alpha = 30^\circ \dots 75^\circ$ and $K_1 K_2 = 0.02 R$, it is recommended to choose the center distance between the centers of the mechanism's earrings in within $(2.08 \div 2.1) R$, and in the absence of deformations in the hinges $K_1 K_2 = 0$, the center distance $2 R$ is proposed. Formulas are obtained for determining the length of the levers, taking into account the deformation in the compound hinges and the distance $K_1 K_2$ and without them. Graphical dependences of the change in the length of the levers as a function of the angle of divergence between the shafts of the lever-articulated coupling are constructed.

Formulas have been obtained for calculating the angles that determine the positions of the link and connecting rods, taking into account the angle of divergence of the shafts and deformations of the elastic elements of the coupling. The graphical patterns of angle changes that determine the positions of the link and the connecting rod as a function of the angular displacement of the coupling shaft at different values of the angle of divergence of the driving and driven shafts are determined. Using the method of moving coordinates and vector equations, formulas were obtained for determining the angular velocities of the coupling halves of the couplings, taking into account the angle of divergence of the shaft axes and the deformation of the elastic elements of the driven shaft support and the hinge of the coupling with the connecting rod. Graphical dependences of the change in the angular velocities of the coupling halves as a function of the angular displacements of the driving and driven shafts are obtained, taking into account the angle of their divergence.

A formula is derived for determining the transfer function between the drive and driven shafts of a articulated-lever coupling, taking into account the angle of divergence of the shaft axes and the deformation of the elastic elements.

The dependences of the change in the amplitude of oscillations of the transfer function of the articulated-lever coupling on the change in the angle of divergence of the shaft axes and deformations of the elastic elements are obtained.

Dynamic and mathematical models of a machine unit with a lever-articulated clutch are compiled, taking into account the mechanical characteristics of the drive, the variability of the transfer function of the clutch, the elastic-dissipative properties of elastic elements, and the characteristics of the technological load of a vehicle of the KaVZ-685 type. Based on the solution of the problem of the dynamics of the machine unit by the numerical method Mathcad, the laws of change of angular velocities, angular accelerations and torques for various values of the technological load, the moments of inertia of the shafts, the angle of their divergence, and the characteristics of elastic elements are obtained.

The dependences of the change in the amplitude of oscillations of the angular velocities, accelerations and torques of the coupling shafts on the change in the technological load, the reduced stiffness coefficient, the dissipation coefficient and the angle of divergence of the axes of the driving and driven shafts are obtained. Recommended parameter values: $I_{n1} = 0,12 \div 0,13 Hmc^2$;
 $I_{n2} = 0,14 \div 0,15 Hmc^2$; $M_c = (450 \div 550) Hm$; $\delta M_c = \pm(2,0 \div 2,2) Hm$;
 $C_y = (750 \pm 850) Hm / pa\delta$; $B_y = (6,4 \div 8,5) Hmc / pa\delta$, $\alpha \leq (10^\circ \div 25^\circ)$

Experimental studies using the strain gauge method have obtained patterns of change in torques on the drive and driven shafts of the lever-articulated coupling of the cardan mechanism with a change in the angle of divergence of the axes of the shafts, technological resistance when using different brands of rubber. Comparative dependences of the change in the average values of the range of torque oscillations on the driving and driven shafts of the coupling are obtained as a function of the reduced stiffness

coefficient of the elastic elements of the coupling. It was revealed that an increase in the rigidity of the elastic elements of the coupling leads to a decrease in the range of oscillations of the shaft torques according to a non-linear pattern. The difference between theoretical and experimental studies is 6.5÷8.5%. As the elastic elements of the coupling, the most acceptable is the use of rubber brand 7V-14MVS, with a hardness of 820-875 Nm / rad, at which $\delta_1 \leq 0.075 \div 0.11$ and $\delta_2 \leq 0.12 \div 0.15$ are provided.

Clutch as a function of the moment of resistance in the transmission of the KaVZ-685 vehicle are obtained . It has been established that with an increase in the moment of resistance, the difference between the amplitudes of the values of the torques of the shafts increases. Recommended parameter values are: $\alpha \leq 5^\circ \div 10^\circ$; $M_s \leq 420 \div 450$ Nm at $\delta M_2 \leq (0.05 \div 0.1) M_s$; $C_p = 700 \div 850$ Nm / rad. Using the harmonic analysis method, analytical forms of the patterns of changes in torques on the driving and driven shafts of a lever-hinge coupling with elastic elements are obtained.

Comparative tests revealed that the use of a lever-articulated coupling with elastic elements in the cardan transmission mechanism of the KAVZ-685 car made it possible, compared with the existing design: reduction of fuel consumption by 5.2÷7.7%; increase in efficiency . in a dirt road by 10÷15%, and in an asphalt road by 8.0÷12%; transmission resource increases by 10÷15%; Reduced vehicle failures due to transmission reliability.

LIST OF USED LITERATURE

1. Лысов М.И. Карданные механизмы. МашГИЗ 1945г.
2. Малаховский Я.Э., Лапин А.А., Веденив Н.К. Карданные передачи. под. ред. проф. Липгарта А.А. Москва-1962.
3. Гольд Б.В., Тверсков Б.М. Карданы равных угловых скоростей, НИИН АВТОПРОМ, 1967г.
4. Артоболевский И.И., Теория механизмов и машин, «Наука», -1975 г.
5. Баранов Г.Г. Курс теории механизмов и машин, М., «Маш-ние», 1975 г.
6. Левитская О.Н. Левитская Н.И. Курс теории механизмов и машин, «Высшая школа», М., 1978 г.
7. Решетов Л.Н. Конструирование рациональных механизмов, Детали машин. М.: Машиностроение. -1974. -655 б. М., «Машиностроение», 1972 г.
8. Решетов Л.Н. и Будыка Е.Ю., К вопросу определения избыточных связей в механизмах, «Известия ВУЗов» «Машиностроение», № 3, 1976 г.
9. Решетов Л.Н. и Будыка Е.Ю., Избыточные связи в механизмах автомобиля ВАЗ и их устранение, «Известия ВУЗов» «Машиностроение», № 4, 1977 г.
10. Акулов В.Я., Определение избыточных связей и подвижностей в механизмах, «Известия ВУЗов» «Машиностроение», № 4, 1977 г.
11. Корон Г. и Корон Т., Справочник по математике (для научных работников и инженеров), «Наука», М., 1973 г.
12. Зиновьев В.А., Курс теории механизмов и машин, М., «Наука», 1972 г.
13. Артоболевский И.И., Теория механизмов для воспроизведения плоских кривых, изд-во АН СССР, М., 1959 г.
14. Войлоков И.Т., О синтезе пространственных четырехзвенников по предельным положениям, «Известия ВУЗов», Машиностроение, № 9, 1969 г.
15. Левитский Н.И. и Шахбазян К.Х., Синтез пространственных четырехзвенных механизмов с низшими парами, «Труды семинара по

- ТММ», т. ХУ, вып. 54, изд-во АН СССР, 1954 г.
16. Ананьев Г.Д., Кинематика пространственных шарнирных механизмов сельскохозяйственных машин, МашГИЗ, 1968 г.
 17. Дижечко Н.Н Кислицин С.Г., Аналитические методы исследования сложных пространственных механизмов, сб «Анализ и синтез механизмов и теория передач» изд-во «Наука», М., 1965 г.
 18. Кунада Г., Кинематика сложных сферических механизмов, сб. статей по ТММ «Анализ синтез механизмов» изд-во Машиностроение, М., 1969 г.
 19. Дудица Ф., К теореме Гарсгофа для четырехзвенных пространственных механизмов, Сб. статей по ТММ «Анализ синтез механизмов» изд-во Машиностроение, М., 1969 г.
 20. Тавхелидзе Д.С., Некоторые вопросы кинематического анализа четырехзвенных пространственных механизмов, Сообщения АН ГССР, 2, 1964 г.
 21. Тавхелидзе Д.С., Ромбоиды в стержневых механизмах и их свойства, сб. статей по ТММ «Анализ синтез механизмов» изд-во Маш-ние, М., 1969 г.
 22. Лысов М.И., Карданные механизмы, МашГИЗ, 1945 г.
 23. Малаховский Я.Э. и др., Карданные передачи МашГИЗ, 1962 г.
 24. Гольд Б.Д. и Тверсков Б.М. Карданы равных угловых скоростей, НИИН АВТОПРОМ, 1967 г.
 25. Гафанович А.А., Шарнирные передачи сельскохозяйственных машин, «Сельхозмашина», №4, 1955 г.
 26. Тартаковский Н.К., Некоторые вопросы кинематики пространственного двойного универсального шарнира, «Вестник машиностроения», № 5, 1965 г.
 27. Свальев Л.Ф. и Хижняков И.П., Определение угловой подвижности в карданных сочленениях, «Автомобильная промышленность», № 11, 1972 г.
 28. Иванов С.Н. и Мамаева В.П., Об углах установки отдельных карданных шарниров в мног шарнирной карданной передаче трансмиссии, «Автомобильная промышленность», № 3, 1976 г.

29. Бысоцкий М.С. и др., Неравномерность вращения двухшарнирного вала, «Автомобильная промышленность», № 6, 1978 г.
30. Савелова А.А., Кинематика карданного механизма, «Известия ВУЗ, Машиностроение», № 6, 1979 г.
31. Павлов Б.И., Механизмы приборов и систем управления, «Машиностроение», Л., 1972 г.
32. Арапбаев С., Исследование нового синхронного карданного механизма. Кандидатская Диссертация. Алматы, 1982 г., 153 с.
33. Кислицин С.Г., Определение положений некоторых пространственных механизмов, Ученые записки Ленинградского госпед. Института им. А.И.Герцена, т. 125, 1956 г.
34. Мудров П.Г., Пространственные механизмы с вращательными парами, изд-во Казанского университета, 1976 г.
35. Кузьмин И.В. и Лебедев И.А., Алгоритмы определения функции положения ведомого звена пространственного кривошипно-коромыслового четырехзвенника с учетом зазоров в шарнирах, «Машиноведение», № 3, 1976 36. Амбарцумян Р.В. и Горовой О.Г., Кинематический анализ шестизвенного зубчато-рычажного механизма, «Известия ВУЗ, Маш-ние», № 3, 1979 г.
36. Линвин Ф.Л., Определение функции положения пространственного механизма способом условного размыкания, «Машиноведение», № 4, 1970 г.
37. Литвин Ф.Л. и Карпович С.Е., Применение метода условного размыкания контура для определения параметров движения семи-шести-, пятизвенных пространственных рычажных механизмов, «Машиноведение», № 6, 1975 г.
38. Литвин Ф.Л. и Карпович С.Е., Геометро-аналитическое определение области существования пространственного четырехзвенного механизма ВССВ, «Машиноведение», № 4, 1976 г.
39. Гантмарех Ф.Р., Теория матриц, «Наука», М., 1966 г.
40. Ефимов Н.В., Квадратичные формы и матрицы, «Наука», М., 1967 г.
41. Су и Рэдклифф, Применение матриц перемещения для синтеза сферических механизмов, «Труды американского общества инженеров-механиков», серия В, № 2, 1967 г.

42. Литвин Ф.Л., Теория зубчатых зацеплений, «Наука», М., 1968 г.
43. Воробьев Е.И., Анализ кинестатики пространственного четырехзвенного механизма методом матриц, «Машиноведение», № 4, 1970
45. Воробьев Е.И., Кинематический анализ пространственных исполнительных механизмов манипуляторов методом матриц, «Механика машин», вып. № 27-28, «Наука», М., 1971 г.
44. Кулюгин В.И., Алгоритм для получения изображения пространственного механизма, «Машиноведение», № 1, 1973 г.
45. Гупта К.С., Кинематический анализ плоских и пространственных механизмов, «Труд американского общества инженеров-механиков», серия В, изд-во «Мир», № 2, 1973 г.
46. Воробьев Е.И., Аналитический метод анализа пространственных кинематических цепей и его приложение к механизмам манипуляторов и автооператоров, «Механика машин», АН СССР, вып. № 43, М., 1974 г.
47. Заморюев Г.Б., Алгоритм для определения относительных скоростей движения звеньев, «Известия ВУЗ, Машиностроение», № 1, 1976 г.
48. Лебедев П.А. и Ростовцев В.Н., Аналитическое определение функции перемещения ведомого звена кривошипных пространственных четырехшарнирников, «Машиноведение», № 5, 1976 г.
49. Корн Г. и Корн Т., Справочник по математике (для научных работников и инженеров), «Наука», М., 1973 г.
50. Добронравов В.В., и др., Курс теоретической механики, «Высшая школа», М., 1974 г.
51. Юдин В.А. и Петрокас Л.В., Теория механизмов и машин, «Высшая школа», М., 1977 г.
52. Габель Р., Силы, действующие на шарнирные валы, «Машиностроение за рубежом», № 3, 1959 г.
53. Иванов С.И. и др., Крутильные колебания карданной передачи в трансмиссии автомобиля, «Автомобильная промышленность», № 4, 1974 г.
54. Тверсков Б.М. и др., Исследование нагруженности трансмиссии одноосных тягачей с асинхронными карданными шарнирами в приводе к управляемым колесам, «Автомобильная промышленность»,

№ 4, 1967 г.

55. Лебедев П.А., О статическом и динамическом условиях проворачиваемости кривошипно-коромыслового механизма, «Известия ВУЗ, Технология легкой промышленности», № 4, 1967 г.
56. Черкудинов С.А. и Полухин В.П., Угол давления однокривошипном шарнирном четырехзвеннике, «Механика машин», № 3, «Наука», 1966 г.
57. Полухин В.П., Некоторые вопросы динамического синтеза пространственных механизмов, Сб. статей «Анализ и синтез механизмов», М., «Машиностроение», 1969 г.
58. Сатерленд Г.И. и Росс Б., Критерий передачи движения в пространственных механизмах, «Труды американского общества инженеров-механиков», серия В, «Мир», № 2, 1973 г.
59. Семенов М.В., Кинематические и динамические расчеты исполнительных механизмов, Л., «Машиностроение», 1974 г.
60. Кулюги В.И., К проворачиваемости звеньев пространственного шарнирного четырехзвенного механизма с учетом допускаемого угла давления, «Машиноведение», № 6 1976 г.
61. Маундер Л. и Бардесс Н.С., Граничные условия для валов, соединенных с помощью шарнира Гука, «Теория машин и механизмов» (сб. посвящен 70-летию академика И.И.Артоболевского), «Наука», М., 1976 г.
62. Ачеркана Н.С. Справочник металлиста под редакцией, изд-во «Машиностроение», 1965 г.
63. Сухарев И.П., Прочность шарнирных узлов машин, М., «Машиностроение», 1977 г.
64. Соловьев А.И., Коэффициент полезного действия механизмов и машин, М., «Машиностроение», 1966 г.
65. Геффнович А.А., Экспериментальное исследование долговечности карданных передач сельскохозяйственных машин, Сб. ВИСХОМа вып.9, «Исследование материалов сельскохозяйственных машин», ЦБТИ, 1956 г.
66. Макарова Р.А., Тензометрия в машиностроении, под редакцией, М., «Машиностроение», 1975 г.

67. Резник В. Легенда о кардане. <http://www.cardan.com.ua/history/>.
68. Внедорожники России. <http://www.avto4x4.narod.ru/staty/varmiy.htm>.
69. Шугуров Л. ШРУС. <http://auto.whatodo.ru/csn/07-98/dev.htm>.
70. Кожевников С.Н., Есипенко Я.И., Раскин Я.М. Элементы механизмов. «Оборонгиз». Москва-1956.
71. Решетов Л.Н. Конструирование рациональных механизмов. Москва-1972.
72. Белкин Л.И., Бученков Н.С., Горелов Л.Р., Горячий Я.В., Евланов В.И., Захаров Э.Г., Липгарт С.А., Сморгонский Л.И., Столяров Е.А., Тапинский В.Н., Филюнов А.Г. Автомобиль АЗЛК-2141. Москва - 1989.
73. BMW серия 5. Руководство по техническому обслуживанию и ремонту. Москва, Фолио-2003.
74. Джураев А.Д., Давидбаев Б., Давидбаева Н. Б...Анализ процесса выпадения частиц хлопка в зоне взаимодействия с амортизирующим отражателем сепаратора \ \ Научно-технический-журнал Ферганского политехнического института, 144-147
75. Иванов С.Н., Соколев О.В. Карданные валы с трубами из композиционного материала, Ж.: автомобильная промышленность. №1, 1986г. 19-20 с.
76. Иванов С.Н., Лунев И.С., Есеновский Ю.К. Конструкции легких карданных валов и особенности их производства. –М.: автомобильная промышленность, 1982, №4, с. 14-16.
77. Артоболевский И.И. Теория механизмов. Москва-1967.
78. Джураев А.Д., Давидбаев Б., Мирзахонов Ю .Теоретическая исследование механический и транспортирующим машины с плоскоременной передачи с натяжным роликам\ \ Научно-технический журнал № 1 Фер ПИ г Фергана 2013 г.76-79
79. Ганиев А.А., Джураев А.Д., Алимухамедов Ш.П., Хикматов Ш.И., Ортиков Р.Я., Заявка Ўт ўргич-майдалагич.
80. Джураев А. и др., Шарнирная муфта, Авт. Свед., № 1693288, Бюл. Изб., № 43, 1991 г.
81. Джураев А. и др., Шарнирная муфта, Авт. Свед., № 1640471, Бюл. №

13, 1991 г.

82. Джураев А.Д., Давидбаев Б., Зулпиев С. М., Мирзахонов Ю., Давидбаева Н. Б. Шарнирно-рычажное муфта, КР. Авторское свидетельство.116
83. Джураев А., Давидбаев Б.Н., Зулпиев С.М., Шарнирная муфта, патент Рес. Узб. № 8513, от 4.08.10 г.
84. Портгитер Ф. М., Применение универсальных шарниров в сельхозмашинах, сб. переводов, «Сельскохозяйственное машиностроение», изд. Иностранной литературы, 1954 г.
85. Зулпиев С., Давидбаев Б. Структурный анализ шарнирной муфты. «Проблемы механики» Фан, 2009, № 2, с. 85-86.
86. Джураев А.Д., Давидбаев Б., Умаров Б. Структурный анализ натяжного механизма плоскоременной передачи.\\ Теория машин и рабочих процессов сборник трудов Международная научно – практическая конференция, посвященная 90-летию со дня рождения академика О.Д. Алимова Бишкек, 17-18 сентября 2013.
87. Зулпиев С., Давидбаев Б. Джураев А. Шарнирная муфта с расширенными кинематическими возможностями. Сб. Трудов РНПК, Наукоёмкие технологии в хлопкоочистительной, текстильной, легкой промышленности и полиграфическом производстве, Ташкент, 2010 г. с. 69-70.
88. Зулпиев С., Давидбаев Б. Джураев А. К метрическому анализу шарнирной муфты из упругих элементов. РНПК «Участие молодых ученых в решении проблемных вопросов техники и технологии», Ташкент, 2011, с. 92.
89. Воронков И.М. Курс теоретической механики, изд. техник.-теор., литературы, М., 1964 г., с. 552.
90. Левитский Н.И. Теория механизмов и машин. Изд. «Наука», 1979, с. 76.
91. Нарбут А.Н., А.Мухитдинов. Система двигатель- трансмиссия. Ж. Автомобильная промышленность. М., 2011, № 4, с.13-14.
92. Мухитдинов А. Совершенствование характеристик двигателей автомобилей. Ж., Вестник транспорта. М., 2002, № 7, с. 27-31.
93. Джураев А. Д., Давидбаев Б. Н., Зулпиев С. М., Структурный синтез рычажно-шарнирной муфты. Ж.Наука и новые технологии № 4 2009,

Бишкек.

94. Фаварин М.В. Момент инерции тел. Справочник. Изд. Машиностроение, М., 1977, с. 511.
95. 98. Ривин Е.И. Динамика привода станков. Изд. Машиностроение, М., 1966, с. 204.
96. Мирзахонов Ю. У. и др. Применение параметров натяжного ролика при теоретическом изучении динамики транспортирующих лент // Энерго-ресурсосберегающие технологии и оборудование в дорожной и строительной отраслях. – 2019. – С. 134-138.
97. Методы динамических испытаний для резины (Общие требования) ГОСТ 23326-78, М., 1978, с. 18.
98. Джураев А. Зулпиев С. и др. Эксплуатационные характеристики шарнирной муфты с составными кинематическими парами. Материалы РНПК «Ресурсо сберегающие технологии на железнодорожном транспорте», Ташкент, 2010 г., с. 73-75.
99. Джураев А., Зулпиев С., Давидбаев Б. Повышение эксплуатационных характеристик шарнирной муфты. Тезисы докладов первого международного Джолдасбековского симпозиума, Алматы, 2011, с 70-71.
100. Джураев А., Давидбаев Б., Зулпиев С. Кинематический и динамический анализ рычажно-шарнирных муфт с упругими элементами карданных механизмов. V Всемирный Конгресс инжиниринга и технологии –WCET-2011 «Содействие развитию передовых технологий УММАН» Алматы, 2011 г.
101. АД Джураев, БН Давидбаев, НБ Давидбаева. Обоснование параметров амартизирующей пластины резиновой подушке сепаратора хлопко-сырца\\ Наманганский инженерно-технологически институт. Научно-технический журнал №4 2019
102. И.Немец Практическое применение тензометров. Перев. с чешского М., Энергия, 1970, с. 144.
103. Н.И.Воронцов и др. Тензометрирование деталей автомобиля. Изд. Машиностроение, М., 1962, с. 232.
104. А.Джураев и др. Теория механизмов и машин. Изд. Г.Гуляма, Ташкент, 2004, с. 592.

105. Веденяпин Г.В. Общая методика экспериментального исследования и обработка опытных данных. М.: Колос. -1973. –199 б.
106. Менли Р. Анализ и обработка записей колебаний. М.: Машиностроение. -1972. стр. 368.
107. А.Джураев Моделирование динамики машинных агрегатов хлопкоперерабатывающих машин. Изд. «Фан», Ташкент , 1984, 128с.
108. Джураев А.Д., Давидбаев Б.Н.,Мамахонов А. Қайишқоқ элементли ва таранглаш қурилмалари занжирли механизмлари кинематик ва динамик тахлили\\ Монография Ташкент 2014,139стр.
109. Джураев А.Д., Давидбаев Б., Давидбаева Н.Б. Анализ влияния радиуса натяжного ролика на силу взаимодействия с ремнем при переменном его натяжении\\ Научно-технический журнал № 3 Фер ПИ г Фергана 2015 г.
110. Джураев А. Д., Давидбаев Б. Н., Зулпиев С. М., Структурный анализ рычажно – шарнирной муфты. Ж.«Фер.ПИ илмий техника журналари», № 2 2009. Фергана.
111. Джураев А. Д., Давидбаев Б. Н., Зулпиев С. М., Определение расстояния между центрами шарнирных соединений валов с серьгами рычажно-шарнирной муфты с упругими элементами. Фер.ПИ. Научно - технический журнал. № 4 2011 г.
112. Джураев А. Д., Давидбаев Б. Н., Зулпиев С. М., Влияние угла расхождения валов рычажно-шарнирной муфты на характер движения системы. Ж. Известия вузов № 3 2011г. Бишкек
113. Джураев А. Д., Давидбаев Б. Н., Зулпиев С. М., Гармонический анализ крутящего момента на ведомом валу рычажно – шарнирной муфты. Ж. Известия вузов № 4 2011г. Бишкек
114. Джураев А. Д., Давидбаев Б.Н., Зулпиев С. М. Давидбаева Н. Б., Влияние параметров упругих элементов на динамику машинного агрегата с рычажно – шарнирной муфтой. Фер.ПИ. Научно - технический журнал. № 4 2011 г.
115. Джураев А. Д., Давидбаев Б. Н., Зулпиев С. М., Исследование рычажно – шарнирной муфты карданного вала автомобилей. Труды Кыргызско – Узбекского университета. Ж. Наука, образование, техника № 1 2009 г. Ош.

116. Джураев А. Д., Давидбаев Б.Н., Зулпиев С. М., Шарнирная муфта с расширенными кинематическими возможностями. Сб. трудов РНПК наукоемкие технологии в хлопкоочистительной, текстильной, легкой пром-ти и полиграфическом производстве Ташкент 2010. Стр.101-103
117. Джураев А.Ж., Давидбаев Б.Н., Жаляев А.А., Мирзахонов Ю.У. Плоскоременная передача с натяжным роликом. // Патент Уз. Рес. UZ IAP 4228, 31.03.97.№ 1
118. Джураев А.Ж Давидбаев Б.Н Мирзахонов Ю.У., Давидбаева Н.Б. Умаров Б.Х. Плоскоременная передача с натяжным роликом. Патент Узбекистан FAR 00780 № 12 2012г.
119. Давидбаев Б., Давидбаева Н.Б . Кўтариш-ташиш машиналари. \\ Тошкент “Наврўз” нашрети 2017й
120. Джураев А.Д., Давидбаев Б.Н., Зулпиев С.М., Давидбаева Н.Б. Структурный анализ шарнирных муфт с упругими элементами\\ Научно-технический журнал ФерПИ №4 2012
121. Джураев А.Д, Давидбаев Б.Н, Зулпиев С. Влияние параметров упругих элементов на динамику рычажно-шарнирной муфты карданного механизмов.\\Новые и нетрадиционные технологии в ресурсо и энергосбережении. Материалы научно-технической конференции (19-22сентября 2011г., г. Одесса)
122. Джураев А.Д., Давидбаев Б.Н., Зулпиев С.М., Давидбаева Н.Б. Структурной анализ шарнирных муфт с упругими элементами . Научно технический журнал Фер.ПИ № 3 2012г
123. B.N Davidbaev,, N.B Davidbaeva. IMPROVEMENT OF THE DESIGN OF THE COTTON SEPARATOR SS-15A \\ Innovative Technologica: Methodical Research Journal 3 (11), 64-69.
124. Джураев А.Д., Зулпиев С., Давидбаев Б.Н .. Влияние угла расхождения валов рычажного-шарнирной муфты на колебания скорости , ускорения и нагруженность ведущего вала карданного механизма. Материалы научно-технической конференции 19-22.09.2011г Одесса
125. Джураев А.Д., Давидбаев Б.Н., Зулпиев С.М., Производителельной испытаний рычажно-шарнирной муфты карданного механизма. Научно технический журнал Фер.ПИ № 2 2013г

126. Джураев А.Д., Давидбаев Б.Н., Джураев Н.Н. Икки киримли тўлкинсимон сиртли винтнинг урта тебранишлари тахлили.\\ Наманган курилиш меҳандислик институти НТЖ №2 2022.
127. Джураев А.Д., Давидбаев Б.Н., Зулпиев С.М., Повышение эксплуатационных характеристик шарнирной муфты. Тезисы докладов первого международного Джолдасбековского симпозиума, Алматы, 2011, с 70-71
128. Джураев А.Д., Давидбаев Б.Н., Зулпиев С.М. Кинематический и динамический анализ рычажно-шарнирных муфт с упругими элементами карданных механизмов\\ V Всемирном Конгрессе инжиниринга и технологии –WCET-2011 «Содействие развитию передовых технологий УММАН» Алматы, 2011 г.
129. Джураев А.Д., Давидбаев Б., Зулпиев С. М. К метрическому анализу шарнирной муфты с упругим элементом\\ РНПК «Участие молодых ученых в решении проблемных вопросов техники и технологии», Ташкент, 2011, с. 92.
130. Джураев А.Д., Давидбаев Б.Н., Зулпиев С., Давидбаева Н.Б. Производительной испытаний рычажно-шарнирной муфты карданного механизма\\ Научно-технический журнал № 2 Фер. ПИ г Фергана 2013г
131. Джураев А.Д., Давидбаев Б., Давидбаева Н.Б Структурный анализ рычажных-шарнирных муфт с упругими связями и элементами карданных механизмов.\\ Материалы с международной научно – практической конференции “Актуальные проблемы внедрения инновацион техники – технология на предприятиях по производству строительных материалов, химической промышленности и в смежных отраслях” 24 – 25. 05. 2019 част 4 2019. 80-85стр.
132. Djuraev A., Davidbaev B. N., Jumaev A. S. Improvement of the design of the belt conveyor and scientific basis for calculation of parameters //Global Book Publishing Services. – 2022. – С. 1-144.
133. *Djurayev, B. N. Davidbayev, N.B.Davidbayeva. Determination Of Oscilation Anpelitude Of Cotton Particle at Interaction with.Plate Shpok Absocter Of The Separator.*\\ International Journal Of Abvanced Research in Science, Engieering and Technology (India) Volume 7, Issue 9,September 2020.14977-14981.

134. Djurayev A., Davidbayev B. N., Jurayev N. N. Scientific basis of the design and parameter calculation of the construction and parameters of a double-inlet and wavy surface resource controller screw conveyor for spillable materials //Global Book Publishing Services. – 2022. – С. 1-113.
135. Джураев А.Д., Давидбаев Б., Давидбаева Н.Б. О передаточной функции рычажно-шарнирной муфты с учетом упругих элементов в шарнирах механизма. Научный журнал Механика и технология Наманганского инженерно-строительного института. №2. 2021г Наманган. стр.9-15
136. Зулпиев С.М, Давидбаев Б., Джураев А.Д., Давидбаев Б., Зулпиев А.М. Давидбаева Н.Б. Плоскоременная передача с натяжным роликом. Патент Кырг. Рес. По заявке № 20220007.2 от 28.04.23 г. №354.
137. A Juraev, BN Davidbaev, AA Zhalyaev - Slippage gear with tension roller. Patent Uz. Res. UZIAP.4228,03-31.
138. АЖ Джураев, БН Давидбаев, АА Жаляев, РЮ Мелемедов, ЮУ Мирзахонов Натяжной ролик плоскоремённой передачи. Патент Уз. Рес. UZ №50
139. АД Джураев, БН Давидбаев, О Алимов, НБ Давидбаева. Сепаратор для волокнистых материалов. - Патент Узбекистан IAP, 2020
140. Б.Н.Давидбоев. Кутариш-ташиш машиналари. Тошкент, “Укитувчи, 1989
141. Джураев А., Давидбоев Б. Н., Давидбоева Н. Б. Разработка и расчет шарнирно-рычажных муфт карданных механизмов Монография //Монография. Изд. LAP Lambert Academic Publishing. – 2021.
142. Зулпиев С.М, Давидбаев Б., Джураев А.Д., Давидбаев Б., Зулпиев А.М. Давидбаева Н.Б. Цепная передача . Патент Кырг. Рес. По заявке № 20220025.1 от 28.04.23 г. №2341.
143. Зулпиев С.М, Давидбаев Б., Джураев А.Д., Давидбаев Б., Зулпиев А.М. Давидбаева. Сепаратор для хлопка-сырца. Патент Кырг. Рес. По заявке № 20230011,2 от 30.08.23 г. №360.
144. Juraev A. D. et al. Results of dynamic analysis of double-inlet screw conveyor machine assembly //E3S Web of Conferences. – 2023. – Т. 417. – С. 06005.
145. B.N.Davidbaev, Mirzaxonov Yu.U, Davidboyeva N.B. Teoriticheskoye

- issledovaniye i opredeleniye parametrov sdvigayushchix sil v natyajnom rolake s uprugimi elementami transportiruyushchix i texnologicheskix mashinax // International Scientific Journal Theoretical & Applied Science 2022.07.11. 382-385
146. Djurayev A., Yuldashev K. Dynamics of the Screw Conveyor for Transportation and Cleaning of Fiber Material //International Journal of Advanced Science and Technology. – 2020. – Т. 29. – №. 5. – С. 8557-8566.
147. АД Джураев, БН Давидбаев, СМ Зулпиев, НБ Давидбаева. Структурный кинематический и динамический анализ рычажно-шарнирных муфт с упругими элементами карданного механизма. Фергана: Фаргона.
148. Джураев А., Давидбаев Б., Давидбаева Н. Влияние взаимодействие летучки с амортизирующей пластин. Сепаратора на качественные показатели хлопка-сырца //Збірник наукових праць ЛОГОС. – 2020. – С. 72-76.
149. Джураев А. Ж., Мирзаханов Ю. У. Совершенствование Конструкций И Обоснование Параметров Центрирующего Натяжного Устройства Транспортёра //Central Asian Journal of Theoretical and Applied Science. – 2021. – Т. 2. – №. 11. – С. 237-247.
150. Мирзаханов Ю. У., Сиддиков М. З. Ё., Уришев Д. И. Ё. Исследование бокового схода ремня в плоскоремённых передачах и транспортирующих механизмах //Oriental renaissance: Innovative, educational, natural and social sciences. – 2022. – Т. 2. – №. 5. – С. 773-781.
151. Зулпиев С. М., Давидбаев Б. Н., Давидбаева Н. Б. О движение летучки хлопка-сырца по поверхности перфорированной сетки сепаратора сс-15а //известия национальной академии наук кыргызской республики. – 2022. – №. 5. – С. 173-178.
152. Зулпиев С. М., Асамидинов Ф. М., Дуйшоева Г. М. Экспериментальное исследование резин различных марок для установки в шарнирно-рычажной муфте //Синергия. – 2016. – №. 3. – С. 88-94.
153. Davidboev B. et al. Research of lateral assembly of the belt in flat-belt transmissions and transport mechanisms //International Journal of

- Scientific and Technology Research. – 2020. – Т. 9. – №. 1. – С. 3666-3669.
154. Djuraevich D. A., Nizomitdinovich D. B., Bakhtiyerdjanovna D. N. Substantiation Parameters Of Reflector With Rubber Shock Absorber Of Cotton Separator //Solid State Technology. – 2020. – Т. 63. – №. 6. – С. 1718-1726.
155. Djuraev A., Davidboev B. N., Davidboeva N. B. Determination of Oscillation Amplitude of Cotton Particle at Interaction with Plate and Shock Absorber of the Separator //International Journal of Advanced Research in Science, Engineering and Technology. – 2020. – Т. 7. – №. 9. – С. 14977-14981.
156. Джураев А., Давидбаев Б., Давидбаева Н. Анализ процесса выпадения частиц хлопка в зоне взаимодействия с амортизирующим отражателем сепаратора //Научно-технический-журнал Ферганского политехнического института. – 2020. – С. 144-147.
157. Давидбаев Б., Джураев А., Давидбаева Н. Исследование взаимодействия частицы хлопка–сырца с амортизирующей пластиной сепаратора //Збірник наукових праць ЛОГОС. – 2020. – С. 82-86.
158. Anvar D., Kuliev T. M. Designing and methods of calculating parameters of a fibrous material cleaner from large litter //International Journal of Advanced Science and Technology. – 2020. – Т. 29. – №. 8 Special Issue. – С. 444-452.

CONTENTS

INTRODUCTION	1
1. ANALYSIS OF THE WORK OF THE STRUCTURE OF HINGE, GARDEN MECHANISMS AND METHODS OF THEIR IMPROVEMENT	3
1.1. Overview of the work of articulated-cardan mechanisms	3
1.2 Analysis of design features and schemes of synchronous cardan mechanisms	5
1.3. Some design features of asynchronous cardan mechanisms.....	15
1.4. Development of new schemes of articulated-lever couplings.....	19
1.5. Classification of articulated couplings in cardan mechanisms	27
2. STRUCTURAL AND METRIC ANALYSIS OF A HINGE COUPLING	29
2.1. Structural Analysis of Swivel Couplings	29
2.2 . Structural Analysis of Swivel Couplings with Elastic Elements	33
2.3. Metric mechanism analysis.....	41
3. KINEMATIC AND DYNAMIC ANALYSIS OF A LINKAGE COUPLING	55
3.1. Kinematic analysis of a lever-hinge coupling with elastic elements.....	55
3.1.1. Analysis of the positions of the links of the mechanism.....	55
3.2. Determination of the transfer function of a lever-articulated coupling, taking into account the elastic elements in the hinges of the mechanism	63
3.3. Dynamics of the machine unit of a lever-articulated coupling with elastic elements.	73
3.3.1 Calculation scheme and mathematical model of the machine unit of the lever-articulated coupling.	73
3.3.2. Solution of the problem and analysis of results.....	80
4. EXPERIMENTAL INVESTIGATIONS OF A LEVER - HINGED COUPLING WITH ELASTIC ELEMENTS	94
4.1. Experimental methodology.....	94

4.2. Processing and analysis of experimental results	101
4.3 . Harmonic Analysis of Torque on the Driven Shaft of a Lever-Hinge Clutch	117
4.4. The results of production tests of the lever-articulated coupling of the cardan mechanism in the vehicle KAVZ-685	123
CONCLUSION	128
LIST OF USED LITERATURE	132
CONTENTS	146

B.N. Davidbaev, A. Juraev, S.M. Zulpiev B.N., Davidbaeva N.B.

**DEVELOPMENT OF EFFECTIVE STRUCTURES AND METHODS
FOR CALCULATING PARAMETERS OF HARNESS-LEVER
COUPLINGS OF CARDAN MECHANISMS WITH ELASTIC
ELEMENTS**

MONOGRAPH

Approved for printing:

Academic Council of Fergana Polytechnic Institute

**MINISTRY OF SCIENCE AND INNOVATION OF THE REPUBLIC OF
UZBEKISTAN**

ISBN: - 978-1-957653-20-4

DOI: - <https://doi.org/10.37547/gbps-15>

GBPS



9 781957 653204

Global Book Publishing Services
1211 Polk St, Orlando, FL 32805, USA
Email info@scientificpublication.org

B.N. Davidbaev, A. Juraev,
S.M. Zulpiev ,N.B. Davidbaeva

**Development of effective structures and methods
for calculating parameters of harness-lever couplings
of cardan mechanisms with elastic elements.**

Fergana 2023, 139 p.